

UNCLASSIFIED

SECURITY CLASSIFICATION OF THIS PAGE (When Data Entered)

REPORT DOCUMENTATION PAGE		READ INSTRUCTIONS BEFORE COMPLETING FORM
1. REPORT NUMBER NORDA Technical Note 195	2. GOVT ACCESSION NO.	3. RECIPIENT'S CATALOG NUMBER
4. TITLE (and Subtitle) Comparison of Observed Data and GDEM/Standard Ocean Data, Part II: Monthly Sea Surface Temperature (SST) Plots and Temperature/Salinity Vertical Cross-Sections Along Great Circle Tracks in the Mediterranean Sea		5. TYPE OF REPORT & PERIOD COVERED Final
7. AUTHOR(s) S.C. Daubin, Jr. (Pacific-Sierra Research Corp.) E. Hashimoto (ODSI, Defense Systems, Inc.)		6. PERFORMING ORG. REPORT NUMBER
9. PERFORMING ORGANIZATION NAME AND ADDRESS ODSI, Defense Systems, Inc. 3255 Wing St. Suite #550 San Diego, CA 92110		8. CONTRACT OR GRANT NUMBER(s) NOOO14-81-C-0316
11. CONTROLLING OFFICE NAME AND ADDRESS Naval Ocean Research and Development Activity NSTL Station, Mississippi 39529		10. PROGRAM ELEMENT, PROJECT, TASK AREA & WORK UNIT NUMBERS
14. MONITORING AGENCY NAME & ADDRESS (if different from Controlling Office)		12. REPORT DATE January 1983
		13. NUMBER OF PAGES 142
		15. SECURITY CLASS. (of this report) Unclassified
		15a. DECLASSIFICATION/DOWNGRADING SCHEDULE
16. DISTRIBUTION STATEMENT (of this Report) Distribution Unlimited		
17. DISTRIBUTION STATEMENT (of the abstract entered in Block 20, if different from Report)		
18. SUPPLEMENTARY NOTES		
19. KEY WORDS (Continue on reverse side if necessary and identify by block number) Ocean model Acoustic model Sound speed Marine climatology Underwater acoustics		
20. ABSTRACT (Continue on reverse side if necessary and identify by block number) This report compares the results of the Generalized Digital Environmental Model, (GDEM), developed by Dr. T. Davis of the Naval Oceanographic Office (NOO), with measured and analyzed data from the Mediterranean Sea. Monthly Sea Surface Temperature (SST) analyses are compared and evaluated. Vertical cross-sections along Great Circle tracks of temperature and salinity are compared and evaluated. Comparisons and evaluations of monthly SST and vertical cross-sections along Great Circle tracks are compared for the major basins of the Mediterranean.		

DD FORM 1 JAN 73 1473

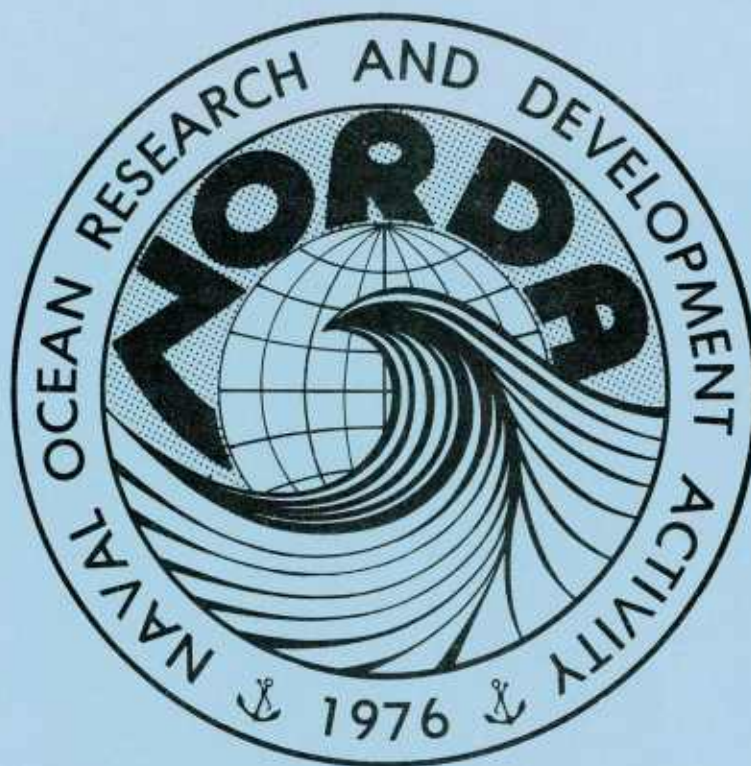
EDITION OF 1 NOV 65 IS OBSOLETE
S/N 0102-LF-014-6601

UNCLASSIFIED

SECURITY CLASSIFICATION OF THIS PAGE (When Data Entered)

Naval Ocean Research
and Development Activity
NSTL Station, Mississippi 39529

Comparison of Observed Data and GDEM/Standard Ocean
Data, Part II: Monthly Sea Surface Temperature (SST)
Plots and Temperature/Salinity Vertical Cross-Sections
Along Great Circle Tracks in the Mediterranean Sea



Superintendent (Code 1424)
Naval Post Graduate School
Monterey, California 93940

Approved for Public Release
Distribution Unlimited

Prepared for
CDR M. McCallister
NORDA Code 520

S.C. Daubin, Jr.
Pacific-Sierra Research Corporation

E. Hashimoto
ODSI, Defense Systems, Incorporated

January 1983



ODSI DEFENSE SYSTEMS, INC.

6110 EXECUTIVE BLVD., SUITE 320, ROCKVILLE, MD 20852 • 301/984-6006

Prepared For:
NAVAL OCEAN RESEARCH AND DEVELOPMENT ACTIVITY
NSTL Station, Mississippi

Prepared Under:
Contract Number N00014-81-C-0316

COMPARISON OF OBSERVED SURVEY/ANALYZED
DATA and GDEM/STANDARD OCEAN DATA

Part II: Monthly Sea Surface Temperature (SST)
Plots and Temperature/Salinity Vertical
Cross-Sections Along Great Circle Tracks
in the Mediterranean Sea

Technical Report
January 1983

Prepared by:
Eigoro Hashimoto
OCEAN DATA SYSTEMS, INC.
San Diego, California

ABSTRACT

This report compares the results of the Generalized Digital Environmental Model, (GDEM), developed by Dr. T. Davis of the Naval Oceanographic Office (NOO), with measured and analyzed data from the Mediterranean Sea. Monthly Sea Surface Temperature (SST) analyses are compared and evaluated. Vertical cross-sections along Great Circle tracks of temperature and salinity are compared and evaluated. Comparisons and evaluations of monthly SST and vertical cross-sections along Great Circle tracks are compared for the major basins of the Mediterranean.

TABLE OF CONTENTS

<u>SECTION</u>	<u>PAGE</u>
TABLE OF CONTENTS	ii
LIST OF FIGURES	iv
LIST OF TABLES	ix
PREFACE	x
1.0 SUMMARY.	1-1
2.0 INTRODUCTION	2-1
2.1 Description of the Model (GDEM MOD-3)	2-2
2.2 Organization of the Technical Report	2-3
3.0 GENERAL DESCRIPTION OF THE MEDITERRANEAN SEA	3-1
3.1 General Oceanography	3-1
3.2 General Meteorology	3-3
4.0 COMPARISON OF GDEM MONTHLY SEA SURFACE TEMPERATURE (SST) PLOTS FOR THE MEDITERRANEAN SEA	4-1
4.1 Monthly SST Comparison.	4-1
5.0 VERTICAL CROSS SECTIONAL COMPARISONS ALONG GREAT CIRCLE TRACKS OF TEMPERATURE AND SALINITY.	5-1
5.1 Vertical Temperature and Salinity Comparisons For MX-01 (Alboran Sea).	5-1
5.1.1 Regional Description	5-1
5.1.2 Comparison	5-3
5.2 Vertical Temperature and Salinity Comparisons For MX-02 (Balearic Sea)	5-12
5.2.1 Regional Description	5-12
5.2.2 Comparison	5-14
5.3 Vertical Temperature and Salinity Comparisons For MX-03 (Tyrrhenian Sea)	5-19
5.3.1 Regional Description	5-19
5.3.2. Comparison	5-21
5.4 Vertical Temperature and Salinity Comparisons For MX-04 (Ionian Sea)	5-27
5.4.1 Regional Description	5-27
5.4.2 Comparison	5-32

TABLE OF CONTENTS (Continued)

<u>SECTION</u>		<u>PAGE</u>
5.5	Vertical Temperature and Salinity Comparisons	
	For MX-05 (Aegean Sea)	5-41
5.5.1	Regional Description	5-41
5.5.2	Comparison	5-42
5.6	Vertical Temperature and Salinity Comparisons	
	For MX-06 (Levantine Sea)	5-43
5.6.1	Regional Description	5-43
5.6.2	Comparison	5-49
5.7	Vertical Temperature and Salinity Comparisons	
	For MX-07 (Balearic Sea)	5-55
5.7.1	Regional Description	5-55
5.7.2	Comparison	5-57
5.8	Vertical Temperature and Salinity Comparisons	
	For MX-08 (Ionian Sea)	5-62
5.8.1	Regional Description	5-62
5.8.2	Comparison	5-67
5.9	Vertical Temperature and Salinity Comparisons	
	For MX-09 (Levantine Sea)	5-73
5.9.1	Regional Description	5-73
5.9.2	Comparison	5-79
5.10	Vertical Temperature and Salinity Comparisons	
	For MX-10 (Balearic Sea)	5-85
5.10.1	Regional Description	5-85
5.10.2	Comparison	5-87
5.0	REFERENCES	6-1

LIST OF FIGURES

<u>FIGURE</u>		<u>PAGE</u>
1-1	LOCATIONS OF VERTICAL TEMPERATURES/ SALINITY COMPARISONS ALONG GREAT CIRCLE TRACKS.	1-2
4-1	ATLAS - JANUARY SEA SURFACE TEMPERATURE (SST) FOR THE MEDITERRANEAN SEA	4-6
4-2	GDEM - JANUARY SEA SURFACE TEMPERATURE (SST) FOR THE MEDITERRANEAN SEA	4-7
4-3	ATLAS - FEBRUARY SEA SURFACE TEMPERATURE (SST) FOR THE MEDITERRANEAN SEA	4-8
4-4	GDEM - FEBRUARY SEA SURFACE TEMPERATURE (SST) FOR THE MEDITERRANEAN SEA	4-9
4-5	ATLAS - MARCH SEA SURFACE TEMPERATURE (SST) FOR THE MEDITERRANEAN SEA	4-10
4-6	GDEM - MARCH SEA SURFACE TEMPERATURE (SST) FOR THE MEDITERRANEAN SEA	4-11
4-7	ATLAS - APRIL SEA SURFACE TEMPERATURE (SST) FOR THE MEDITERRANEAN SEA	4-12
4-8	GDEM - APRIL SEA SURFACE TEMPERATURE (SST) FOR THE MEDITERRANEAN SEA	4-13
4-9	ATLAS - MAY SEA SURFACE TEMPERATURE (SST) FOR THE MEDITERRANEAN SEA	4-14
4-10	GDEM - MAY SEA SURFACE TEMPERATURE (SST) FOR THE MEDITERRANEAN SEA	4-15
4-11	ATLAS - JUNE SEA SURFACE TEMPERATURE (SST) FOR THE MEDITERRANEAN SEA	4-16
4-12	GDEM - JUNE SEA SURFACE TEMPERATURE (SST) FOR THE MEDITERRANEAN SEA	4-17
4-13	ATLAS - JULY SEA SURFACE TEMPERATURE (SST) FOR THE MEDITERRANEAN SEA	4-18
4-14	GDEM - JULY SEA SURFACE TEMPERATURE (SST) FOR THE MEDITERRANEAN SEA	4-19
4-15	ATLAS - AUGUST SEA SURFACE TEMPERATURE (SST) FOR THE MEDITERRANEAN SEA	4-20
4-16	GDEM - AUGUST SEA SURFACE TEMPERATURE (SST) FOR THE MEDITERRANEAN SEA	4-21

LIST OF FIGURES (Continued)

<u>FIGURE</u>		<u>PAGE</u>
4-17	ATLAS - SEPTEMBER SEA SURFACE TEMPERATURE (SST) FOR THE MEDITERRANEAN SEA	4-22
4-18	GDEM - SEPTEMBER SEA SURFACE TEMPERATURE (SST) FOR THE MEDITERRANEAN SEA	4-23
4-19	ATLAS - OCTOBER SEA SURFACE TEMPERATURE (SST) FOR THE MEDITERRANEAN SEA	4-24
4-20	GDEM - OCTOBER SEA SURFACE TEMPERATURE (SST) FOR THE MEDITERRANEAN SEA	4-25
4-21	ATLAS - NOVEMBER SEA SURFACE TEMPERATURE (SST) FOR THE MEDITERRANEAN SEA	4-26
4-22	GDEM - NOVEMBER SEA SURFACE TEMPERATURE (SST) FOR THE MEDITERRANEAN SEA	4-27
4-23	ATLAS - DECEMBER SEA SURFACE TEMPERATURE (SST) FOR THE MEDITERRANEAN SEA	4-28
4-24	GDEM - DECEMBER SEA SURFACE TEMPERATURE (SST) FOR THE MEDITERRANEAN SEA	4-29
5-1	JANUARY TEMPERATURE ISOTHERMS AT THE 100 METER SURFACE LEVEL	5-5
5-2	MARCH TEMPERATURE ISOTHERMS AT THE 100 METER SURFACE LEVEL	5-6
5-3	GDEM - WINTER VERTICAL TEMPERATURE CROSS SECTION ALONG GREAT CIRCLE TRACK MX-01	5-7
5-4	WINTER VERTICAL SALINITY CROSS SECTION ALONG GREAT CIRCLE TRACK MX-01	5-8
5-5	GDEM - WINTER VERTICAL SALINITY CROSS SECTION ALONG GREAT CIRCLE TRACK MX-01	5-9
5-6	SUMMER VERTICAL SALINITY CROSS SECTION ALONG GREAT CIRCLE TRACK MX-01	5-10
5-7	GDEM - SUMMER VERTICAL SALINITY CROSS SECTION ALONG GREAT CIRCLE TRACK MX-01	5-11
5-8	WINTER VERTICAL TEMPERATURE CROSS SECTION ALONG GREAT CIRCLE TRACK MX-02	5-15
5-9	GDEM - WINTER VERTICAL TEMPERATURE CROSS SECTION ALONG GREAT CIRCLE TRACK MX-02	5-16

LIST OF FIGURES (Continued)

<u>FIGURE</u>		<u>PAGE</u>
5-10	WINTER VERTICAL SALINITY CROSS SECTION ALONG GREAT CIRCLE TRACK MX-02	5-17
5-11	GDEM - WINTER VERTICAL SALINITY CROSS SECTION ALONG GREAT CIRCLE TRACK MX-02	5-18
5-12	WINTER VERTICAL TEMPERATURE CROSS SECTION ALONG GREAT CIRCLE TRACK MX-03	5-23
5-13	GDEM - WINTER VERTICAL TEMPERATURE CROSS SECTION ALONG GREAT CIRCLE TRACK MX-03	5-24
5-14	WINTER VERTICAL SALINITY CROSS SECTION ALONG GREAT CIRCLE TRACK MX-03	5-25
5-15	GDEM - WINTER VERTICAL SALINITY CROSS SECTION ALONG GREAT CIRCLE TRACK MX-03	5-26
5-16	LOCATIONS OF THE SALINITY CORE LAYER WITHIN THE LEVANTINE INTERMEDIATE WATER IN THE WINTER (WUST, 1961).	5-30
5-17	LOCATIONS OF THE SALINITY CORE LAYER WITHIN THE LEVANTINE INTERMEDIATE WATER IN THE SUMMER (WUST, 1961)	5-31
5-18	WINTER VERTICAL TEMPERATURE CROSS SECTION ALONG GREAT CIRCLE TRACK MX-04	5-34
5-19	GDEM - WINTER VERTICAL TEMPERATURE CROSS SECTION ALONG GREAT CIRCLE TRACK MX-04	5-35
5-20	WINTER VERTICAL SALINITY CROSS SECTION ALONG GREAT CIRCLE TRACK MX-04	5-36
5-21	WINTER VERTICAL SALINITY CROSS SECTION ALONG GREAT CIRCLE TRACK MX-04	5-37
5-22	GDEM - WINTER VERTICAL SALINITY CROSS SECTION ALONG GREAT CIRCLE TRACK MX-04	5-38
5-23	SUMMER VERTICAL SALINITY CROSS SECTION ALONG GREAT CIRCLE TRACK MX-04	5-39
5-24	GDEM - SUMMER VERTICAL SALINITY CROSS SECTION ALONG GREAT CIRCLE TRACK MX-04	5-40
5-25	LOCATIONS OF THE SALINITY CORE LAYER WITHIN THE LEVANTINE INTERMEDIATE WATER IN THE WINTER (WUST, 1961).	5-46

LIST OF FIGURES (Continued)

<u>FIGURE</u>		<u>PAGE</u>
5-26	LOCATIONS OF THE SALINITY CORE LAYER WITHIN THE LEVANTINE INTERMEDIATE WATER IN THE SUMMER (WUST, 1961)	5-47
5-27	LOCATIONS OF THERMAL FRONTS IN THE IONIAN AND LEVANTINE SEAS (LEVINE AND WHITE, 1972) . .	5-48
5-28	FALL VERTICAL TEMPERATURE CROSS SECTION ALONG GREAT CIRCLE TRACK MX-06	5-51
5-29	GDEM - FALL VERTICAL TEMPERATURE CROSS SECTION ALONG GREAT CIRCLE TRACK MX-06 . . .	5-52
5-30	FALL VERTICAL SALINITY CROSS SECTION ALONG GREAT CIRCLE TRACK MX-06	5-53
5-31	GDEM - FALL VERTICAL SALINITY CROSS SECTION ALONG GREAT CIRCLE TRACK MX-06	5-54
5-32	WINTER VERTICAL TEMPERATURE CROSS SECTION ALONG GREAT CIRCLE TRACK MX-07	5-58
5-33	GDEM - WINTER VERTICAL TEMPERATURE CROSS SECTION ALONG GREAT CIRCLE TRACK MX-07 . . .	5-59
5-34	WINTER VERTICAL SALINITY CROSS SECTION ALONG GREAT CIRCLE TRACK MX-07	5-60
5-35	GDEM - WINTER VERTICAL SALINITY CROSS SECTION ALONG GREAT CIRCLE TRACK MX-07	5-61
5-36	LOCATIONS OF THE SALINITY CORE LAYER WITHIN THE LEVANTINE INTERMEDIATE WATER IN THE WINTER (WUST, 1961).	5-65
5-37	LOCATIONS OF THE SALINITY CORE LAYER WITHIN THE LEVANTINE INTERMEDIATE WATER IN THE SUMMER (WUST, 1961)	5-66
5-38	WINTER VERTICAL TEMPERATURE CROSS SECTION ALONG GREAT CIRCLE TRACK MX-08	5-69
5-39	GDEM - WINTER VERTICAL TEMPERATURE CROSS SECTION ALONG GREAT CIRCLE TRACK MX-08 . . .	5-70
5-40	WINTER VERTICAL SALINITY CROSS SECTION ALONG GREAT CIRCLE TRACK MX-08	5-71

LIST OF FIGURES (Continued)

<u>FIGURE</u>		<u>PAGE</u>
5-41	GDEM - WINTER VERTICAL SALINITY CROSS SECTION ALONG GREAT CIRCLE TRACK MX-08	5-72
5-42	LOCATIONS OF THERMAL FRONTS IN THE IONIAN AND LEVANTINE SEAS (LEVINE AND WHITE, 1972)	5-73
5-43	FALL VERTICAL TEMPERATURE CROSS SECTION ALONG GREAT CIRCLE TRACK MX-09	5-79
5-44	GDEM - FALL VERTICAL TEMPERATURE CROSS SECTION ALONG GREAT CIRCLE TRACK MX-09	5-80
5-45	FALL VERTICAL SALINITY CROSS SECTION ALONG GREAT CIRCLE TRACK MX-09	5-81
5-46	GDEM - FALL VERTICAL SALINITY CROSS SECTION ALONG GREAT CIRCLE TRACK MX-09	5-82
5-47	SUMMER VERTICAL SALINITY CROSS SECTION ALONG GREAT CIRCLE TRACK MX-10	5-86
5-48	GDEM - SUMMER VERTICAL SALINITY CROSS SECTION ALONG GREAT CIRCLE TRACK MX-10	5-87

LIST OF TABLES

<u>TABLE</u>		<u>PAGE</u>
1-1	MONTHLY SEA SURFACE TEMPERATURE (SST) COMPARISONS FOR THE MEDITERRANEAN SEA	1-3
1-2	VERTICAL TEMPERATURE/SALINITY CROSS- SECTIONAL COMPARISONS ALONG GREAT CIRCLE TRACKS IN THE MEDITERRANEAN SEA BETWEEN GDEM AND SURVEY ANALYSIS DATA	1-5

PREFACE

This technical report has been written in support of the Generalized Digital Environmental Model (GDEM) Standard Ocean Evaluation Project sponsored by the Surveillance Environmental Acoustic Support (SEAS) Program at the Naval Ocean Research and Development Activity (NORDA). This report is Part 2 of the evaluation of GDEM MOD-3 for the Mediterranean Sea. Monthly Mediterranean Sea Surface Temperature (SST) contoured plots were compared. Vertical cross-sectional comparisons were also conducted along selected great circle tracks. These great circle track comparisons were performed on temperature and salinity.

Earlier in FY-81, GDEM comparisons of seasonal temperature, salinity and sound speed vertical profiles at six selected site locations in the Mediterranean Sea were conducted and the results were presented in NORDA Technical Note 154-S dated December 1981 and titled "Comparison of Observed Data and GDEM/Standard Ocean Data, Part I: Vertical Temperature, Salinity and Sound Speed Profiles at Six Selected Site Locations in the Mediterranean Sea," by S. C. Daubin, Jr. and E. Hashimoto. Other publications related to previous GDEM evaluations have been: "Recent Standard Ocean Evaluation Results," June 1980, SEAS Report 80-037; and "GDEM/Standard Ocean Results for the North Pacific," December 1980, NORDA Technical Note 101-S.

This report has been technically reviewed by Dr. T. Davis (NORDA), Dr. M. Carron (NOO), Mr. P. Bucca (NORDA), Mr. R. VanWyckhouse (NORDA), Mr. G. Kerr (NORDA), and Mr. K. Countryman (NOO) and their comments and suggestions are greatly appreciated. The GDEM vertical cross-sections and sea surface temperature contoured plots for comparison were provided by Dr. M. Carron and Mr. K. Countryman. Comparisons and evaluations have been limited to materials which were available in present literature.

In memory of the fine work and friendship of

Scott C. Daubin, Jr.

July 1946 - August 1981

1.0 SUMMARY

This report evaluates the Generalized Digital Environmental Model (GDEM) developed by Dr. T. Davis of the Naval Oceanographic Office (NOO), and compares its results with ocean climatological atlas, oceanographic surveyed and analyzed data for the European Mediterranean Sea. Monthly Mediterranean Sea Surface Temperature (SST) contoured plots were compared. Vertical cross-sectional comparisons were also conducted along great circle tracks (Figure 1-1).

The comparisons were conducted on two major physical parameters: temperature and/or salinity. The comparisons of monthly sea surface temperature contoured plots were conducted on the five secondary Mediterranean basins (Alboran, Balearic, Tyrrhenian, Ionian and Levantine). Excluded from the comparisons were the marginal seas such as the Black Sea, Adriatic Sea, Aegean Sea, and the Red Sea. The comparisons along great circle tracks were performed either on temperature, on salinity, or on both. The temporal resolutions compared were either monthly or seasonal (four three-month seasons) identified as winter (January, February, March), spring (April, May, June), summer (July, August, September), and fall (October, November, December).

A brief summary of the comparisons is provided below. Each comparison described in the summary reflects the exact sequence (order) of the comparisons which were made (e.g. monthly, then tracks MX-01 through MX-10).

- Monthly Sea Surface Temperature Comparisons:

Monthly GDEM sea surface temperature plots were compared with Mediterranean Sea climatological atlas data (Robinson, Bauer and Schroeder, 1979). The results are presented on Table 1-1 for each major region.

The Alboran Sea and Levantine Sea were considered similar to the atlas for each of the twelve months (January to December). The Balearic

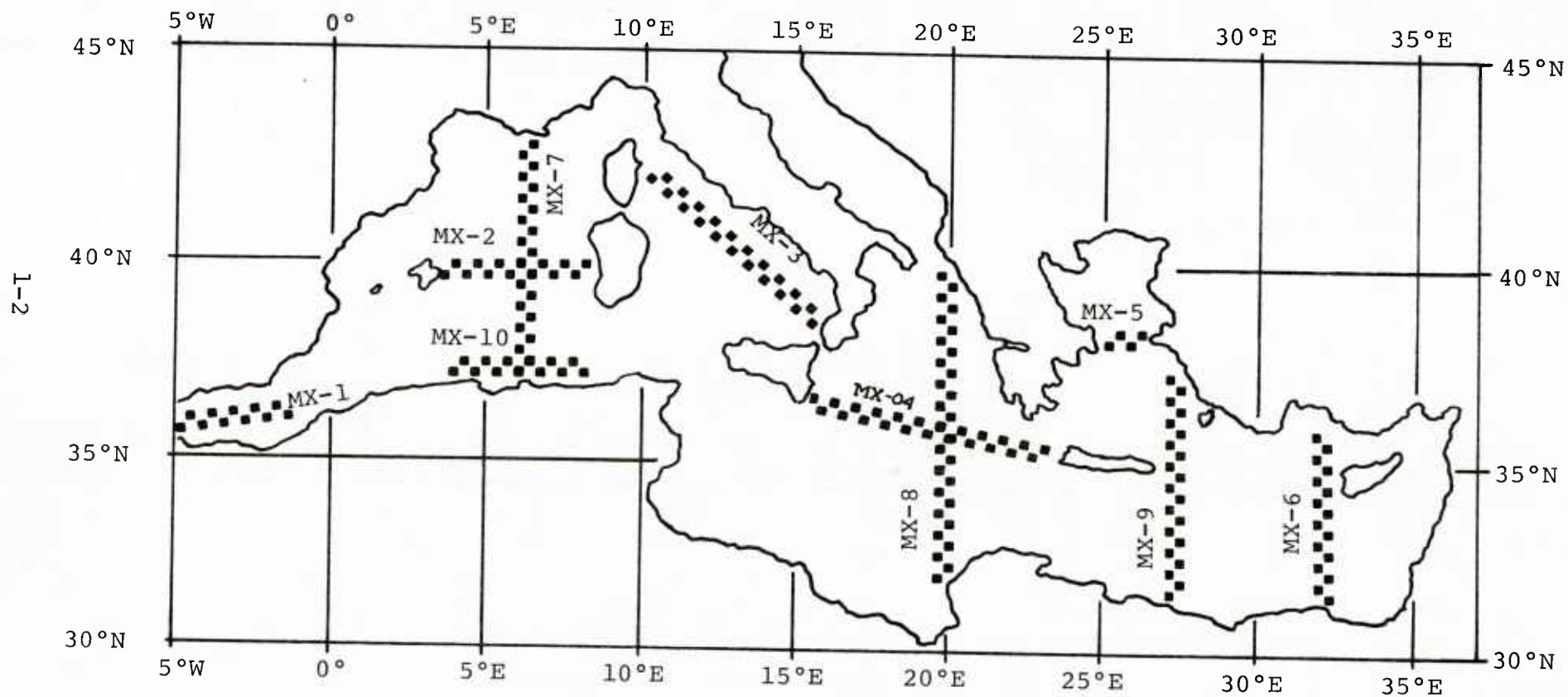


FIGURE 1-1: LOCATIONS OF VERTICAL TEMPERATURE/SALINITY
COMPARISONS ALONG GREAT CIRCLE TRACKS IN
THE MEDITERRANEAN SEA

TABLE 1-1: MONTHLY SEA SURFACE TEMPERATURE (SST) COMPARISONS
FOR THE MEDITERRANEAN SEA

BASINS OF THE MEDITERRANEAN	MONTHLY SST COMPARISONS/EVALUATIONS		
	Similar	Similar with Slight Differences	Similar with Major Differences
Alboran Sea	January February March April May June July August September October November December		None
Balearic Sea	January February March April June July August September October November December	May	None
Tyrrhenian Sea	January February March April May July August September October November December	June	None
Ionian Sea	January February March April May June August September October November	July December	None
Levantine Sea	January February March April May June July August September October November December		None

Sea was considered similar for eleven of the twelve months. The GDEM-atlas Balearic SST comparison for May was considered similar with slight differences in either orientation (direction) or proximity (location) of SST isotherms. The Tyrrhenian Sea was considered similar for eleven of the twelve months. The GDEM-atlas Tyrrhenian SST comparison for June was considered similar with slight differences in either orientation or proximity of the SST isotherms. The Ionian Sea was considered similar for ten of the twelve months. The GDEM-atlas Ionian SST comparisons for July and December were considered similar with slight differences in either orientation or proximity of the SST isotherms.

- Vertical Temperature and/or Salinity Cross Sectional Comparisons Along Great Circle Tracks

Comparisons of vertical cross sections were conducted along selected great circle tracks (Figure 1-1). The results are presented on Table 1-2 for each MX (Mediterranean Cross Section) track (MX-01 through MX-10). Brief comparisons of the GDEM outputs with surveyed/analyzed vertical cross sections are described.

GDEM vertical cross sections were considered similar for the following regions; in the Alboran Sea (MX-01); in the Balearic Sea (MX-02, MX-07 and MX-10) in the Tyrrhenian Sea (MX-03); in the Ionian Sea (MX-04 and MX-08); and in the Levantine Sea (MX-06 and MX-09). Comparisons for MX-05 (Aegean Sea) were not conducted due to the shallow and restrictive barrier topography of this region. Temperature comparisons for MX-01 and MX-10 were not available for comparison. Similarities with slight temperature differences were determined for MX-02 and MX-03. There were no comparisons which were determined as having major differences.

In summary, GDEM adequately reproduced most large and meso-scale temperature and salinity features in both the monthly sea surface temperature and vertical cross section comparison. Fine structures, if present, were reviewed but not compared. Such comparisons were viewed inappropriate

TABLE 1-2: VERTICAL TEMPERATURE/SALINITY CROSS-SECTIONAL COMPARISONS ALONG GREAT CIRCLE TRACKS IN THE MEDITERRANEAN SEA BETWEEN GDEM AND SURVEY/ANALYZED DATA

	Cheney - Winter	Wust - Winter	Wust - Summer		R.V. Atlantis I #263 Winter		R.V. Atlantis I #275 Winter		R.V. Chain #21 Fall		R.V. Atlantis II #59 Summer		LEGEND:
													A = Similar A+d = Similar with slight differences D = Major differences -- = No comparisons made S = Salinity T = Temperature
SITE	S	S	T	S	T	S	T	S	T	S	T	S	COMMENTS
MX-01	A	A+d	--	A									Similar in temperature at 100 meter surface (Cheney). Similar in salinity.
MX-02					A+d	A							Similar in salinity. Similar in temperature.
MX-03							A+d	A					Similar in salinity. Similar in temperature.
MX-04		A					A	A					Similar in temperature. Similar in salinity.
MX-05									--	--			Shallowness of region viewed inappropriate for comparison.
MX-06									A	A			Similar in temperature. Similar in salinity.
MX-07					A	A							Similar in temperature. Similar in salinity.
MX-08							A	A					Similar in temperature. Similar in salinity.
MX-09									A	A			Similar in temperature. Similar in salinity.
MX-10											--	A+d	Similar in salinity.

for this study. The evaluation was based on several comparisons. GDEM comparisons which properly reflected the following characteristics were determined as being similar and realistic where there were:

- 1) the appropriate duplication of major known isotherms and isohalines,
- 2) the approximate equivalent depths of known isotherms and isohaline layers,
- 3) the duplication of appropriate locations (positions) of major known isotherms and isohalines,
- 4) the duplication of appropriate vertical thicknesses of major known thermal and haline layers.

2.0 INTRODUCTION

This technical report compared output from the MOD-3 version of the Generalized Digital Environmental Model (GDEM), which is being developed by Dr. T. Davis of the Naval Oceanographic Office (NOO), with surveyed/analyzed data from published sources, for the Mediterranean Sea. The comparisons - GDEM graphic outputs with surveyed/analyzed data from present literature - were intended to determine the model's ability to duplicate known and observed oceanographic features as outlined in the sources.

The purpose of this technical report was to determine and evaluate GDEM's capability to reasonably represent the known oceanography of the Mediterranean Sea. Comparisons were made of monthly GDEM Sea Surface Temperature (SST) outputs with recently available Mediterranean Sea SST atlases, (Figures 4-1 through 4-24). Comparisons were also conducted on GDEM outputs (vertical cross-sections) along selected great circle tracks with surveyed and analyzed data found in present literature. Figure 1-1 identifies the locations of each great circle track (cross-hatched bands). Figures 5-1 through 5-53 identify the contoured vertical cross-sectional plots along each great circle track.

The comparisons relied heavily on the work of Miller, Tschernia, Charnock, 1970; Robinson, Schroeder, Bauer, 1979; Morel, 1972; Katz, 1972; Wust, 1961; MEDOC Group, 1970; Cheney, 1977; and other sources cited in the text.

The marginal seas, such as the Black Sea, Red Sea, and the Adriatic Sea were excluded from this comparison.

To provide the reader with additional information, the Introduction has been divided into two parts: Description of the Model (GDEM MOD-3); and Organization of the Technical Report.

2.1 Description of the Model (GDEM MOD-3)

GDEM produces three mean data fields of temperature, salinity and sound speed on a 30-minute latitude by 30-minute longitude grid. GDEM is comprised of three major vertical models: upper, middle, and lower. All of the three mean data fields modeled have been developed to represent continuous vertical and horizontal data fields in an attempt to minimize vertical discontinuities between one model and the other.

- Upper or Near-surface Model* (Surface to 400 m):

The upper or near-surface temperature model can be expressed as either monthly or seasonal mean data fields. The upper or near-surface salinity model is expressed as seasonal mean data fields. The upper or near-surface sound-speed model can be expressed as either monthly or seasonal mean data fields.

- Middle or Mid-depth Model (200 to 2450 m):

The middle or mid-depth temperature and salinity model is expressed as biannual mean data fields. The middle or mid-depth sound-speed model is expressed as seasonal mean data fields.

- Lower or Deep-depth Model (Greater than 2450 m):

The lower or deep-depth temperature, salinity and sound-speed models are expressed as annual mean data fields.

The data set used to develop the GDEM mean data fields was derived through the use of several extensive up to date data sources. Data sets of expendable bathythermograph (XBT); ocean station (Nansen cast) hydrocast; salinity-temperature-depth (STD); and some mechanical bathythermograph (MBT) measurements primarily from the recent Fleet Numerical Oceanography Center (FNOC) Master Ocean Observation Data Set (MOODS) files of

*Other than the monthly GDEM SST comparisons, further results of the monthly GDEM upper or near-surface temperature and sound speed model are not presented in this report. These results are intended to follow during an appropriate phase of the GDEM evaluation.

1980 were accessed and used as well as the data files from the Naval Oceanographic Office (NOO) Oceanographic Data Set of 1980.

2.2 Organization of the Technical Report

The Preface and Summary have preceded this section of the report. Section 2.0 discusses the General Oceanography and Meteorology of the Mediterranean Sea. Section 3.0 discusses the Comparison of GDEM Monthly Sea Surface Temperature (SST) for the Mediterranean Sea. Section 4.0, discusses the Vertical Cross-Sectional Comparisons Along Great Circle Tracks of Temperature and Salinity for Mediterranean Sections MX-01 through MX-10. References for this report are found in Section 5.0.

The following conventions are observed throughout this report. Temperatures are in degrees Celsius ($^{\circ}\text{C}$); and salinity in parts per thousand ($^{\circ}/\text{oo}$). Horizontal gradients, whether of temperature, or salinity are in units of change per 100 km.

Every effort has been made to render the compared plots and sections visually similar. North - south, east - west orientations are always the same. Horizontal positions are nearly always comparable so that a line drawn through both figures passes through the same part of the ocean. The reader should note, however, that vertical scale is not constant and is generally not comparable. In order to publish as much as possible of the GDEM output, we often present a complete GDEM section against a smaller section from the published data. (For example, Figures 5-34 and 5-35.)

3.0 GENERAL DESCRIPTION OF THE MEDITERRANEAN SEA

Brief overviews on the general oceanography and meteorology of the Mediterranean Sea are discussed in Sections 3.1 and 3.2. The purpose of this section is to acquaint the reader with some of the variety of oceanographic and meteorologic features which have been observed in and reported on the Mediterranean. This general overview is primarily intended as general background for both the sea surface temperature (SST) and great circle track comparisons. An extensive "in-depth" treatment and discussion of each feature described are considered by the authors to be inappropriate for this report. More specific oceanographic and meteorological descriptions appropriate to each great circle track comparison are discussed under the Regional Description section of each comparison.

All comparisons in this report are confined to the region often referred to as the European Mediterranean Sea (Sverdrup, Johnson, Fleming, 1942). This region is located in the northern hemisphere between the northern African continent and bounded roughly by the $47^{\circ}00'N$ latitude, the $6^{\circ}00'W$ meridian and the $36^{\circ}00'E$ meridian. It encompasses an area of approximately 1,145,000 square miles and has an average depth of 1500 m, having extensive areas below 3000 m with maximum depths near 5100 m (Fairbridge, 1966).

3.1 General Oceanography

In this report, the Mediterranean Sea is considered to be a semi-enclosed body of water having a primary access (the Strait of Gibraltar) to an open ocean (the eastern North Atlantic). A unique feature of this body of water is that it extends over eight different basins of which each are divided from the other by sills (Wust, 1961). Excluding the Black Sea, the Mediterranean Sea is described as having the total amount of evaporation greatly exceeding the total amount of precipitation and run off (Sverdrup, Johnson and Fleming, 1942). Extensive heat and salt fluxes occur at the sea

surface having net effects of high evaporation, high surface salinities, increase in surface densities and the sinking of unique surface water parcels. The major inflow (addition) of water into the Mediterranean Basin is received from the surface waters of the eastern North Atlantic. Seasonally unique, in the opinion of the author, the Mediterranean Sea may be described as having five to six oceanographic seasons. Mediterranean Sea observations from various data sets (ocean station and XBT) have neither revealed nor depicted the classical four-season temporal division (winter, spring, summer, fall).

For convenience, this particular section has been divided into two subsections: Water Masses and Other Oceanographic Features.

- Water Masses:

The application of the so-called "core method" reveals a convenient method for the identification of existing water masses in the Mediterranean Sea (Wust, 1961). Basically, this method allows one to follow and trace the mixing processes as well as the spreading of primary water masses along their curved core layers. These curved core layers are generally characterized by intermediate maxima or minima of temperature, salinity, and oxygen. By means of the vertical distribution of temperature, salinity, and oxygen, four different core masses can be identified: 1) the near-surface water of Atlantic origin, 2) the intermediate water (between approximately 200 to 600 meters), 3) the deep water (between approximately 1500 to 3000 meters), and 4) the bottom water (below the deep water and down to the bottom).

At this time, there are three significant points regarding the water masses of the Mediterranean which deserve comment. First, the flow of near-surface North Atlantic water is quite noticeable especially in the western Mediterranean Basin; second, the intermediate water originating from the Levantine Basin plays a significant role in the subsurface distribution and circulation of physical properties over major portions of the eastern and western basins; and third, the sources for the deep and bottom waters of the Mediterranean Sea have several locations of origin.

- Other Oceanographic Features

The Mediterranean Sea has been an excellent theater for the observation of other physical features which are of oceanographic interest. To mention just a few: features such as the formation of banded salt finger structures (Linden, 1978), temperature inversions (Fedorov, 1972), vertical and horizontal flows along subsurface density (σ_t) surfaces over sills (Morel, 1972) have all been observed and reported. These features are discussed further in the appropriate sections (which follow) under Regional description.

3.2 General Meteorology

The atmospheric circulation patterns surrounding the Mediterranean are influenced by the passage or prolonged presence of macro-high and low pressure systems over the continental land masses. These large-scale patterns are considered variable over both the western and eastern basins. However, for the purpose of this report, the meteorology over the Mediterranean Sea region is considered by the author in general to be variable to highly variable from season to season, from basin to basin and influential on both the local and regional oceanography.

Certain regions of the Mediterranean Sea are influenced more by cyclogenesis than others. The locations for cyclogenesis are not confined to one primary region. The range of the intensity of the cyclones which traverse over the Mediterranean waters vary from weak to very intense. The development of cyclones are often found to be very rapid in advancement and growth. These features are discussed further in the appropriate sections (which follow) under Regional Description.

4.0 COMPARISON OF GDEM MONTHLY SEA SURFACE TEMPERATURE (SST) PLOTS FOR THE MEDITERRANEAN SEA

Twelve monthly horizontal contoured plots of sea surface temperatures for the Mediterranean Sea were compared. Monthly horizontal contours of sea surface salinities were not compared in this report.

The monthly sea surface temperature outputs for GDEM, employing the ocean-environmental data sources as described in Section 2.0 of this report, were compared with the monthly sea surface temperature charts from the Atlas of North Atlantic-Indian Ocean Monthly Mean Temperature and Mean Salinities of the Surface Layers (1979) by Robinson, Bauer and Schroeder.* This atlas was constructed from charts which were based on bathythermograph (BT) data obtained from 1941 to 1970, hydrocast data, means extracted from published charts, and unpublished tabulations of means. The charts from the atlas were produced from plots of 1° quadrangle temperature means.

Basic differences existed between the GDEM and the atlas data bases regarding the use of the most recent available data set(s). The atlas was based upon the bathythermograph data set of 1970 and on hydrocast data. The GDEM data base was based upon the 1980 MOODS and NOO oceanographic data sets of BT's, hydrocasts, STD's, MBT's, and XBT's. The spatial resolutions employed by the atlas and by GDEM were also different. The analysis of the atlas was based on 1° quadrangles and the GDEM analysis employed by 30' by 30' grid resolution.

4.1 Monthly SST Comparison

- January

Comparisons of January Sea surface temperature contour plots are shown on Figures 4-1 and 4-2. The GDEM-atlas SST

*Note: Hereinafter, all reference to the "Atlas of the North Atlantic-Indian Ocean Monthly Mean Temperature and Mean Salinities of the Surface Layers" (1979) will be referred to as the atlas.

comparisons exhibited realistic orientation of the sea surface isotherms. The GDEM and atlas SST plots were similar. Similarities were reflected in both analyses for the Alboran Sea in the 16.0°C isotherm; for the Balearic Sea in the 13.0°C, 14.0°C, and 15.0°C isotherms; for the Tyrrhenian Sea in the 14.0°C and 15.0°C isotherms; for the Ionian Sea in the 15.0°C, 16.0°C and 17.0°C isotherms; and for the Levantine Sea in the 17.0°C and 18.0°C isotherms.

- February

Comparisons of February sea surface temperature contour plots are shown on Figures 4-3 and 4-4. The GDEM-atlas SST comparisons exhibited realistic orientation of the sea surface isotherms. The GDEM and atlas SST plots were similar. Similarities were reflected in both analyses for the Alboran Sea in the 15.0°C isotherm; for the Balearic Sea in the 13.0°C and 14.0°C isotherms; for the Tyrrhenian Sea in the 14.0°C isotherm; for the Ionian Sea in the 15.0°C and 16.0°C isotherms; and for the Levantine Sea in the 16.0°C, 17.0°C, and 18.0°C isotherms. GDEM reflects the presence of a warm region ($>17.0^{\circ}\text{C}$) off the coast of Libya. This warm region ($>17.0^{\circ}\text{C}$ off the coast of Libya) is not evident in the atlas data.

- March

Comparisons of March sea surface temperature contour plots are shown on Figures 4-5 and 4-6. The GDEM-atlas SST comparisons exhibited realistic orientation of the sea surface isotherms. The GDEM and atlas SST plots were similar. Similarities were reflected in both analyses for the Alboran Sea in the general proximity of the 15.0°C isotherm; for the Ionian Sea in the 15.0°C and 17.0°C isotherms; and for the Levantine Sea in the 16.0°C and 17.0°C isotherms.

- April

Comparisons of April sea surface temperature contour plots are shown on Figures 4-7 and 4-8. The GDEM-atlas SST comparisons were similar and exhibited realistic orientation of the sea surface isotherms. In most regions, the GDEM and atlas SST plots were equivalent with slight dissimilarities. In the Alboran Sea, the atlas had higher values in temperature (atlas: 16.0°C to 17.0°C in lieu of GDEM 15.0°C to 16.0°C) by 1.0°C; the Balearic Sea was similar with slight dissimilarities in the southern displacement of the 14.0°C and 15.0°C isotherms; the Tyrrhenian Sea was similar; the Ionian Sea was similar in the 16.0°C, 16.5°C and 17.0°C isotherms; and the Levantine Sea was similar in the 17.0°C and 18.0°C isotherms.

- May

Comparisons of May sea surface temperature contoured plots are shown on Figures 4-9 and 4-10. The GDEM-atlas SST comparisons exhibited realistic orientation of the sea surface isotherms. The GDEM atlas SST plots were similar. Similarities were reflected in both analyses for the Alboran Sea in the 18.0°C isotherm; for the Balearic Sea in the 16.0°C, 17.0°C and 18.0°C isotherms; for the Tyrrhenian Sea in the 17.0°C and 18.0°C isotherms; for the Ionian Sea in the 18.0°C, 19.0°C and 20.0°C isotherms; and for the Levantine Sea in the 19.0°C, 20.0°C and 21.0°C isotherms.

- June

Comparisons of June sea surface temperature contoured plots are shown on Figure 4-11 and 4-12. The GDEM-atlas SST comparisons exhibited realistic orientation of the sea surface isotherms. The GDEM-atlas SST plots were similar. Similarities were reflected in both analyses for the Alboran Sea in the 19.0°C and 20.0°C isotherms; for the Balearic Sea in the 18.0°C, 19.0°C, 20.0°C, and 21.0°C isotherms; for the Tyrrhenian Sea in the 21.0°C and 22.0°C isotherms; for the Ionian Sea in the 21.0°C, 22.0°C, and 23.0°C isotherms; and for the Levantine Sea in the 22.0°C, 23.0°C, and 24.0°C isotherms.

- July

Comparisons of July sea surface temperature contoured plots are shown on Figures 4-13 and 4-14. The GDEM-atlas SST comparisons exhibited realistic orientation of the sea surface isotherms. The GDEM-atlas SST plots were similar. Similarities were reflected in both analyses for the Alboran Sea in the 22.0°C and 23.0°C isotherms; for the Balearic Sea in the 21.0°C, 22.0°C, 23.0°C and 24.0°C isotherms; for the Tyrrhenian Sea in the 24.0°C and 25.0°C isotherms; for the Ionian Sea in the 24.0°C and 24.5°C isotherms; and for the Levantine Sea in the 24.0°C, 25.0°C, 26.0°C and 27.0°C isotherms.

- August

Comparisons of August sea surface temperature contoured plots are shown on Figures 4-15 and 4-16. The GDEM-atlas SST comparisons exhibited realistic orientation of the sea surface isotherms. The GDEM-atlas SST plots were similar. Similarities were reflected in both analyses for the Alboran Sea in the

22.0°C, 23.0°C and 24.0°C isotherms; for the Balearic Sea in the 22.0°C, 23.0°C, 24.0°C, 25.0°C, and 26.0°C isotherms; for the Tyrrhenian Sea in the 25.0°C and 26.0°C isotherms; and for the Levantine Sea in the 25.0°C, 27.0°C and 28.0°C isotherms.

- September

Comparisons of September sea surface temperature contoured plots are shown on Figures 4-17 and 4-18. The GDEM-atlas SST comparisons exhibited realistic orientation of the sea surface isotherms. The GDEM-atlas SST plots were similar. Similarities were reflected in both analyses for the Alboran Sea in the 22.0°C and 23.0°C isotherms; for the Balearic Sea in the 21.0°C, 22.0°C, 23.0°C and 24.0°C isotherms; for the Tyrrhenian Sea in the 23.0°C, 24.0°C and 25.0°C isotherms; for the Ionian Sea in the 25.0°C and 26.0°C isotherms; and for the Levantine Sea in the 24.0°C, 25.0°C, 26.0°C and 27.0°C isotherms.

- October

Comparisons of October sea surface temperature contoured plots are shown on Figures 4-19 and 4-20. The GDEM-atlas SST comparisons exhibited realistic orientation of the sea surface isotherms. The GDEM-atlas SST plots were similar. Similarities were reflected in both analyses for the Alboran Sea in the 20.0°C and 21.0°C isotherms; for the Balearic Sea in the 18.0°C, 19.0°C, 20.0°C, 21.0°C and 22.0°C isotherms; for the Ionian Sea in the 23.0°C and 24.0°C isotherms; and for the Levantine Sea in the 22.0°C, 23.0°C, 24.0°C, 25.0°C and 26.0°C isotherms.

- November

Comparisons of October sea surface temperature contoured plots are shown on Figures 4-21 and 4-22. The GDEM-atlas SST comparisons exhibited realistic orientation of the sea surface isotherms. The GDEM-atlas SST plots were similar. Similarities were reflected in both analyses for the Alboran Sea in the 18.0°C isotherms; for the Balearic Sea in the 16.0°C, 17.0°C, 18.0°C, and 19.0°C isotherms; for the Tyrrhenian Sea in the 18.0°C isotherm; for the Ionian Sea in the 20.0°C and 21.0°C isotherms; and for the Levantine Sea in the 20.0°C, 21.0°C, 22.0°C and 23.0°C isotherms.

- December

Comparisons of December sea surface temperature contoured plots are shown on Figures 4-23 and 4-24. The GDEM-atlas SST

comparisons exhibited realistic orientation of the sea surface isotherms (with a few differences). Similarities were reflected in both analyses for the western Mediterranean basins. A few similarities were found in the eastern Mediterranean basins. Similarities in both the western and eastern basins were for the Alboran Sea in the 16.0°C isotherm; for the Balearic Sea in the 15.0°C and 16.0°C isotherms; for the Tyrrhenian Sea in the 16.0°C and 17.0°C isotherms; for the Ionian Sea in the 17.0°C and 18.0°C isotherms; and for the Levantine Sea in the 20.0°C isotherm. Dissimilarities were reflected in the Ionian Sea in the presence of an extensive, well-defined GDEM region of $\geq 19.0^{\circ}\text{C}$ located in the southern portion of this basin. The atlas does not reflect either a 19.0°C isotherm or a region of maximum temperature of $\geq 18.5^{\circ}\text{C}$. Dissimilarities were also reflected in the Levantine Basin not in the orientation (directionality) but in the proximities of the 18.0°C and 19.0°C isotherms. The locations of the GDEM 18.0°C and 19.0°C isotherms were displaced farther southward from those of the atlas, as seen on December contoured SST plots. These dissimilarities, however, are not considered as major differences but as differences related to data density and distribution resulting largely from GDEM's use of a more recent and extensive data base.

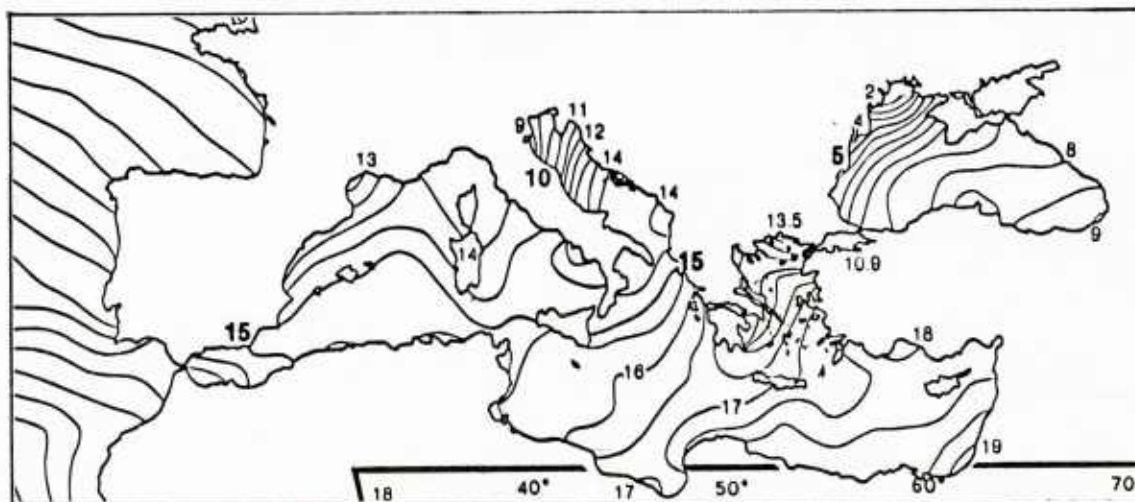


FIGURE 4-1: ATLAS - JANUARY SEA SURFACE TEMPERATURE (SST)
FOR THE MEDITERRANEAN SEA

(Note: Contoured in half-degree centigrade units)

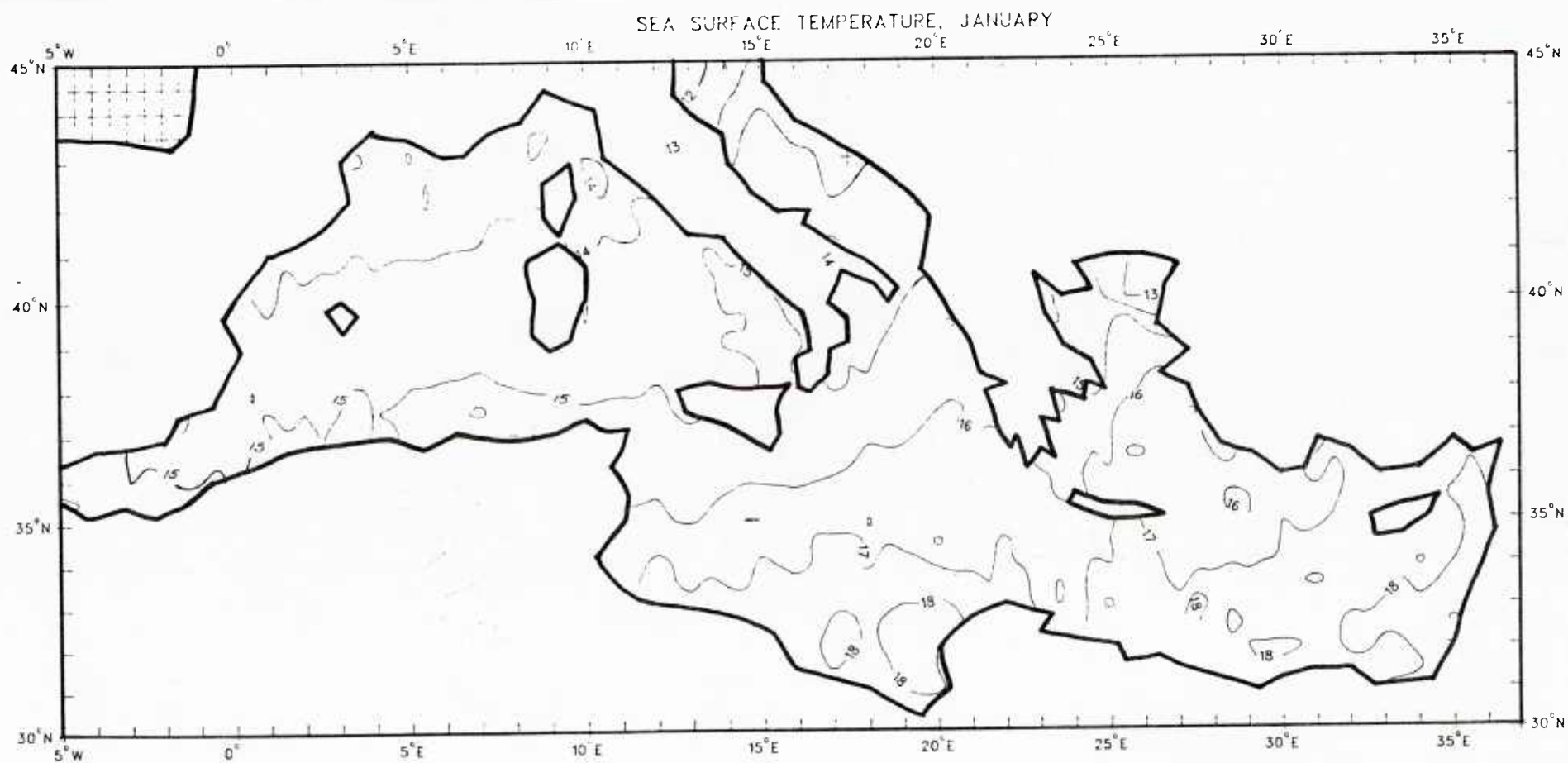


FIGURE 4-2: GDEM - JANUARY SEA SURFACE TEMPERATURE (SST) FOR THE MEDITERRANEAN SEA

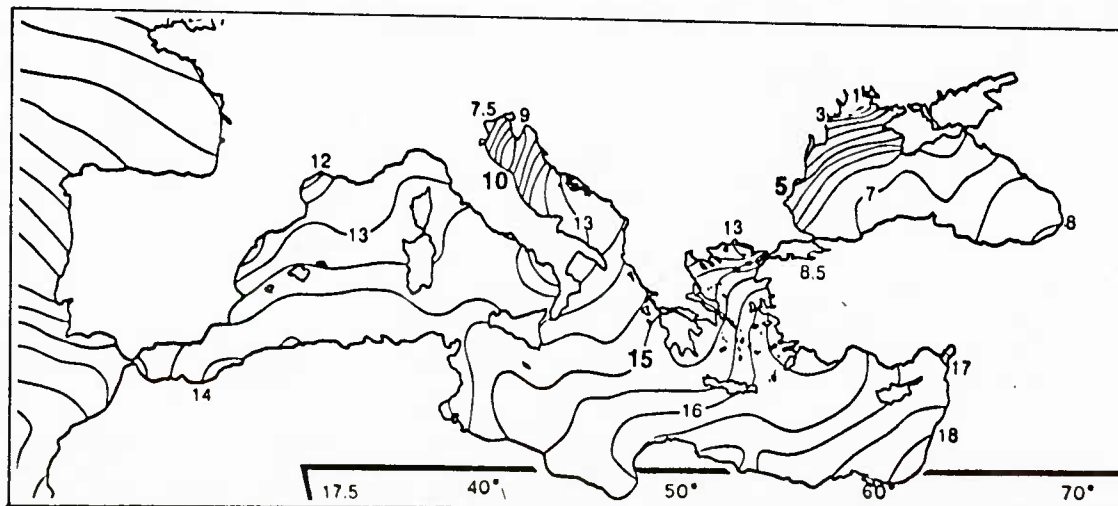


FIGURE 4-3: ATLAS - FEBRUARY SEA SURFACE TEMPERATURE (SST)
FOR THE MEDITERRANEAN SEA

(Note: Contoured in half-degree centigrade units)

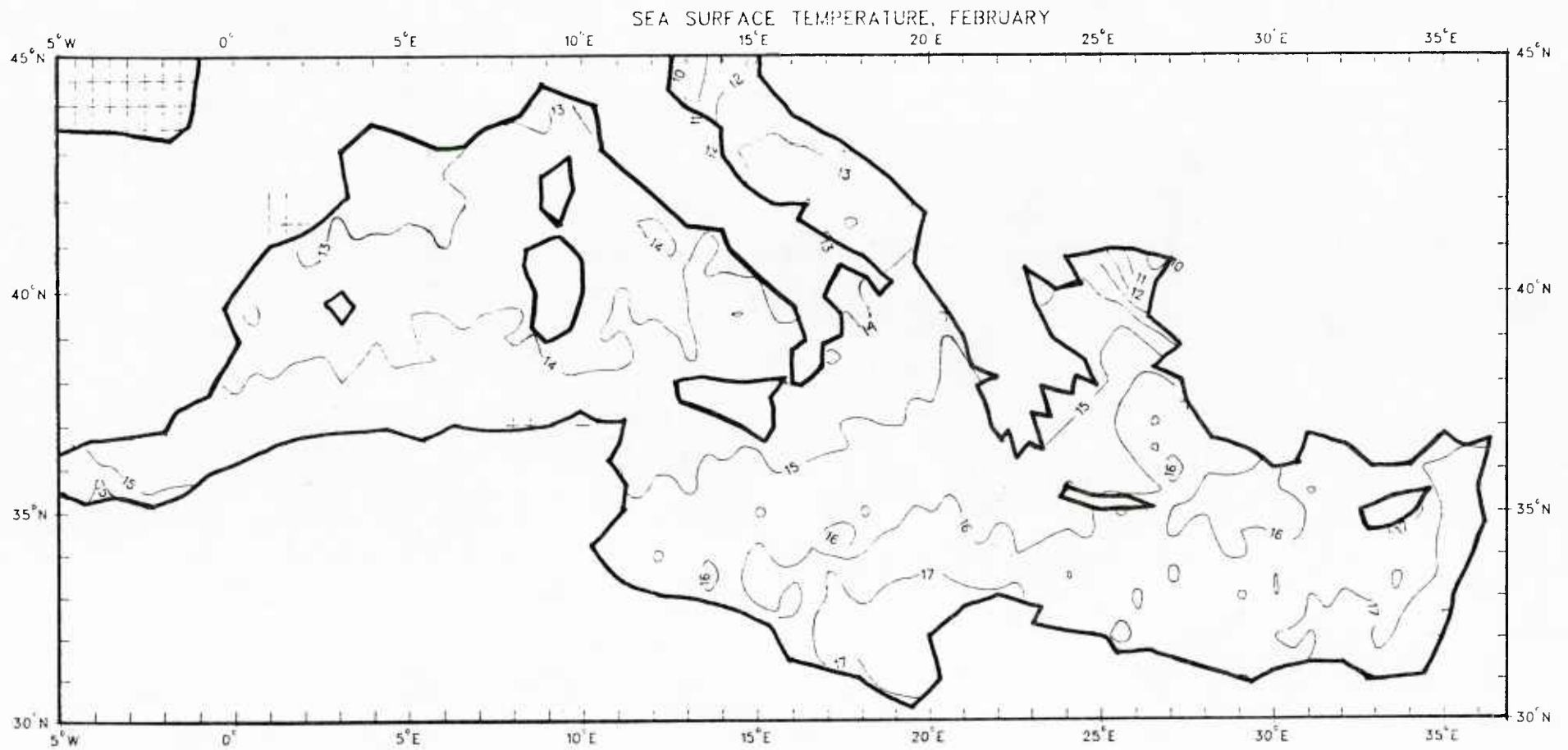


FIGURE 4-4: GDEM - FEBRUARY SEA SURFACE TEMPERATURE (SST) FOR THE MEDITERRANEAN SEA

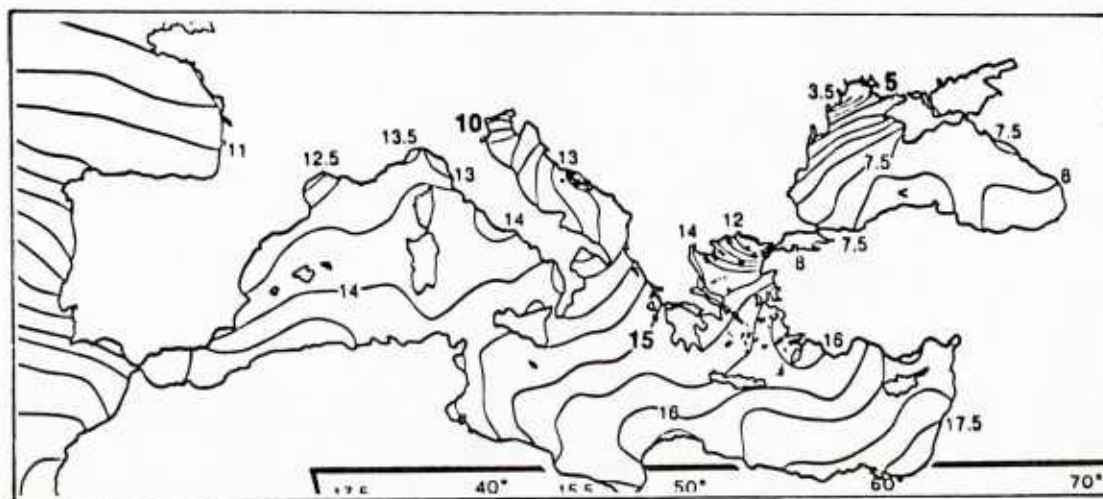


FIGURE 4-5: ATLAS - MARCH SEA SURFACE TEMPERATURE (SST)
FOR THE MEDITERRANEAN SEA

(Note: Contoured in half-degree centigrade units)

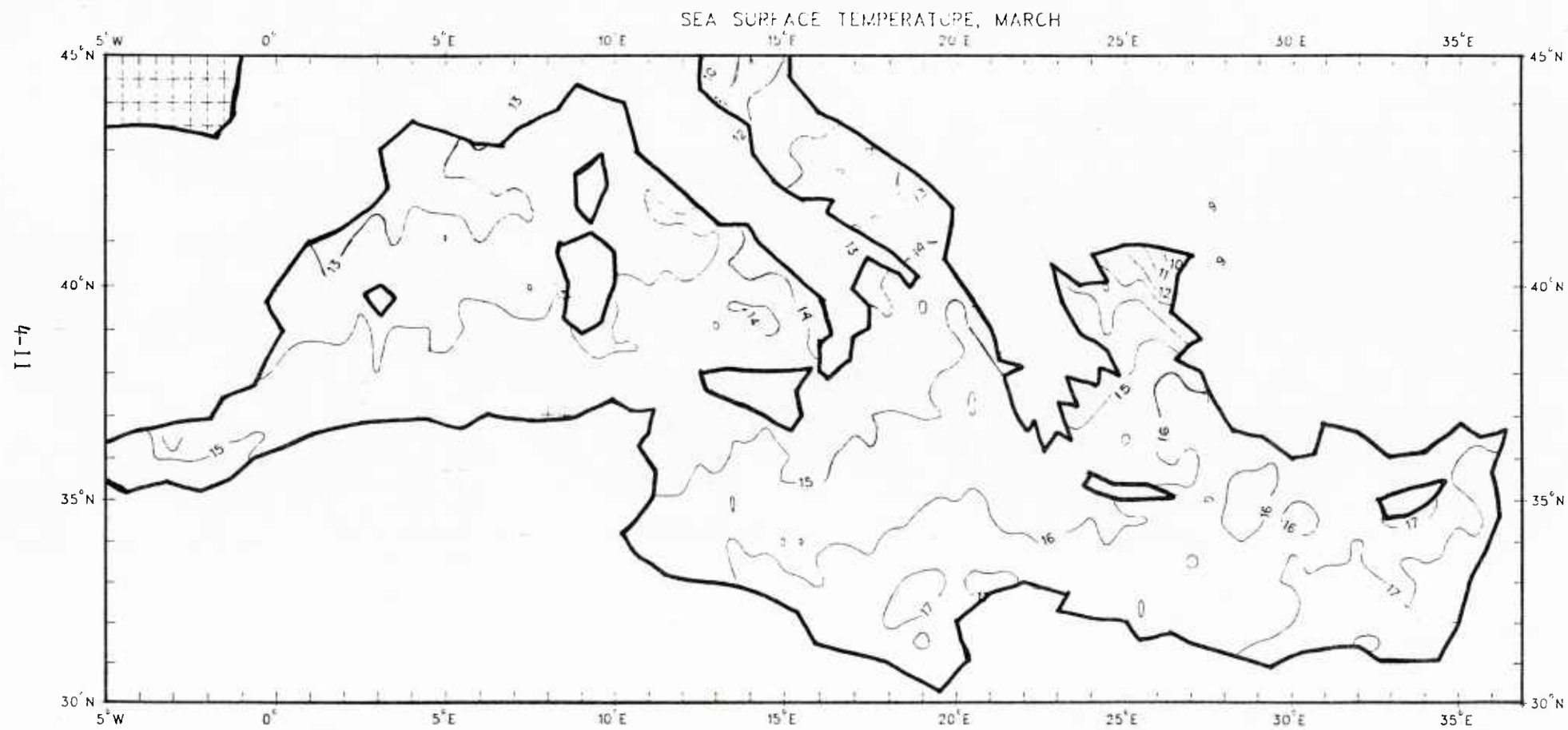


FIGURE 4-6: GDEM - MARCH SEA SURFACE TEMPERATURE (SST) FOR THE MEDITERRANEAN SEA

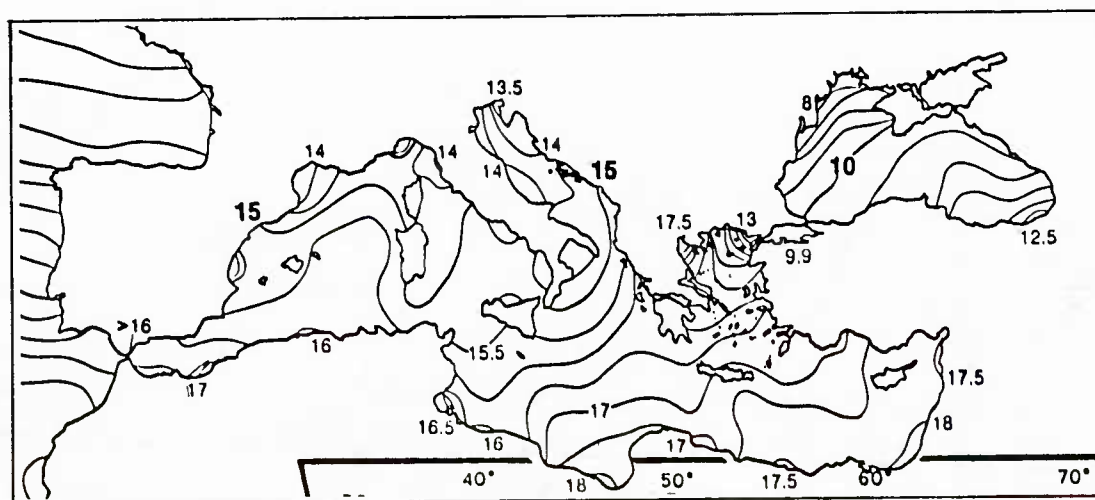


FIGURE 4-7: ATLAS - APRIL SEA SURFACE TEMPERATURE (SST)
FOR THE MEDITERRANEAN SEA

(Note: Contoured in half-degree centigrade units)

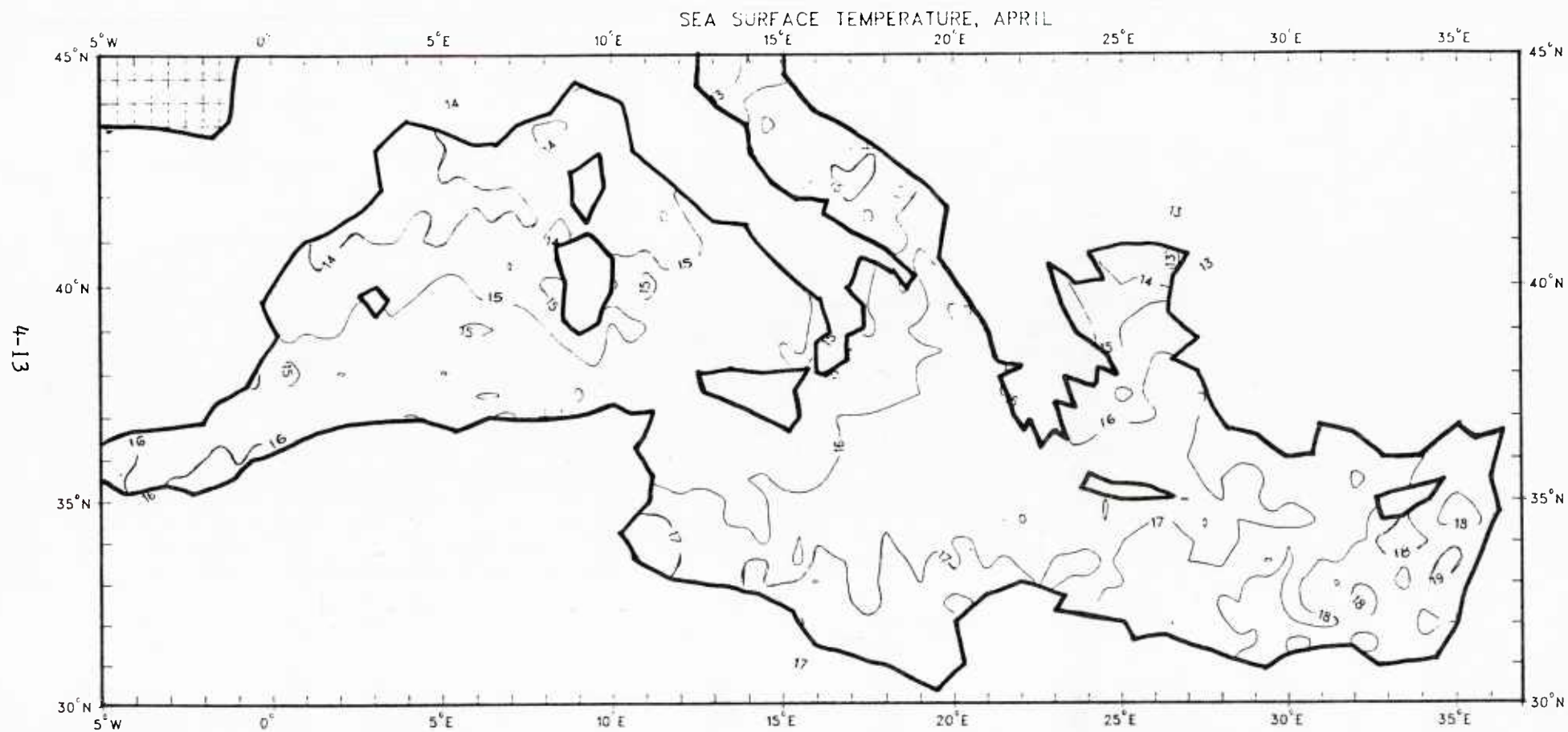


FIGURE 4-8: GDEM - APRIL SEA SURFACE TEMPERATURE (SST) FOR THE MEDITERRANEAN SEA

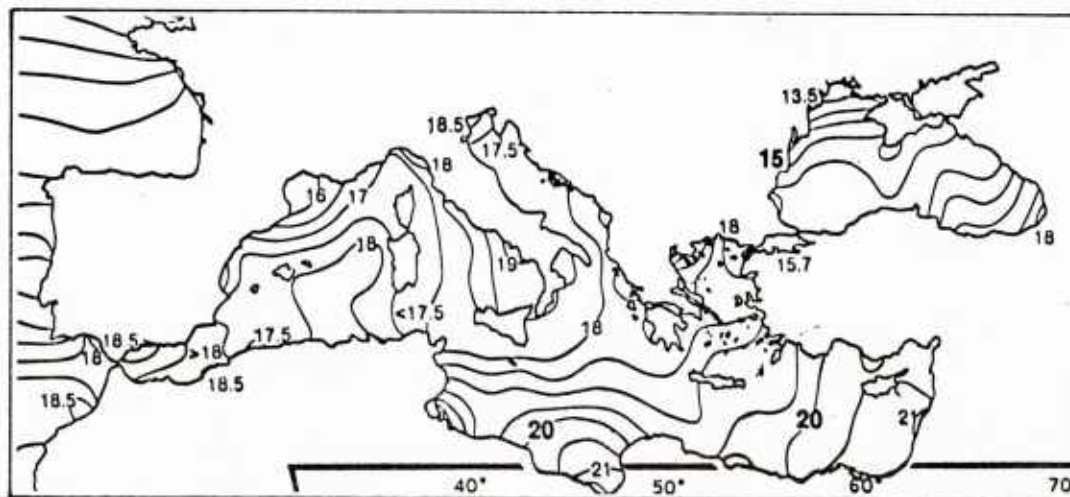


FIGURE 4-9: ATLAS - MAY SEA SURFACE TEMPERATURE (SST)
FOR THE MEDITERRANEAN SEA

(Note: Contoured in half-degree centigrade units)

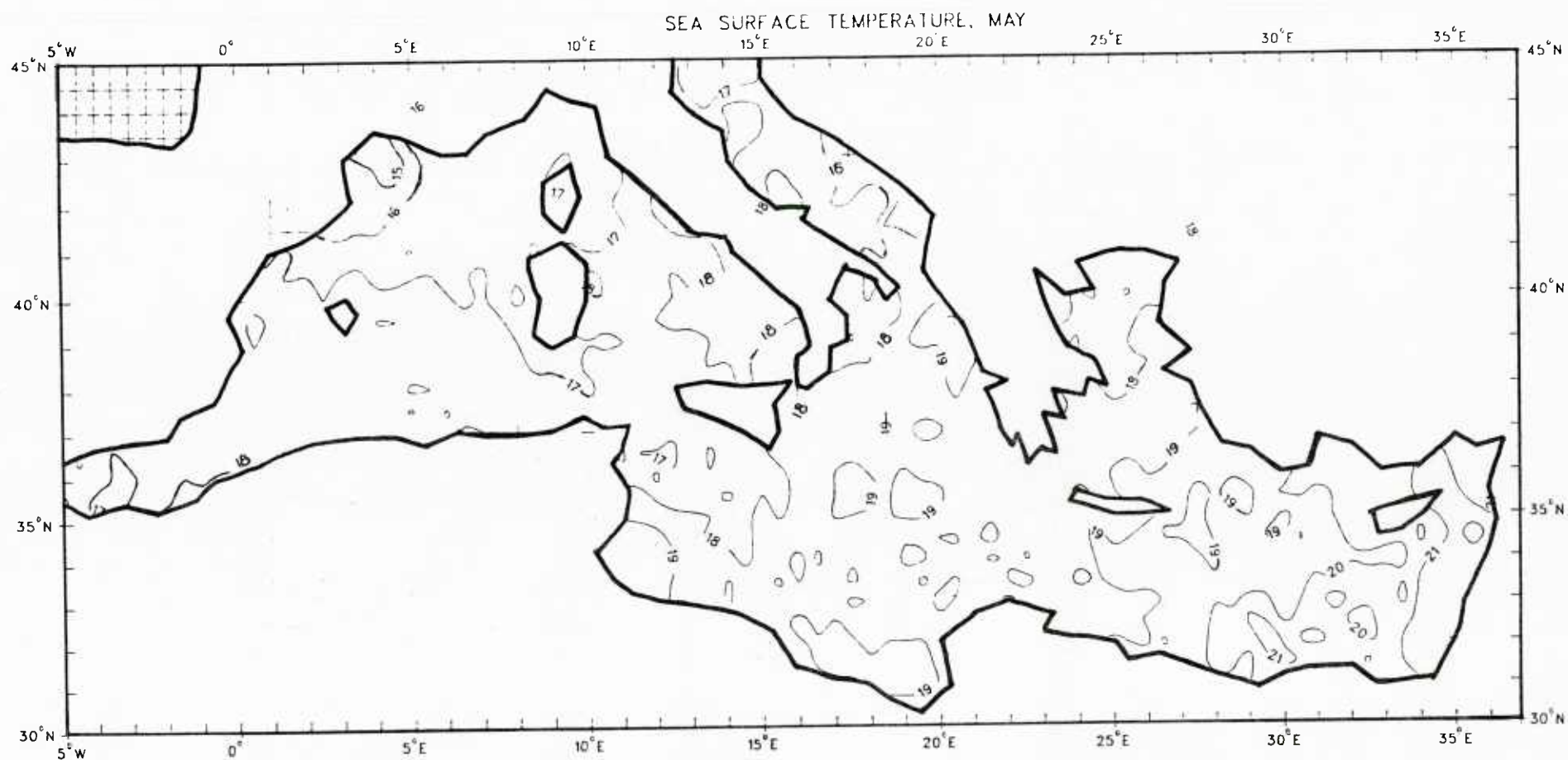


FIGURE 4-10: GDEM - MAY SEA SURFACE TEMPERATURE (SST) FOR THE MEDITERRANEAN SEA

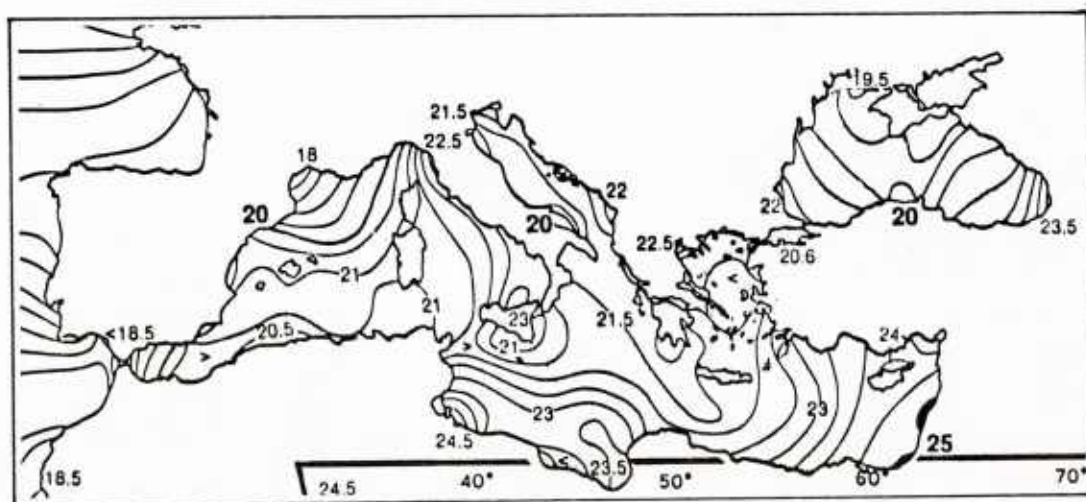


FIGURE 4-11: ATLAS - JUNE SEA SURFACE TEMPERATURE (SST)
FOR THE MEDITERRANEAN SEA

(Note: Contoured in half-degree centigrade units)

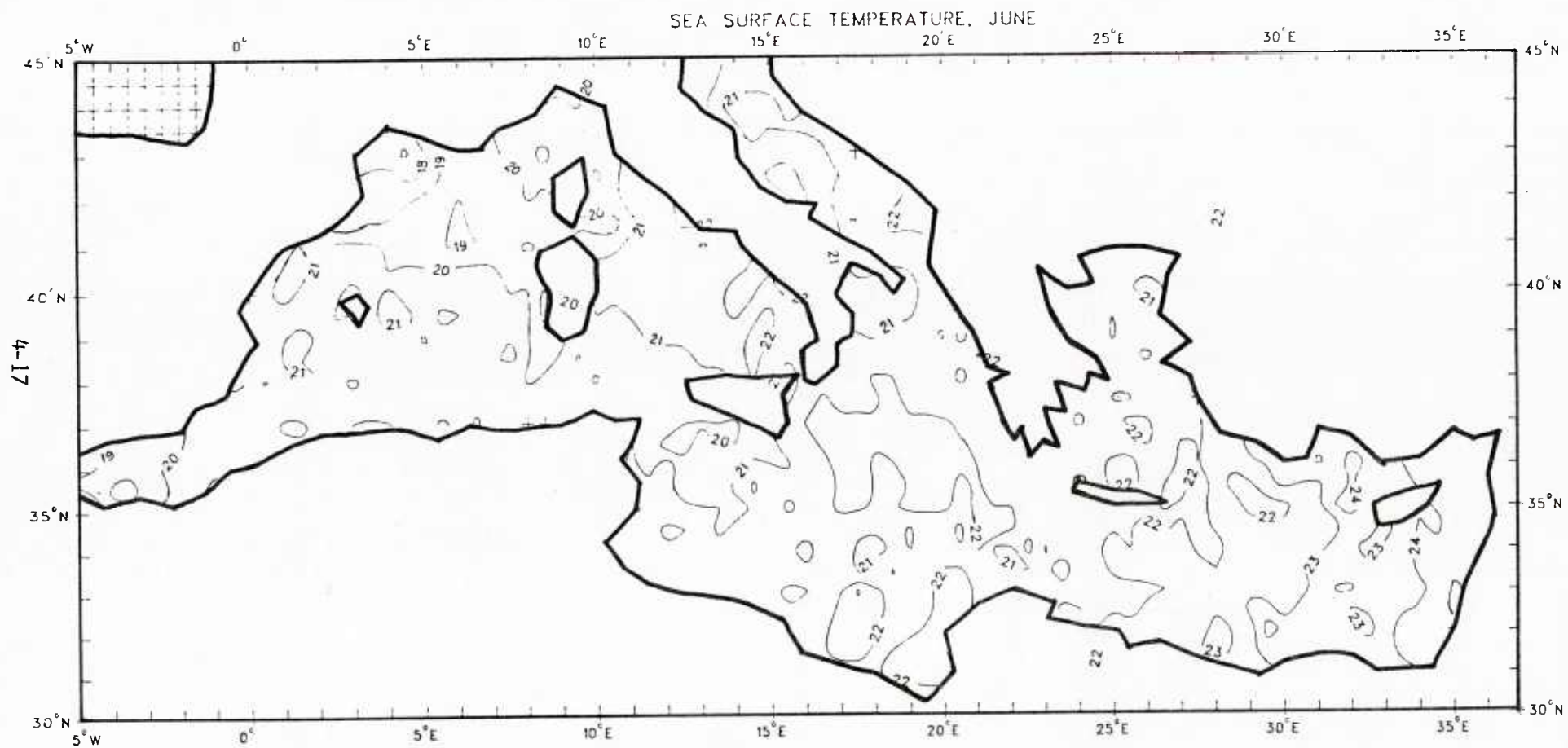


FIGURE 4-12: GDEM - JUNE SEA SURFACE TEMPERATURE (SST) FOR THE MEDITERRANEAN SEA

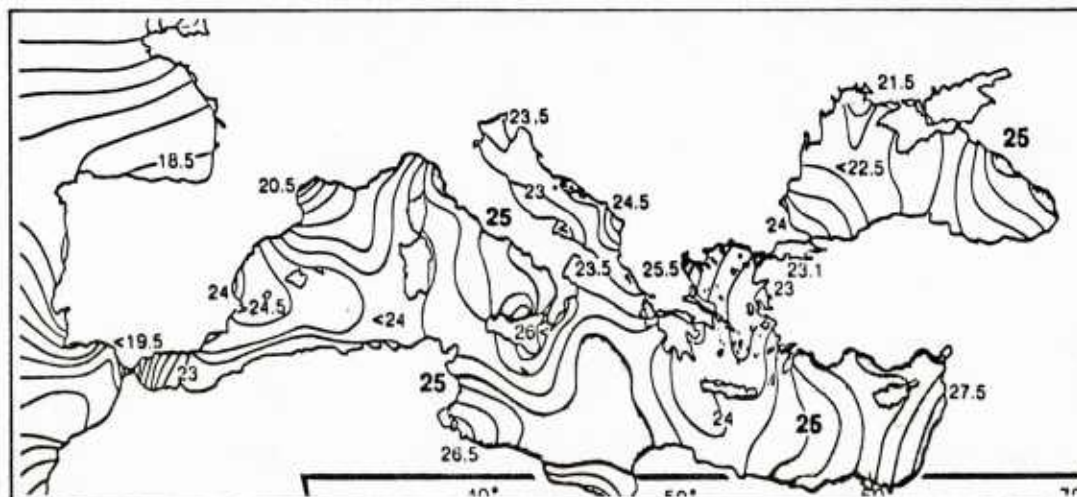


FIGURE 4-13: ATLAS - JULY SEA SURFACE TEMPERATURE (SST)
FOR THE MEDITERRANEAN SEA

(Note: Contoured in half-degree centigrade units)

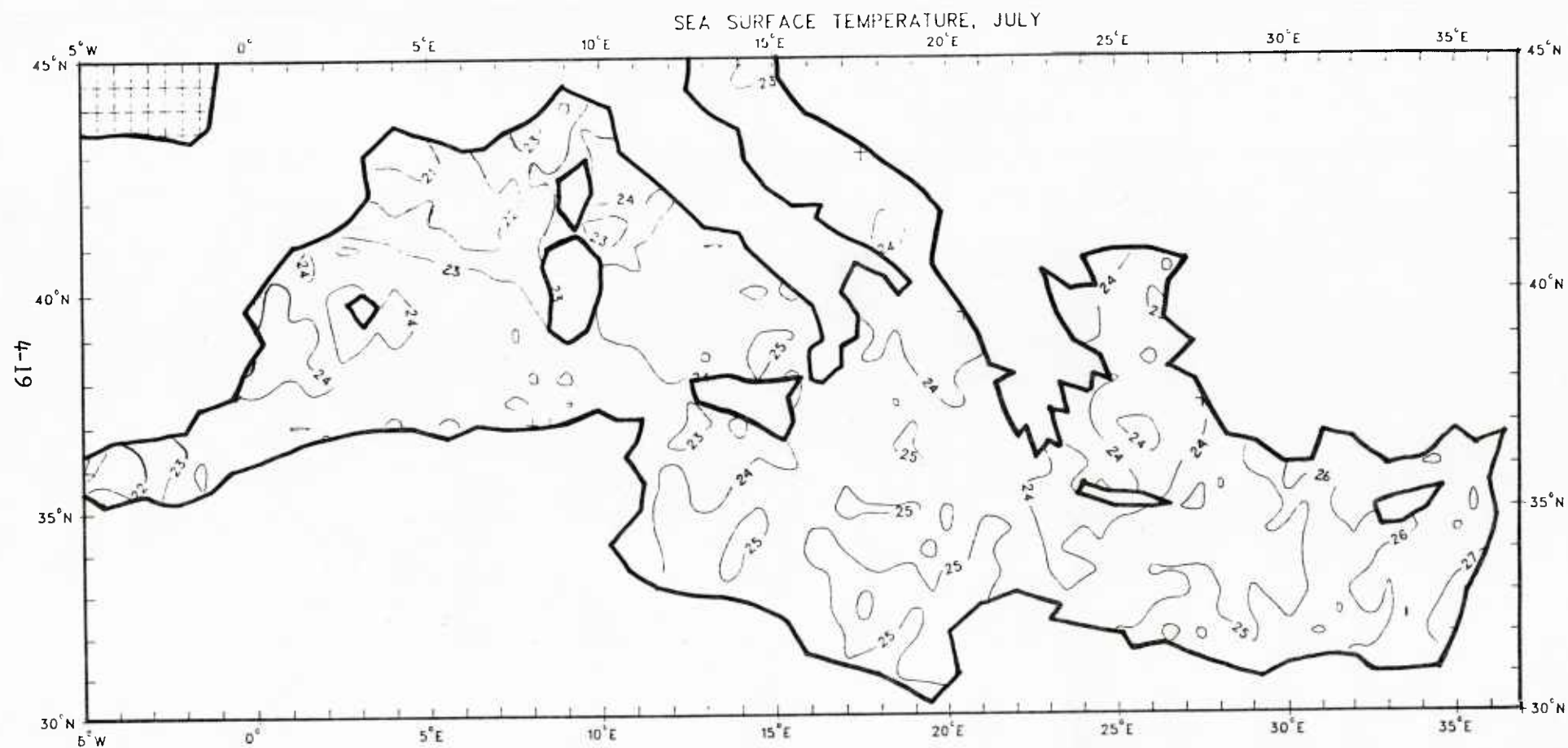


FIGURE 4-14: GDEM - JULY SEA SURFACE TEMPERATURE (SST) FOR THE MEDITERRANEAN SEA

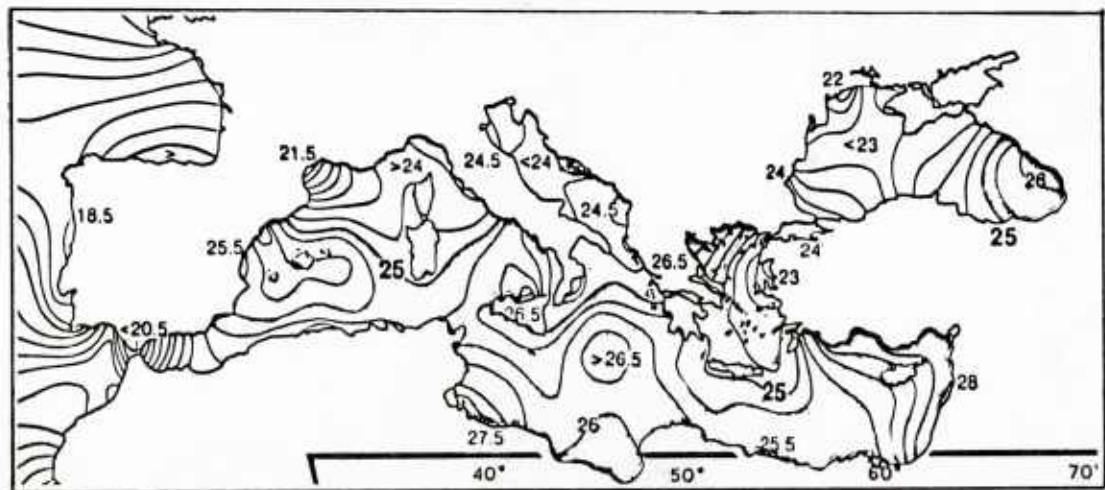


FIGURE 4-15: ATLAS - AUGUST SEA SURFACE TEMPERATURE (SST)
FOR THE MEDITERRANEAN SEA

(Note: Contoured in half-degree centigrade units)

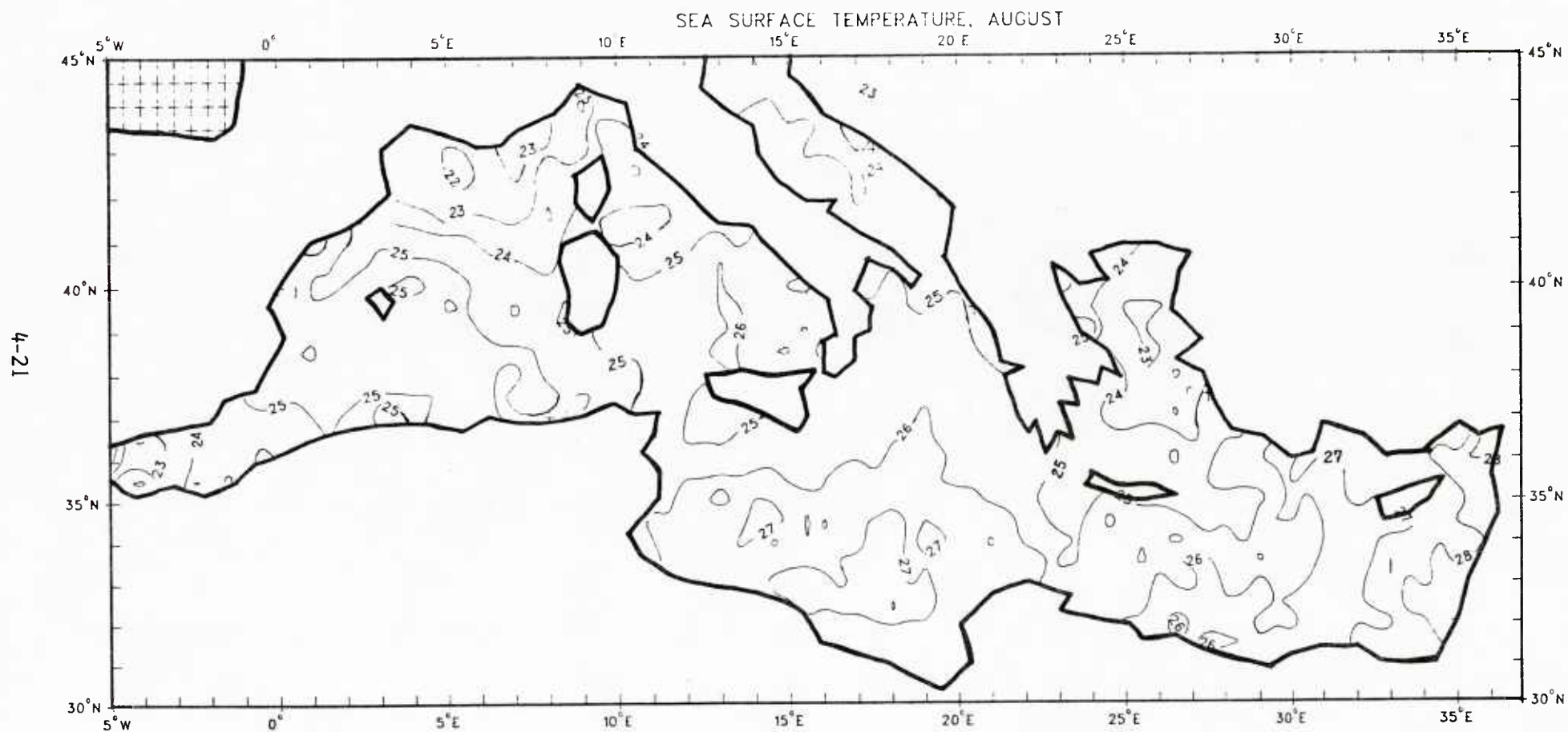


FIGURE 4-16: GDEM - AUGUST SEA SURFACE TEMPERATURE (SST) FOR THE MEDITERRANEAN SEA

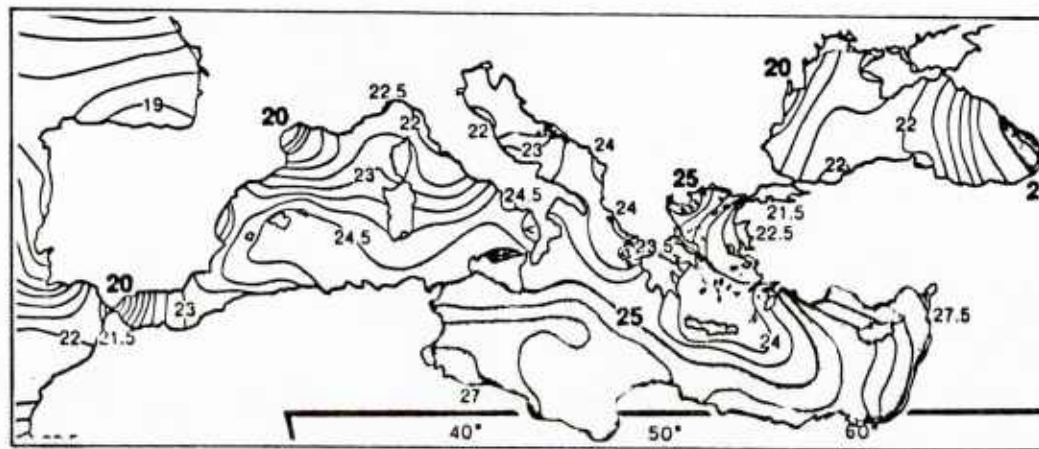


FIGURE 4-17: ATLAS - SEPTEMBER SEA SURFACE TEMPERATURE (SST)
FOR THE MEDITERRANEAN SEA

(Note: Contoured in half-degree centigrade units)

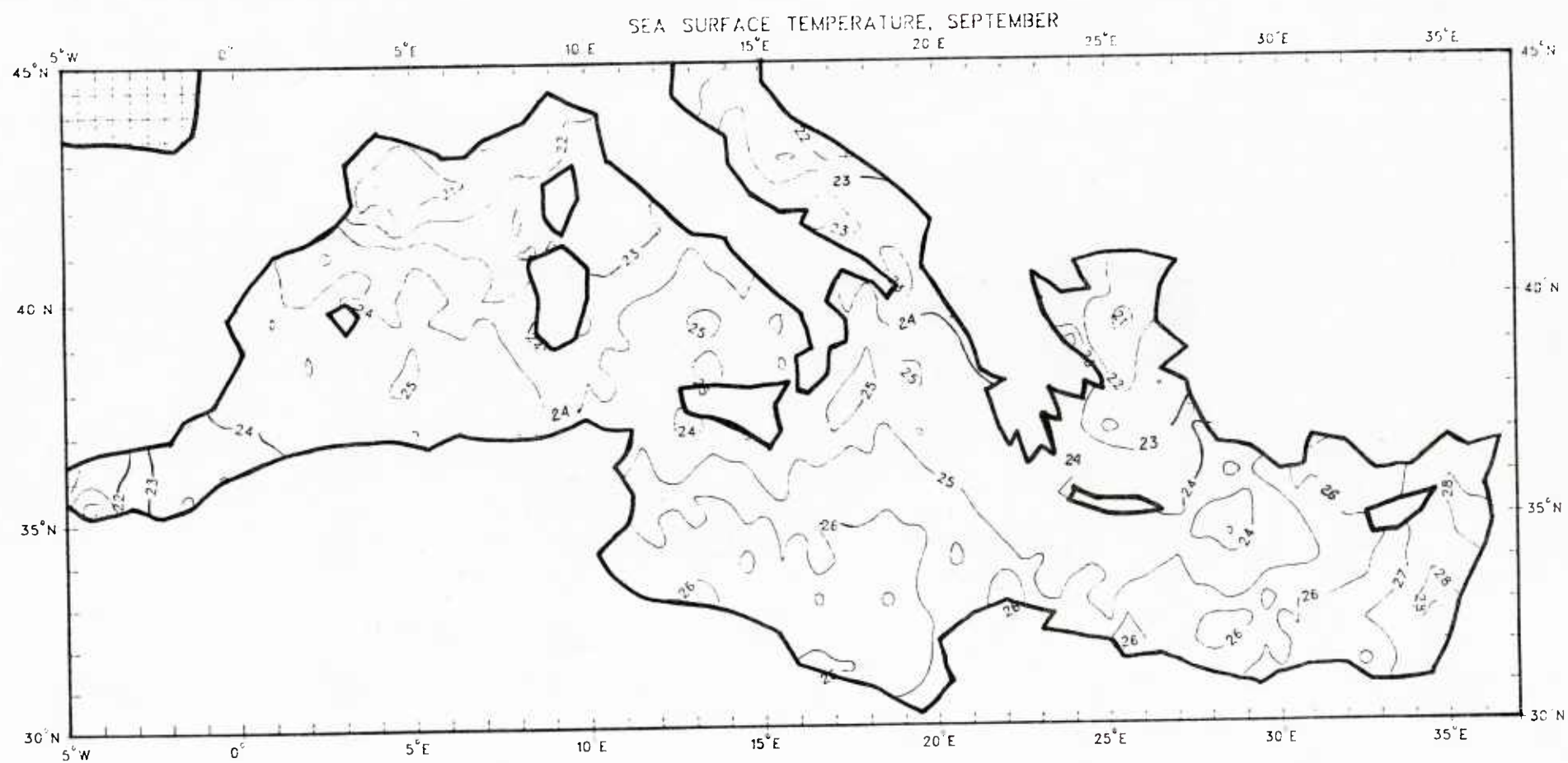


FIGURE 4-18: GDEM - SEPTEMBER SEA SURFACE TEMPERATURE (SST) FOR THE MEDITERRANEAN SEA

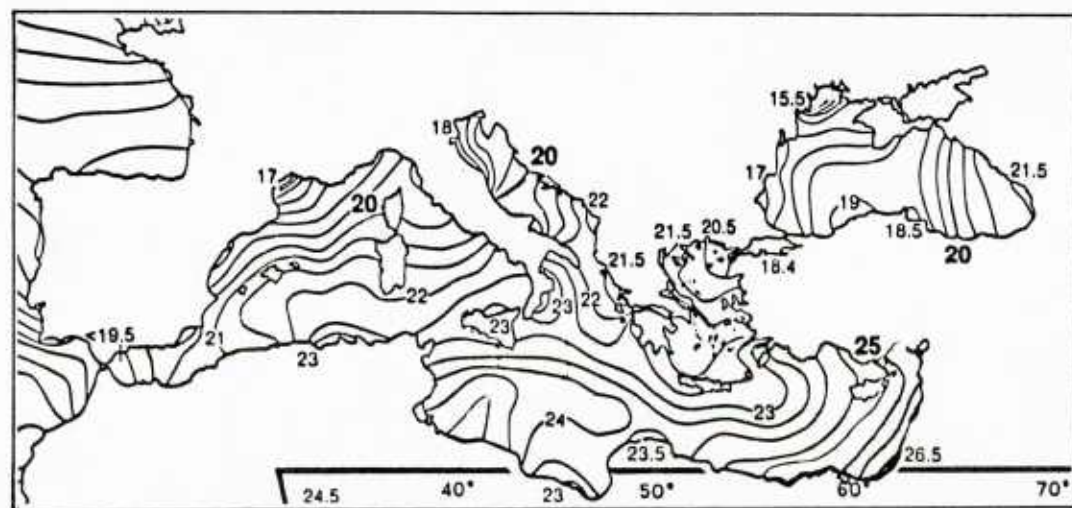


FIGURE 4-19: ATLAS - OCTOBER SEA SURFACE TEMPERATURE (SST)
FOR THE MEDITERRANEAN SEA

(Note: Contoured in half-degree centigrade units)

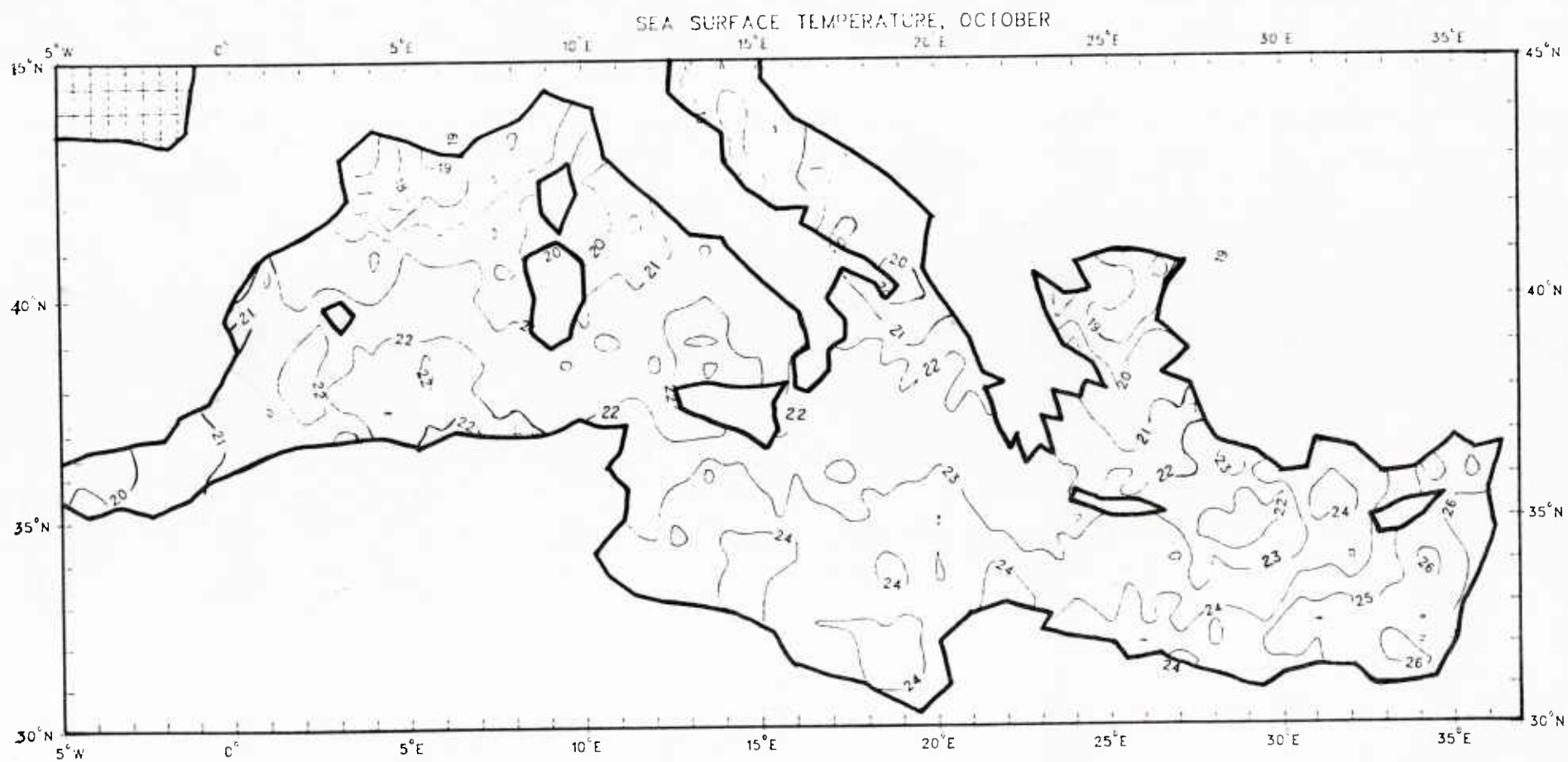


FIGURE 4-20: GDEM - OCTOBER SEA SURFACE TEMPERATURE (SST) FOR THE MEDITERRANEAN SEA

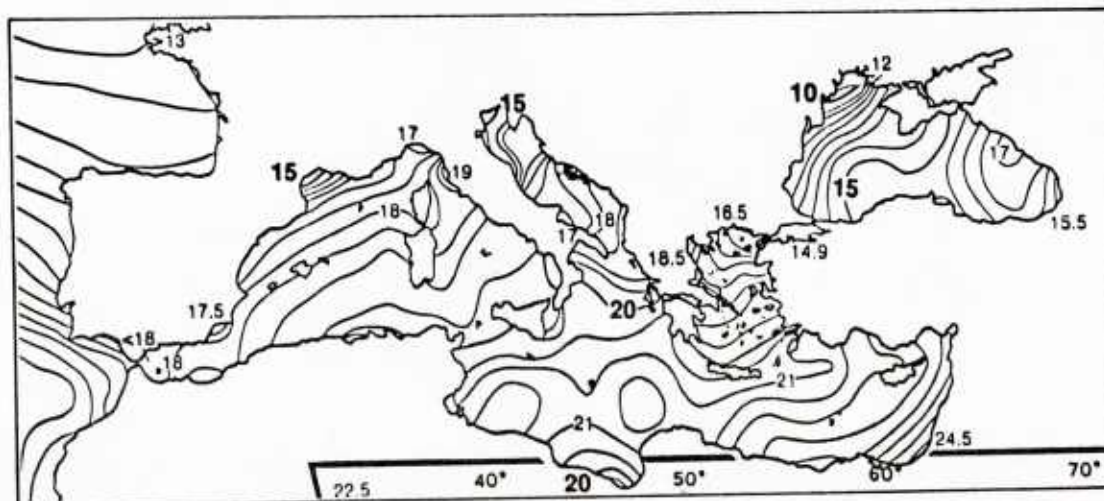


FIGURE 4-21: ATLAS - NOVEMBER SEA SURFACE TEMPERATURE (SST)
FOR THE MEDITERRANEAN SEA

(Note: Contoured in half-degree centigrade units)

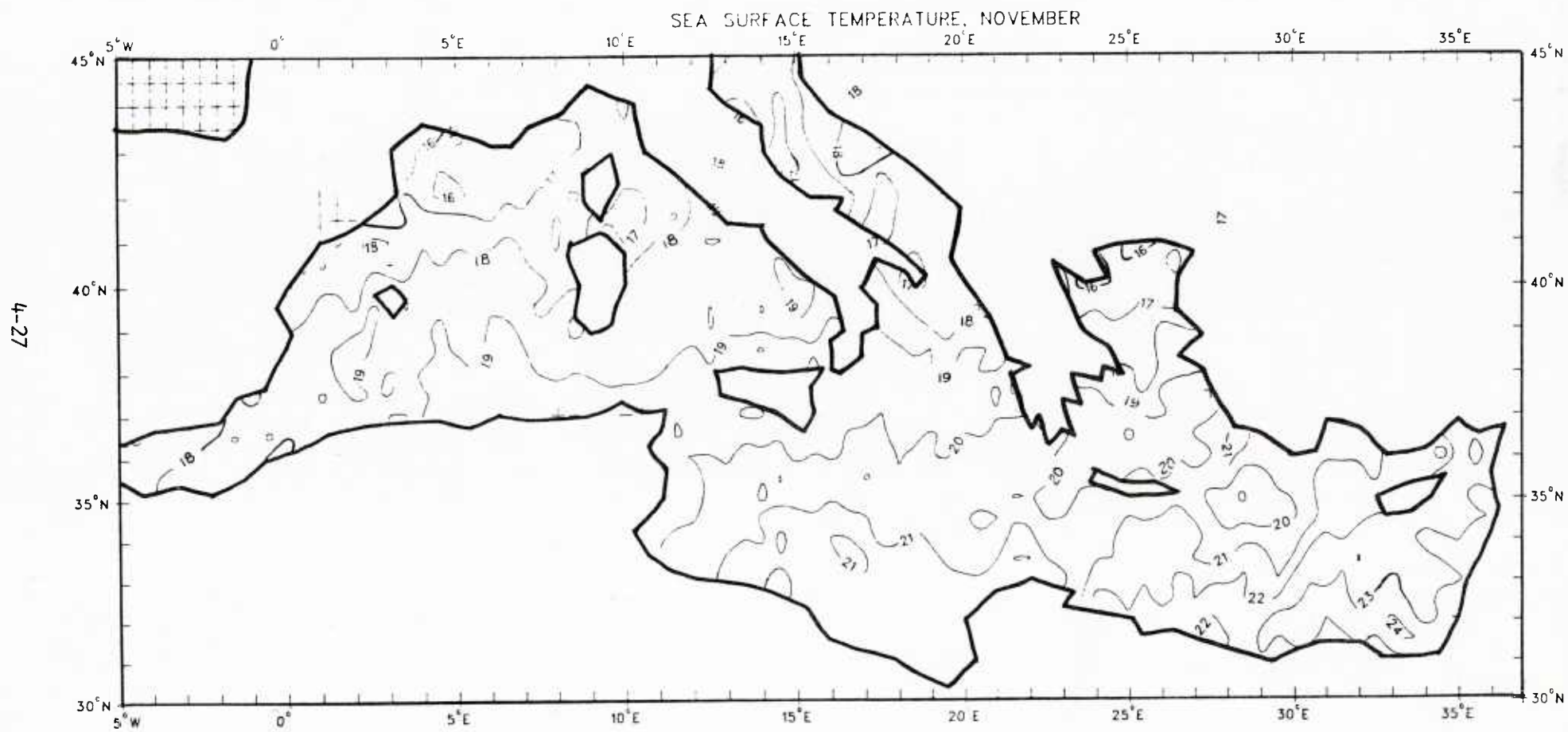


FIGURE 4-22: GDEM - NOVEMBER SEA SURFACE TEMPERATURE (SST) FOR THE MEDITERRANEAN SEA

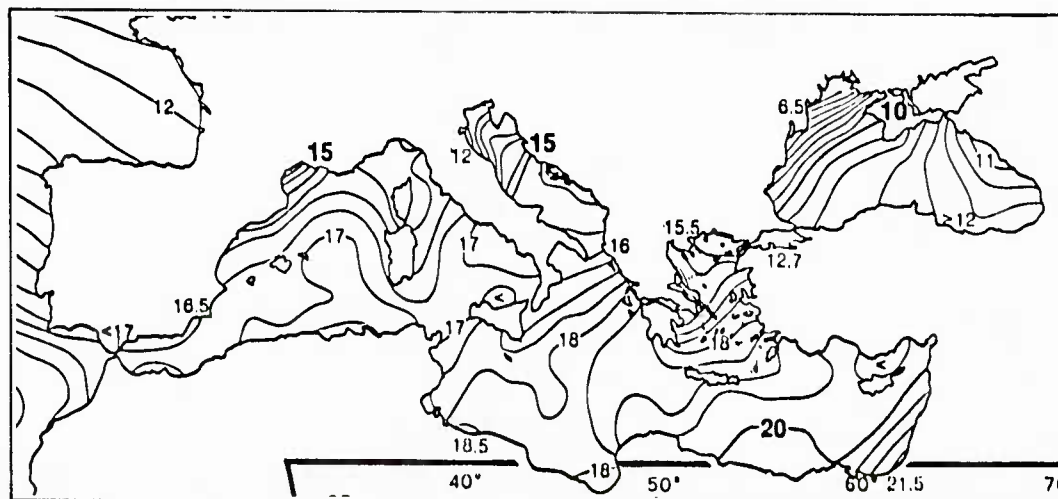


FIGURE 4-23: ATLAS - DECEMBER SEA SURFACE TEMPERATURE (SST)
FOR THE MEDITERRANEAN SEA

(Note: Contoured in half-degree centigrade units)

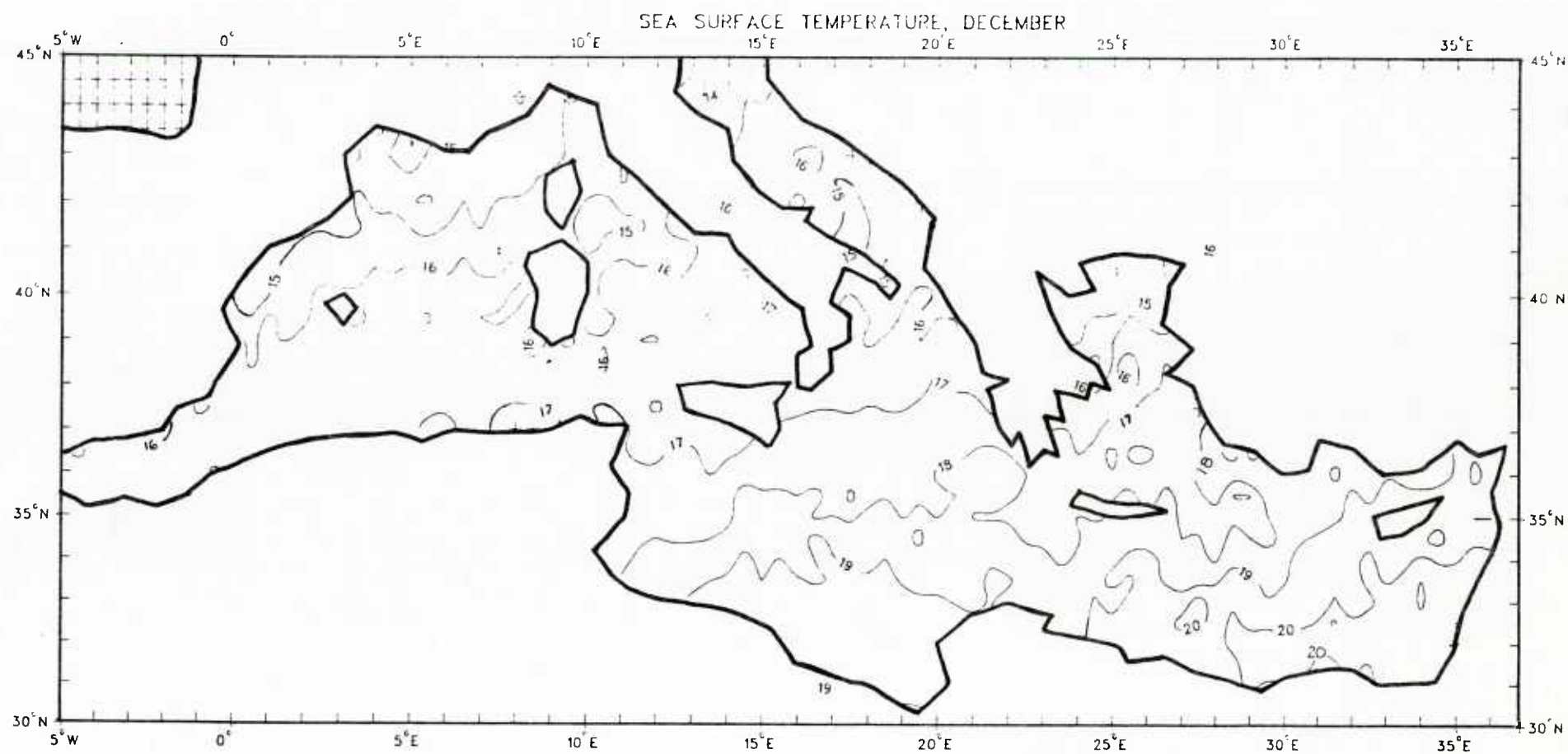


FIGURE 4-24: GDEM - DECEMBER SEA SURFACE TEMPERATURE (SST) FOR THE MEDITERRANEAN SEA

5.0 VERTICAL CROSS SECTIONAL COMPARISONS OF TEMPERATURE AND/OR SALINITY ALONG GREAT CIRCLE TRACKS

Vertical cross-sections of temperature and/or salinity along great circle tracks (Figure 1-1) were compared. Comparisons were made on surveyed/analyzed data found in present literature.

The vertical cross sectional temperature and/or salinity outputs for GDEM, employing the ocean-environmental data sources as described in Section 1.0 of this report, were compared with analyzed vertical cross-sections from Cheney (1977); Miller, Tschernia and Charnock (1970); Morel (1972); Katz (1972) Wust (1961); MEDOC Group (1970); and other sources cited in the text.

5.1 Vertical Temperature and Salinity Comparisons for MX-01 (Alboran Sea)

Vertical cross-sections of salinity (S) for winter and summer were compared. Numerical values for temperature at the 100 m depth level were also compared. The survey cross-sections were taken by the Naval Oceanographic Office during the USNS KANE cruise of 1976-77 and by G. Wust (Lamont Geological Observatory) 1959-60.

5.1.1 Regional Description

Section MX-01 was selected from the Alboran Sea region of the Mediterranean Sea. The vertical cross-sections are defined by a great circle track which originates at 36°00'N, 2°00'W and terminates at 36°00'N, 5°00'W. The location of the Alboran Sea and Section MX-01 are depicted on Figure 1-1. Vertical cross-sections of temperature and salinity for MX-01 are shown on Figures 5-1 through 5-7.

Oceanographically, this region is considered to be highly active, extremely variable, and sufficiently influenced by a number of surface and subsurface physical features; e.g. ocean fronts, ocean eddies, current

boundaries, and zones of convergence/divergence. Proper environmental numerical modeling of this region is problematic. Substantial dynamic activity and variability make proper representation of typical conditions extremely difficult. Past studies of this region have indicated the development and presence of a noticeable summer oceanic front. More recent studies have shown that the Alboran Sea Front is not a summer feature, but a persistent feature that can be identified throughout the year (Cheney, 1977). The frontal system extends in a general eastward pattern establishing cyclonic and anticyclonic gyres. Large amounts of North Atlantic water flow through the Strait of Gibraltar, providing a source for warm water as well as exerting some influence on the meanderings of the Alboran Front.

According to Cheney, the Alboran Front is confined to the upper 200 meters. The width is typically of 35 km. At 100 meters in depth, the horizontal temperature difference is typically 2.0°C to 4.0°C . Characteristic of the Alboran Sea region, in addition to the front itself, are gyres having diameters of approximately 75-100 km exerting influence on the regional circulation patterns. The front is most noticeable (due to higher contrast in values of temperature) when colder surface waters along the southern coast of Spain are entrained in the region along the front. Ovchinnikov (1976) suggested that this anticyclonic gyre of the Alboran Sea is an anomalous feature which on occasion occurs in the summer. In reviewing other data sets before and after Ovchinnikov's study, these data have indicated that this feature is not anomalous but a characteristic feature of the region in spring and summer ((Donguy, 1962; Cheney, 1977, 1978, subsurface hydrostations), (Stevenson, 1977, satellite infrared imagery), (Donguy, 1962; Grousson and Faroux, 1963, surface current measurements)).

The presence and flow of the Levantine Intermediate Water (L.I.W.), whose origin is from the eastern Mediterranean Basin, has been detected and studied by investigators (Wust, 1961; Katz, 1972). Past and recent investigations appear to be in agreement in that the subsurface flow of the L.I.W.

is westerly in this region and characteristically follows along the northern coastline of Africa. Upon encountering the Strait of Gibraltar, the L.I.W. continues its westerly flow over the sill and becomes an outflow into the eastern North Atlantic (Ambar, I., and Howe, M. R., 1979a; Ambar, I. and Howe, M. R., 1979b; Ambar, I., Howe, M. R. and Abdullah, M. I., 1976).

It has been suggested by past investigations that the presence of cold subsurface waters above the L.I.W. may possibly be formed northeast of the Alboran Sea proper near the Balearic Channel and the Island of Mallorca (Miller, Tschernia and Charnock, 1970). This should, however, be treated as only a possibility requiring further investigation.

Surface and near-surface waters of the Alboran Sea are influenced strongly by the influx of North Atlantic surface water directed easterly through the Strait of Gibraltar. Characteristics of this surface and near-surface water have been found to be present outside (east) of the Alboran Sea.

Meteorologically, this region is considered highly variable and seasonally influenced to a great degree by the movement of the semi-permanent Azores anticyclone. In most cases, the local to semilocal surface wind conditions are not produced by the distinct wind patterns associated with either the Sierra Nevada of Spain or the Atlas Mountains of Morocco and Algeria. Channeling and corner effects dominate the local wind patterns in this region. An area of cyclogenesis for the western portion has been identified as being in the center of the Alboran Sea.

5.1.2 Comparison

The GDEM vertical temperature cross-section along great circle track MX-01 was compared with January and March 100 meter surface analyses by Cheney (1977), as well as with the mean numerical values of the January and March. Also, GDEM vertical salinity cross-sections along great circle track MX-01 were compared with Wust (1961) analyses for both winter and summer.

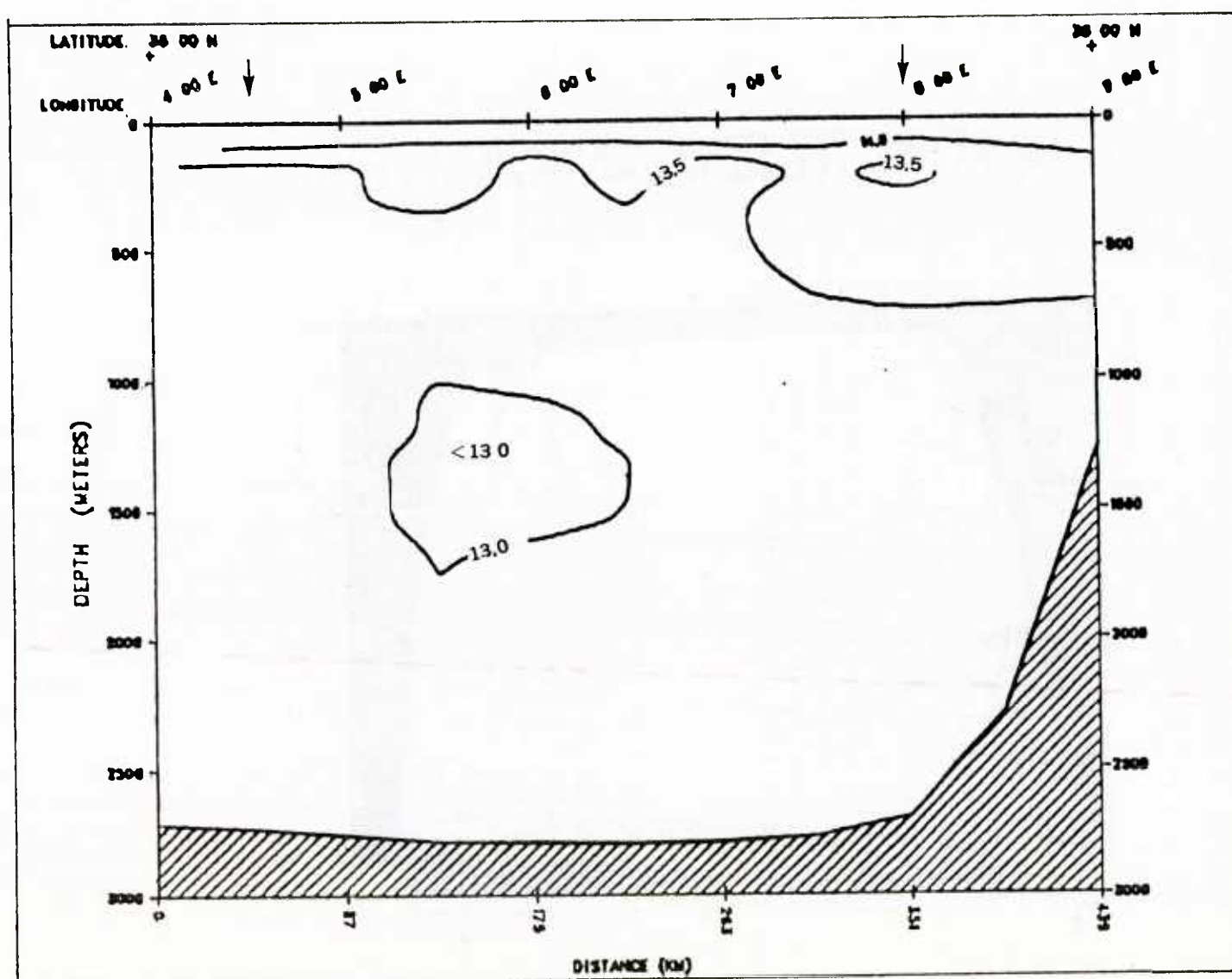


FIGURE 5-9: GDEM - WINTER VERTICAL TEMPERATURE CROSS-SECTION ALONG GREAT CIRCLE TRACK MX-02

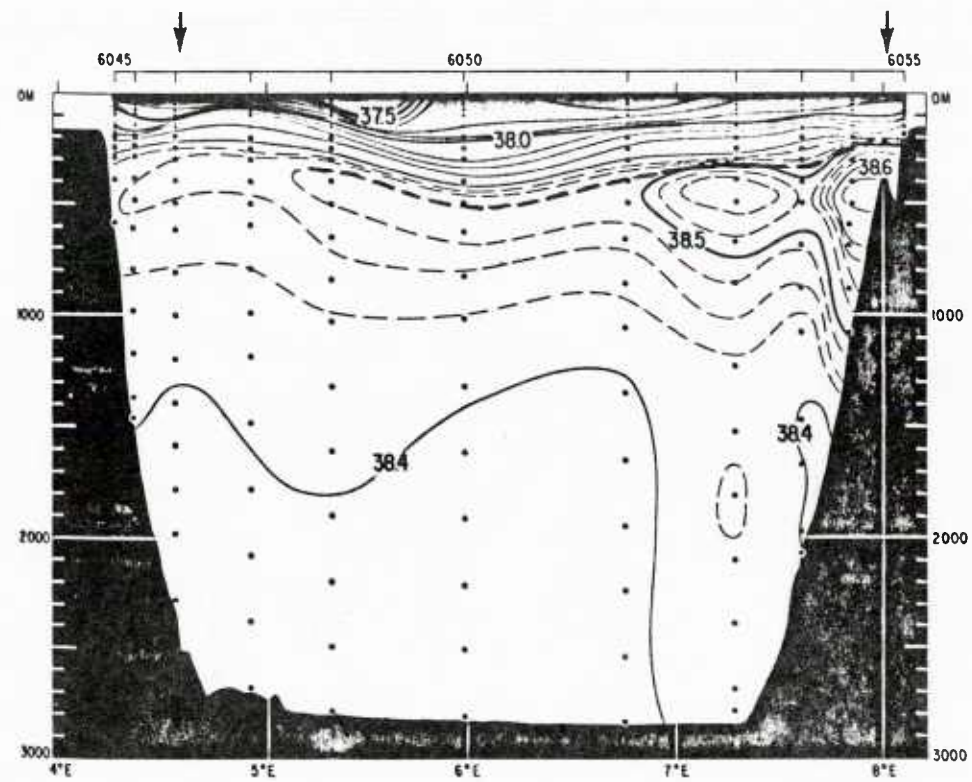


FIGURE 5-10: WINTER VERTICAL SALINITY CROSS-SECTION
ALONG GREAT CIRCLE TRACK MX-02

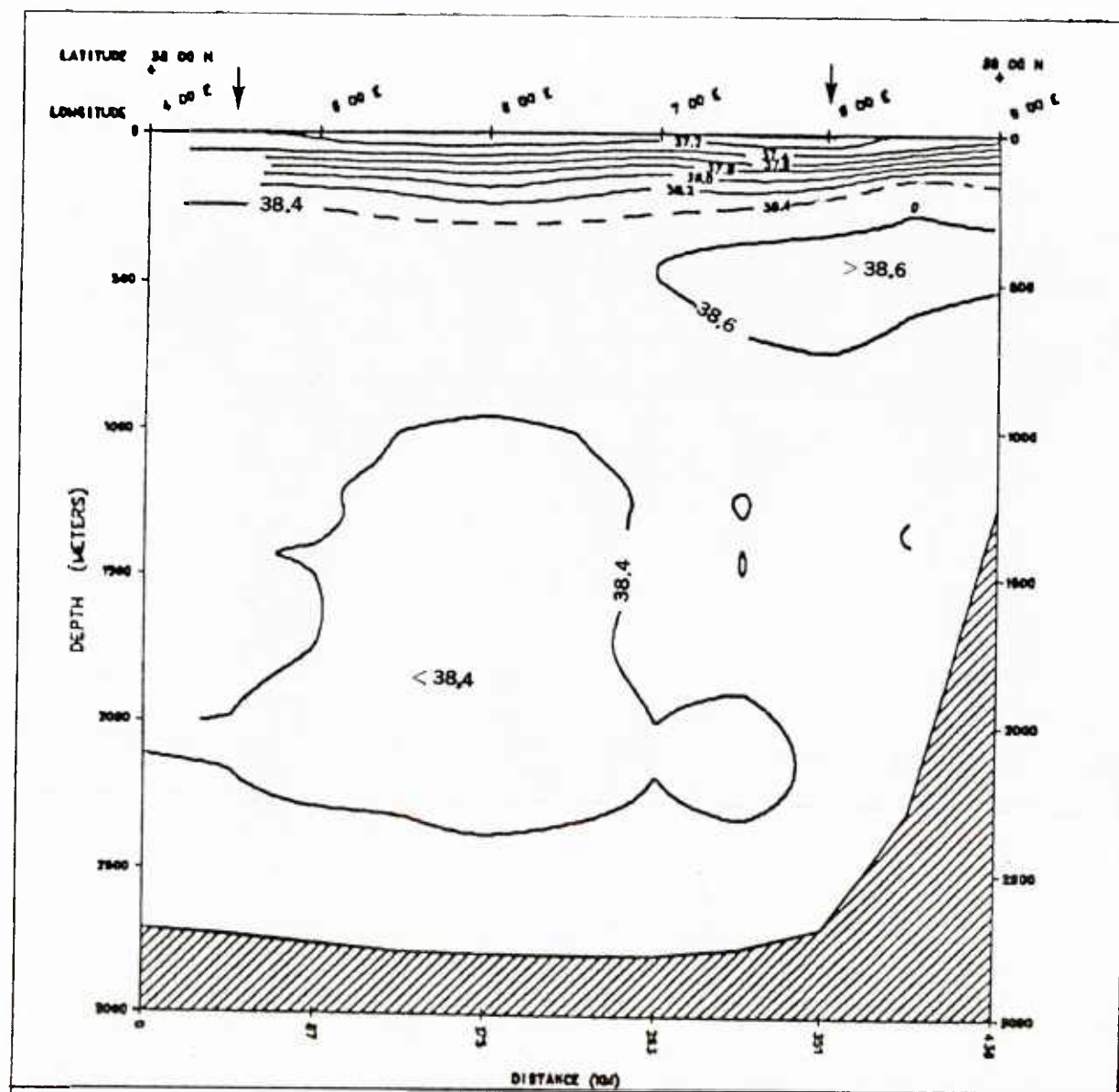


FIGURE 5-11: GDEM - WINTER VERTICAL SALINITY CROSS-SECTION ALONG GREAT CIRCLE TRACK MX-02

5.3 Vertical Temperature and Salinity Comparisons for MX-03 (Tyrrhenian Sea)

Vertical cross-sections of temperature (T) and salinity (S) for the winter time period were compared. The survey cross-sections were taken during the R. V. Atlantis I cruise of 1962.

5.3.1 Regional Description

Section MX-03 was selected from the Tyrrhenian Sea region of the Mediterranean Sea. The vertical cross-sections are defined by a great circle track which originates at 42°30'N, 10°00'E and terminates at 39°00'N, 15°00'E. The locations of the Tyrrhenian Sea region and Section MX-03 are depicted on Figure 1-1. Vertical cross-sections of temperature and salinity for MX-03 are shown on Figures 5-12 through 5-15.

Oceanographically, this region is considered variable. The ocean variability and changes in the vertical water column (more so than in the horizontal) are directly influenced by the impulses received from the path of cyclogenesis which begin in the Gulf of Genoa toward the eastern part of Sicily. The vertical variability throughout the track region can be expected to provide broad and relatively deep seasonal ocean variability.

Unlike some of the other major basins of the Mediterranean, the Tyrrhenian Sea is relatively tame and less active when compared to the other regions. In the opinion of the authors, the Tyrrhenian is a large transitional basin influenced by the exchange of water through the Strait of Sicily, the passageway from the Balearic Sea and, to an undetermined degree, through the Strait of Messina.

The Levantine Intermediate Water (L.I.W.) is primarily channeled into the Tyrrhenian Sea through the Strait of Sicily. No incontrovertible periodicity has been established as existing anywhere in the flow of the L.I.W. throughout the western Mediterranean except along the northernmost coast of Africa (Stommel, Voohris and Webb, 1971). The discharge of L.I.W. into the Tyrrhenian through the Strait of Sicily has been studied and mapped

(to some degree) as proceeding as a subsurface cyclonic flow around the Tyrrhenian Basin and eventually traversing along a passage below Sardinia in a westerly direction (Katz. 1972; Molcard. 1972). The full extent and degree of penetration of this subsurface L.I.W. cyclonic gyre is not fully known. It is logical to infer that the flow will be (to some extent) influenced by the proximate bathymetric configuration. Nevertheless, substantial amounts of L.I.W. do flow westerly south of the island of Sardinia. Although Ovchinnikov (1966) speculated that all of the outflow from the Strait of Sicily goes into the cyclonic gyre circulation in the Tyrrhenian Sea, the authors (in analysis of past Mediterranean data sets) do not fully support this speculation by Ovchinnikov. A more acceptable speculation would be that, on occasion, some undetermined quantities of inflow water from the Strait of Sicily have been reflected in various data sets. The authors agree, however, with Katz in that the bottom layer of Levantine origin flows over the Strait of Sicily into the southern Tyrrhenian Sea region and has the following characteristics: temperature 14.0°C to 14.3°C , salinity $38.70^{\circ}/\text{oo}$ to $38.75^{\circ}/\text{oo}$, and σ_t 29.05 -29.10. In studying Wust's distribution of oxygen within the core layers of the deep waters of the Tyrrhenian Sea, there is an obvious zone of oxygen maxima ($\geq 4.2 \text{ cm}^3/\text{l}$) located at approximately 2500 meters in the central portion of the basin. The origin and significance are not clear to the authors at this time.

Additional studies and investigations conducted in the Tyrrhenian Sea have provided supplemental insights on other physical processes which have been observed in this region. Linden has conducted several investigations on the formation of banded salt finger structure. The Tyrrhenian Sea, between 600 and 1400 meters, is one of the best known regions for the study of this phenomenon. These observed bands of salt fingers have been observed to be on the order of magnitude of several meters in thickness (Tait and Howe, 1971). Investigations on temperature inversions occurring in the Tyrrhenian Sea region have been conducted by Fedorov (1970, 1972). In the Tyrrhenian, the local temperature inversions result when low winter temperatures occur in the coastal regions. These local inversions are related to the intrusion of

cold intermediate layers which slide down from the continental shelf region into the warmer water layer of the open basin. Inversions of this kind are not unique to either the Tyrrhenian or Mediterranean. However, it should be mentioned that this kind of temperature inversion is unique in itself in that it does not occur everywhere in the Mediterranean Sea. The temperature inversions, occurring in the Tyrrhenian Sea occur between the "intrinsically Mediterranean" waters ($38.0^{\circ}/\text{oo} \leq S \leq 38.3^{\circ}/\text{oo}$) and the intermediate waters of Levantine origin are the most frequently encountered type of inversion. And despite the findings of Nielsen (1912) and of Romanovsky and Le Floch (1966), studies by Defant (1940), French and Italian expeditions investigating and mapping spatial distributions of the temperature and salinity maximas of the intermediate waters of the Tyrrhenian Sea reveal that intermediate waters appear to penetrate into the Tyrrhenian not only through the Strait of Sicily, but also through the Strait of Messina (Federov, 1972).

Meteorologically, this region is considered variable and is influenced in part by a region of cyclogenesis located over the Gulf of Genoa. The major geographical feature influencing the role of cyclogenesis in the Gulf of Genoa is the Alps, which are north of Italy. The Alps have been known to play a key role in determining the weather over the Gulf of Genoa, the northern Adriatic Sea, and the Ligurian Sea in terms of fronts, planetary waves, and degree of cyclogenesis. The Gulf of Genoa is perhaps one of the most significant regions of the world for cyclogenesis.

5.3.2 Comparison

GDEM temperature and salinity vertical cross sections along great circle track MX-03 were compared with the Atlantis #275 data of February 1, 1962, to March 24, 1962. and were evaluated as follows for:

- Temperature

Winter comparisons of temperature revealed in both the GDEM and Atlantis 275 analyses the presence of known isotherms (a

well-defined $13.5^{\circ}\text{C} \leq T \leq 14.0^{\circ}\text{C}$ subsurface layer between approximately the 500 and 1000 meter levels) in this region. The GDEM analysis did not reflect this feature as surfacing west of the $12^{\circ}00'\text{E}$ meridian as the Atlantis. However, GDEM did show a warm pool of $\geq 14.5^{\circ}\text{C}$ near the $12^{\circ}00'\text{E}$ meridian. Both analyses reflected the presence of 14.0°C to 14.3°C water above 500 meters.

- Salinity

Winter comparisons of salinity revealed in both the GDEM and Atlantis 275 analyses the presence of the major isohalines ($38.5^{\circ}/\text{oo}$ and $38.60^{\circ}/\text{oo}$) known in this region. Both the GDEM and Atlantis analyses reflected surface similarities; e.g. the surfacing of the $38.0^{\circ}/\text{oo}$ isohaline at the $12^{\circ}00'\text{E}$ meridian; the surfacing of the $37.8^{\circ}/\text{oo}$ and $37.9^{\circ}/\text{oo}$ isohalines near the $14^{\circ}10'\text{E}$ meridian. Both GDEM and the Atlantis analyses reflected a very well-defined salinity maximum subsurface layer of $\geq 38.6^{\circ}/\text{oo}$ between the 250 and 800 meter levels completely along the entire track. Any partials of water of Levantine origin would be enclosed in this subsurface, well-defined salinity band. Immediately above the 250 meter level, both reflected thin $38.3^{\circ}/\text{oo}$, $38.4^{\circ}/\text{oo}$ and $38.5^{\circ}/\text{oo}$ layers paralleling the 1100 to 1500 meter levels. Both analyses reflected the presence of an undulating $38.5^{\circ}/\text{oo}$ isohaline.

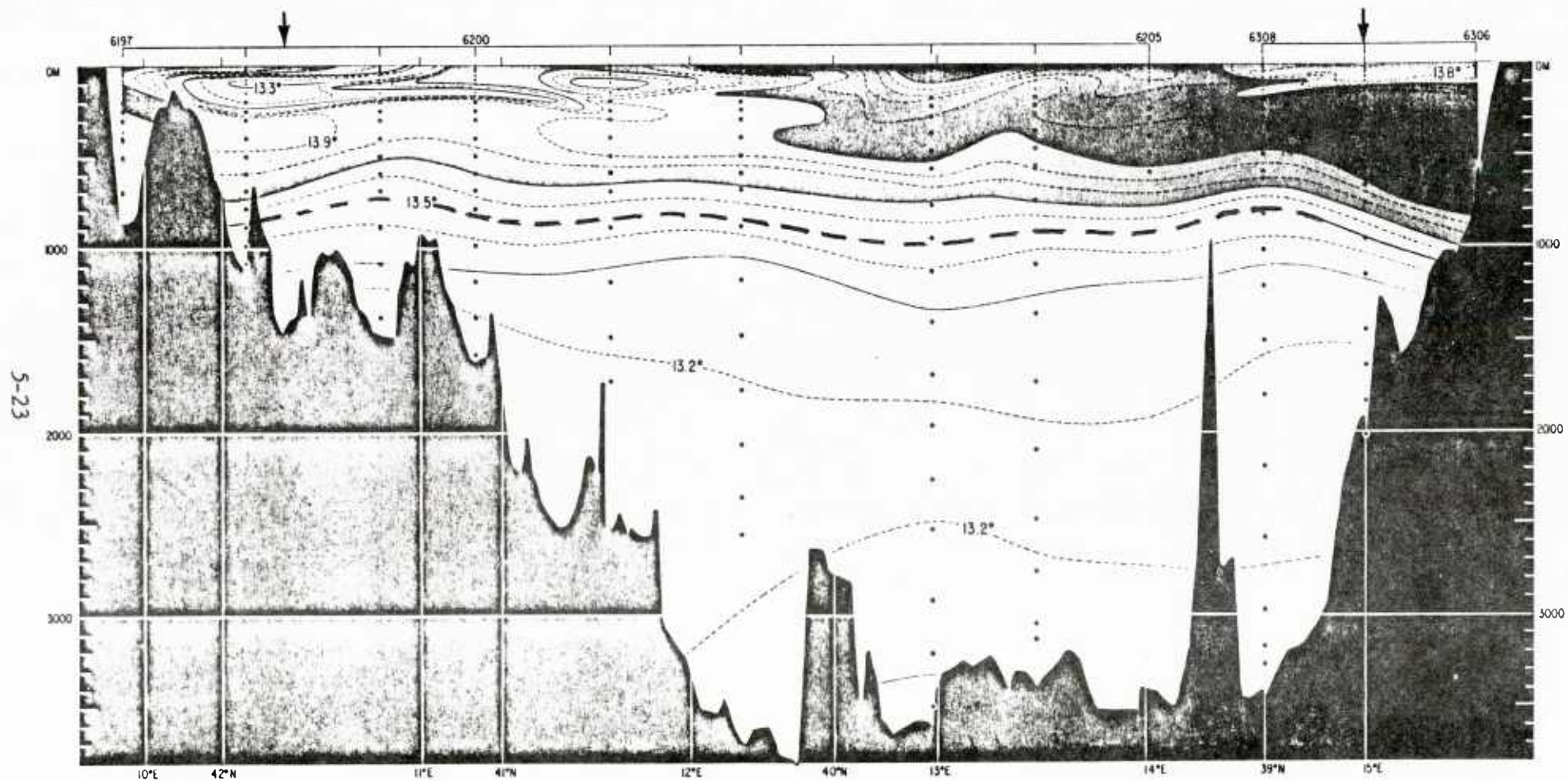


FIGURE 5-12: WINTER VERTICAL TEMPERATURE CROSS-SECTION ALONG GREAT CIRCLE TRACK MX-03

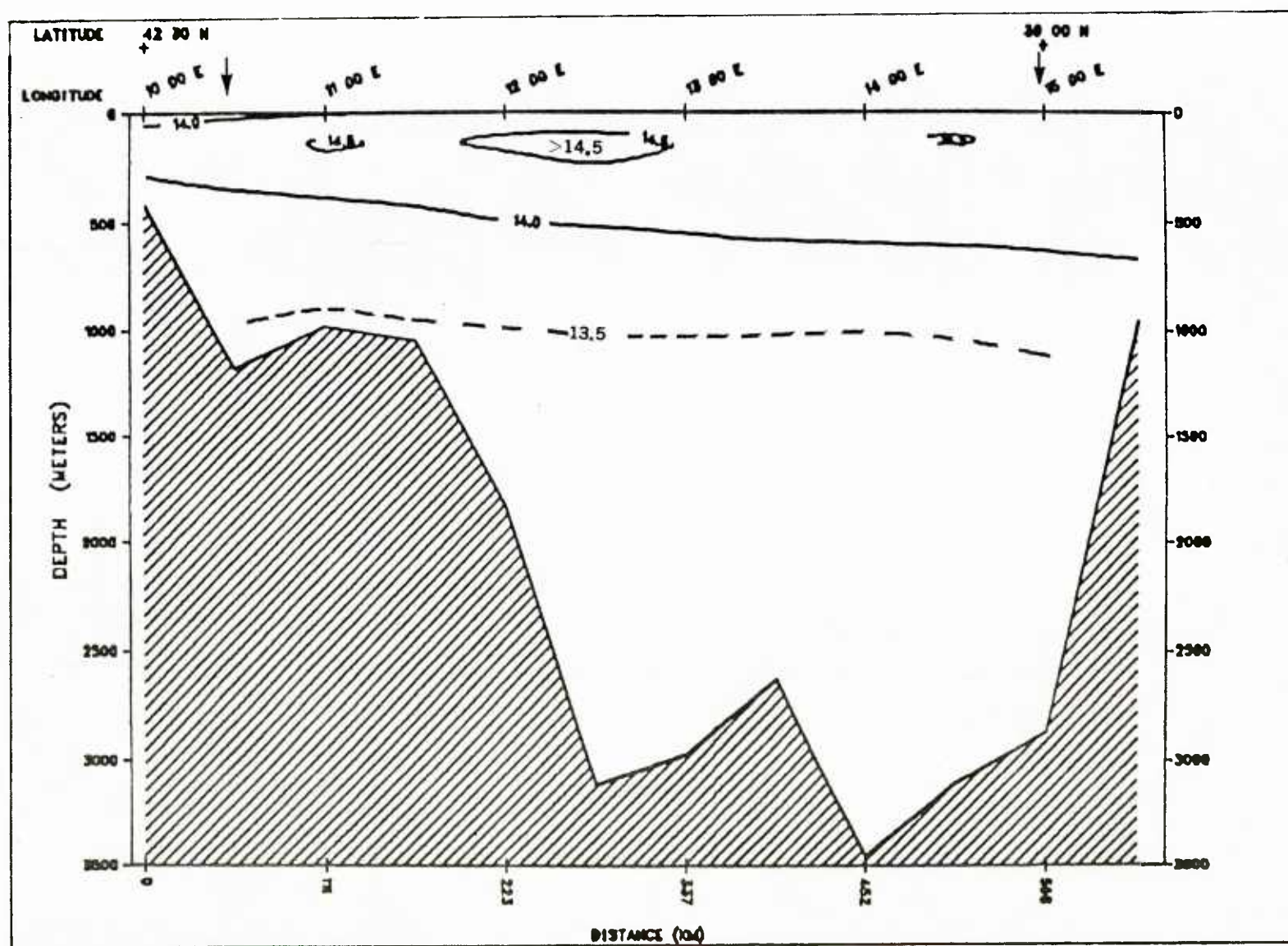


FIGURE 5-13: GDEM - WINTER VERTICAL TEMPERATURE CROSS-SECTION ALONG GREAT CIRCLE TRACK MX-03

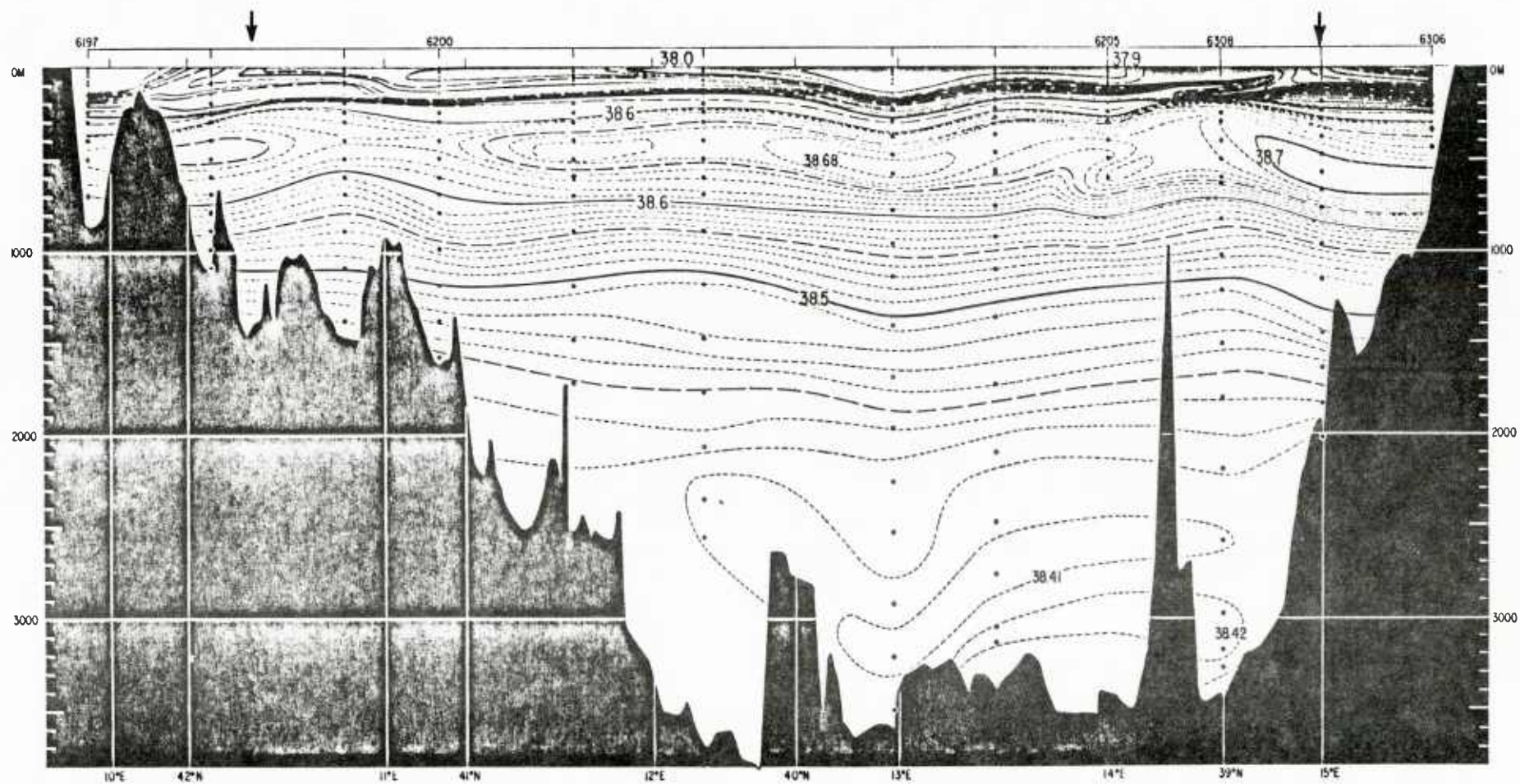


FIGURE 5-14: WINTER VERTICAL SALINITY CROSS-SECTION ALONG GREAT CIRCLE TRACK MX-03

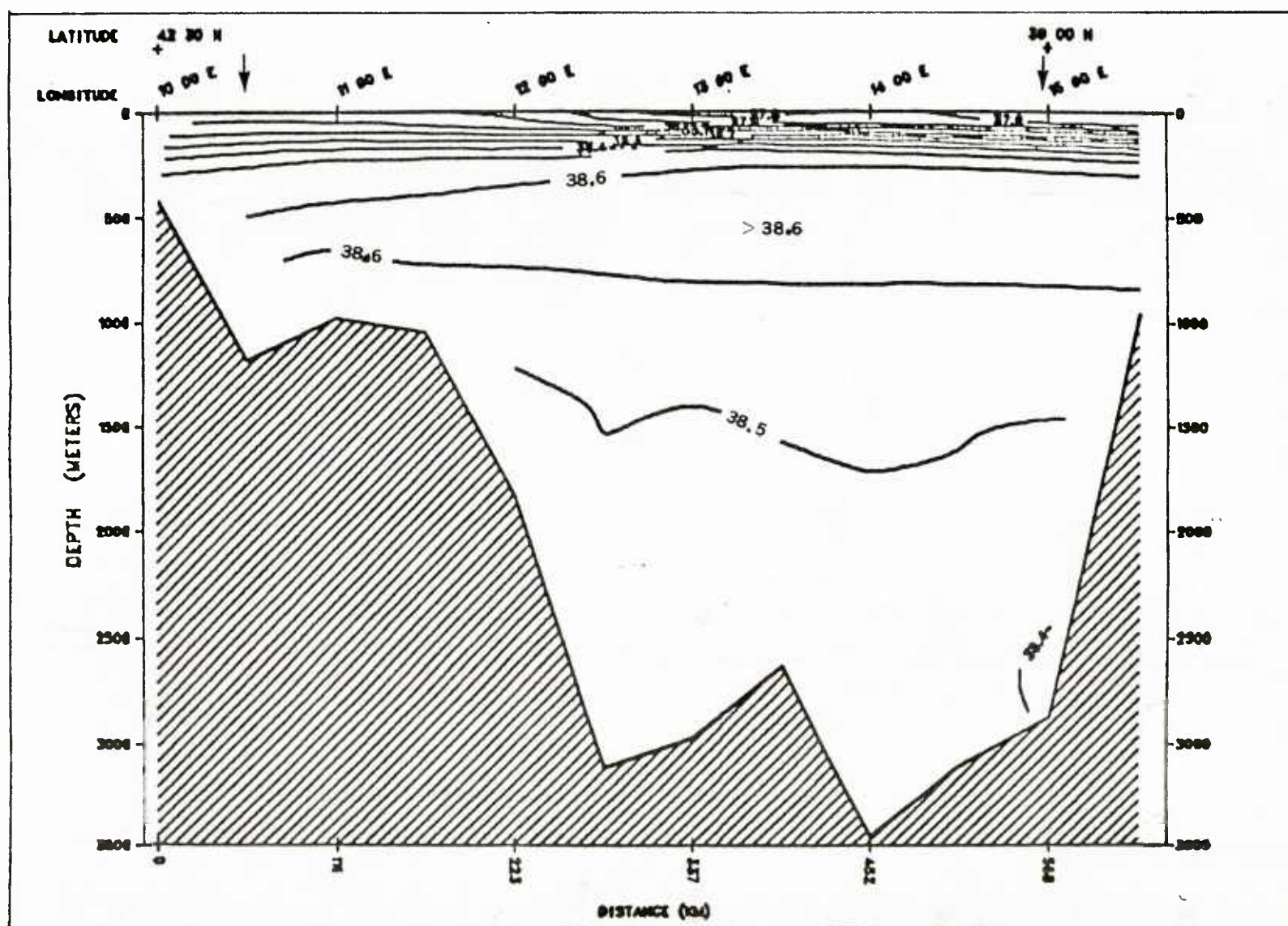


FIGURE 5-15: GDEM - WINTER VERTICAL SALINITY CROSS-SECTION ALONG GREAT CIRCLE TRACK MX-03

5.4 Vertical Temperature and Salinity Comparisons for MX-04 (Ionian Sea)

Vertical cross-sections of temperature (T) and salinity (S) for the winter time periods and salinity for the summer period were compared. The survey cross-sections were taken during the R. V. Atlantis I cruise of 1962.

5.4.1 Regional Description

Section MX-04 was selected from the Ionian Sea region of the Mediterranean Sea. The vertical cross-sections are defined by a great circle track which originates at $36^{\circ}30'N$, $16^{\circ}00'E$, and terminates at $35^{\circ}30'N$, $22^{\circ}30'E$. The locations of the Ionian Sea and Section MX-04 are depicted on Figure 1-1. Vertical cross-sections of temperature and salinity for MX-04 are shown on Figures 5-18 through 5-24.

Oceanographically, this region is considered variable. The ocean variability and changes in the near-surface vertical water column are directly influenced by the impulses received from the paths of cyclogenesis through mechanical mixing (especially in the winter and early spring). Because of the seasonal influence of surface air masses from the Sahara Desert, this area will reflect wide vertical variability in the surface and near-surface stratification, especially in salinity.

The Ionian Sea is an active basin and contributes toward Mediterranean watermass formations, thermal fronts, displacements of the proximity of the Levantine Intermediate Water (L.I.W.), etc. General surveys and in-depth studies have both been conducted in furthering our understanding of the above features.

Early studies by Nielsen (1912) indicate that the deep waters of the Ionian Sea are formed in the southern Aegean Sea (possibly north of Crete). Schott (1915) conducted a review of Nielsen's work. In his review, Schott agreed with Nielsen regarding the location of Ionian deep water formation, but doubted that sufficient quantities of water flow out from the southern Aegean Sea to fill the Levantine Basin. Pollak (1951) expressed a contrary opinion to those of Nielsen and Schott. Pollak concluded that the Ionian

Deep Water is formed north of the Ionian Basin proper and not in the southern Aegean Sea. In reviewing the work of Pollak as well as other foreign data sets available for this particular region, the authors are in agreement with the thesis of Pollak. Characteristics of the Ionian Deep Water existing at roughly 1600 meters are: for temperature, a minimum of 13.57°C ; for salinity, isohaline of $38.65^{\circ}/\text{oo}$; for oxygen, 3.9 to 4.0 ml/l . The physical characteristics of temperature, salinity and dissolved oxygen appear to reflect the properties of water found in the region near the southern limits of the Adriatic Sea (the Strait of Otranto). In this region, it is possible for mixing to occur of waters from a region of relatively fresh water (river effluent) from the north (Adriatic) with the more saline waters of the upper Ionian. This newly mixed parcel of water results due to sufficient surface cooling and vertical convection in winter. The resultant mixture eventually sinks towards the bottom and flows out through the Strait of Otranto into the Ionian Sea. The magnitude and quantity of this outflowing Ionian Deep Water is neither clearly understood nor adequately measured; however, there seems to be little doubt that the impulses of outflow are irregular, depending to a large extent on the prevailing weather regimes from winter to winter. This deep water should be detectable throughout the major Ionian Sea Basin. The outflow originates along the bottom of the western side of the Strait, then flows in a counterclockwise circulation pattern (Pollak, 1951; Wust, 1961). Further evidence of the outflow is that the water at the sill depth of the Strait of Otranto has a higher potential density (the majority of the time in winter) than the deep waters of the eastern Mediterranean. This differential in potential densities can allow for a net downslope flow into the Ionian Sea.

Although some flow has been measured and observed through the Strait of Messina by Nielsen (1912) and Vercelli (1925), this passageway into the Ionian Sea has been ruled out as a major channel for water transport between the eastern and western Mediterranean Basins. The amount of flow and exchange through the Strait of Messina, when compared to that taking place through the Strait of Sicily and the Strait of Otranto, would be very

small by comparison. In the past, investigations have been conducted by Frassetto (1964) revealing that the primary water exchange between the eastern and western Mediterranean Basins occurs in the region of the Strait of Sicily* over at least two sills (or systems of sills) and the exchanges are confined to depths not greater than 558 meters on the Eastern Sill (almost exactly along the $15^{\circ}00'E$ meridian) between the Medina Bank and south of Malta.

Zones of high thermal gradients were found and studied by Levine and White (1972) in the Ionian Sea. The most striking feature of these zones was that thermal fronts were measured and observed having thermal gradients exceeding $1.0^{\circ}C/10\text{ km}$ at either the surface or in the seasonal thermocline. The thermal discontinuity appeared not to be continuous but discontinuous in a step-wise fashion. Other investigations have been conducted on specific regions of the thermal fronts described by Levine and White. Woods and Watson (1970); Woods (1972); Johannessen, De Strobel and Gehin (1971); Johannessen (1971); and Briscoe, Johannessen and Vincenzi (1974) all have studied the western portion known as the Maltese Front. This front extends from the southern tip of Sicily to about $35^{\circ}30'N$ and appears to coincide with the edge of the continental shelf. The northern region of this front revealed changes across the front of $1.0^{\circ}C$ to $1.5^{\circ}C$, in temperature; and $0.6^{\circ}/\text{oo}$ to $1.0^{\circ}/\text{oo}$, in salinity. The width was estimated at approximately eight to ten nautical miles.

The core of the L.I.W. flows in a predominantly westerly direction through the southern region of the Ionian Basin. The placement of the axis of the L.I.W. core layer appears to be seasonally variable. The core layer appears to be displaced southerly in the winter (indicating weaker in strength) and northerly in the summer (indicating stronger in strength). This seasonal displacement can be observed in Figures 5-16 and 5-17 (Wust, 1961).

*Note: The "Strait of Sicily" in the text should be taken in the broadest meaning to include all the area between the Meridian of Malta (or Medina Bank) and a line joining Cape Bon to the Aegates Islands (Marittimo).

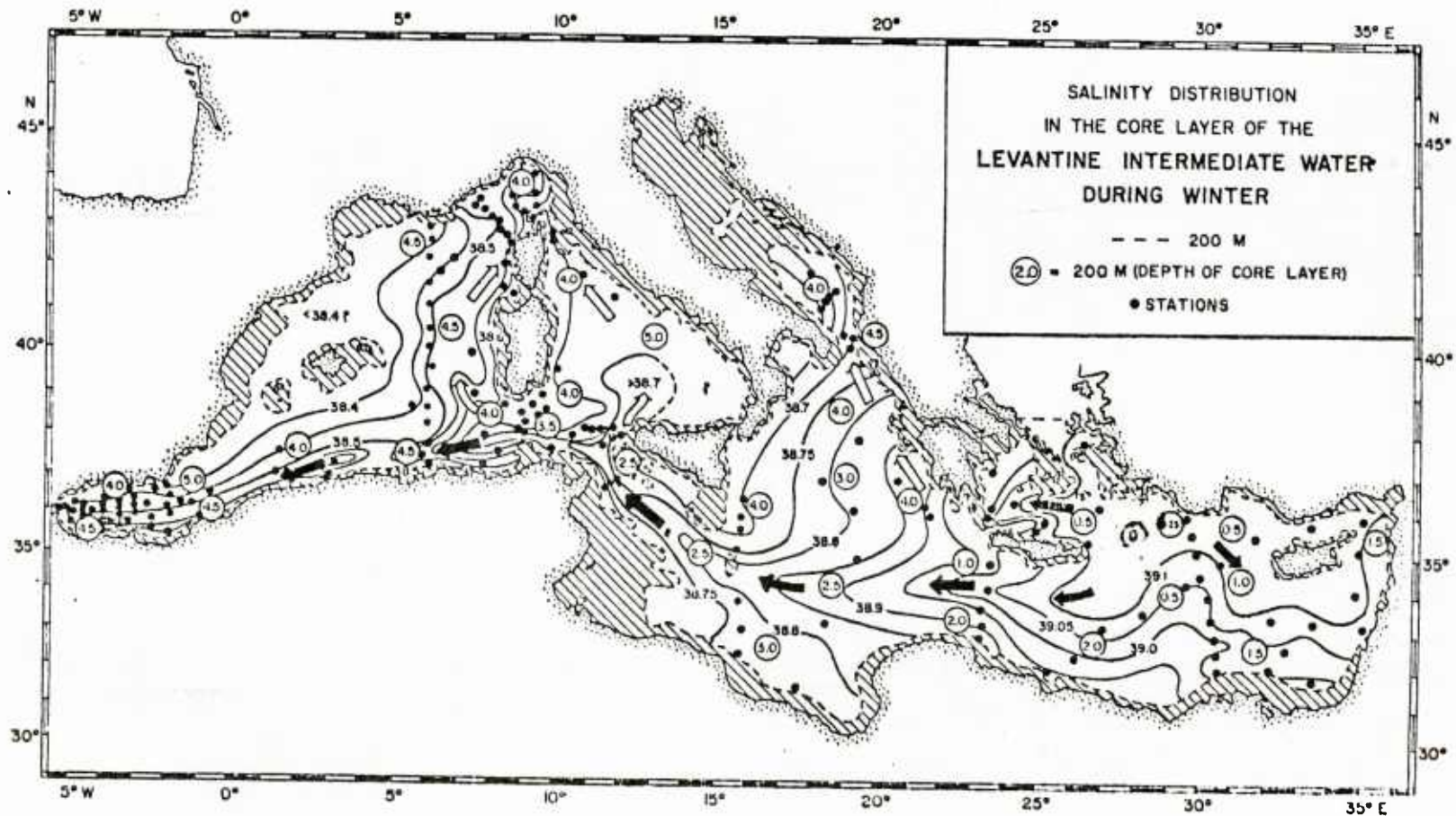


FIGURE 5-16: LOCATIONS OF THE SALINITY CORE LAYER WITHIN THE LEVANTINE INTERMEDIATE WATER IN THE WINTER (WUST, 1961)

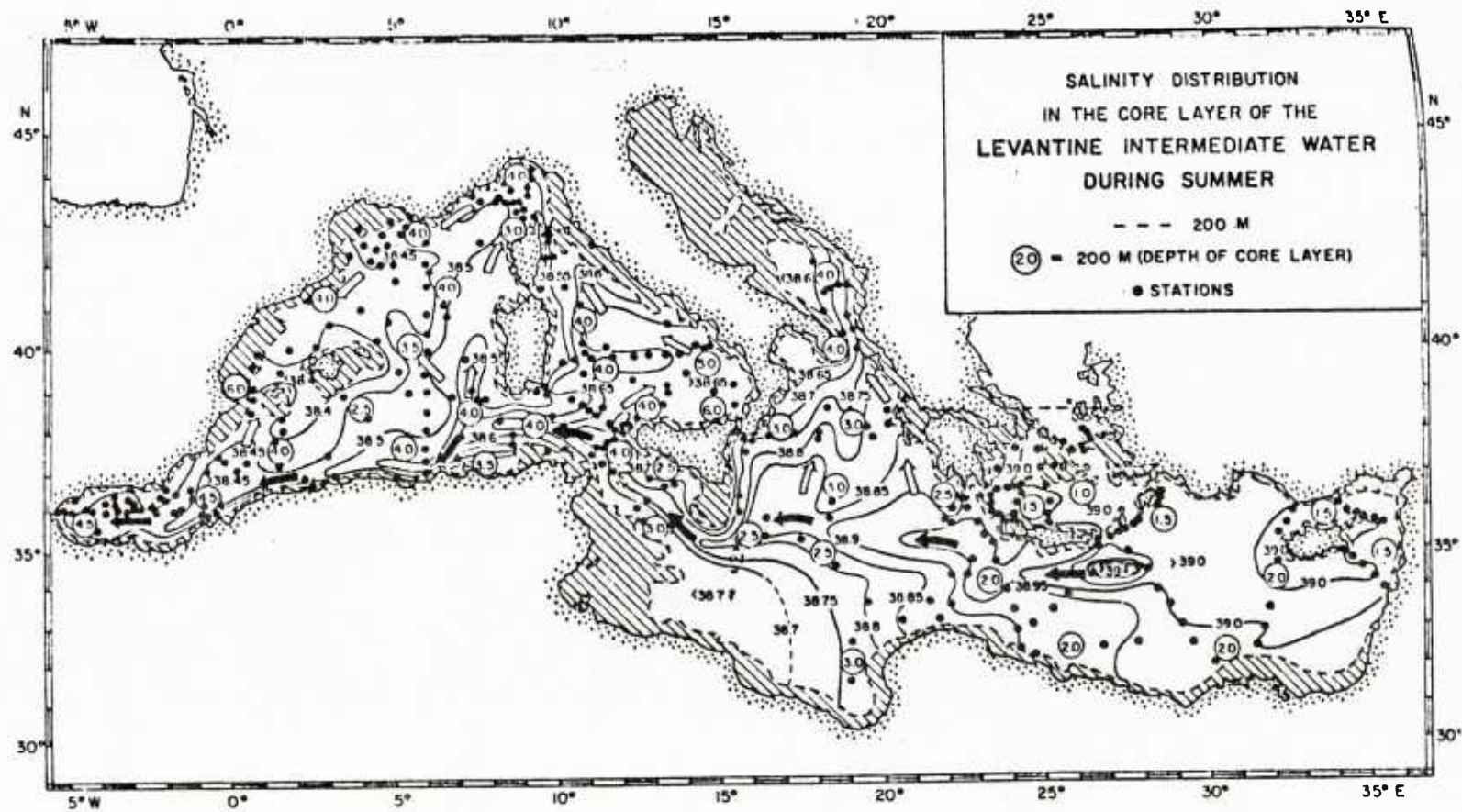


FIGURE 5-17: LOCATIONS OF THE SALINITY CORE LAYER WITHIN THE LEVANTINE INTERMEDIATE WATER IN THE SUMMER (WUST, 1961)

Meteorologically, this region is considered variable and seasonally active. The seasonal patterns are controlled primarily by the monsoonal characteristics of the Sahara Desert to the south and the Eurasian land mass to the north. The winters are characterized by a dominant high pressure with associated unsettled, windy conditions. The summers are characterized by a relatively weak high pressure with associated warm, dry settled conditions and light winds. Cyclogenesis does occur over the Ionian Sea. With their origin in the Atlas Mountains of Algeria and Tunisia, the primary path for the North African cyclones is north-eastward across the Ionian Sea. A secondary zone for Ionian cyclogenesis is located over the northern portion of the Ionian Sea. This region is known to generate southeastward cyclones that are associated with the southerly invasion of cold-air-mass movements from the Adriatic Sea.

5.4.2. Comparison

GDEM temperature and salinity vertical cross sections along great circle track MX-04 were compared with the Atlantis #275 data of February 1, 1962 to March 24, 1962. Also, GDEM salinity vertical cross section along great circle track MX-04 was compared with Wust (1961) winter analysis for this region. The comparisons and evaluations for both were as follows for:

- Temperature

Winter comparisons of temperature revealed in both the GDEM and Atlantis 275 analyses the presence of known isotherms (14.0°C , 15.0°C and 15.5°C) in this region. Both the GDEM and Atlantis analyses reflected the surface temperature maximum of $\geq 15.5^{\circ}\text{C}$ to be approximately 200 meters in thickness. In both analyses this maximum layer extended out to approximately the $018^{\circ}45'\text{E}$ meridian. The 14.0°C isotherm in both analyses maintained itself near the 700 meter level. Below the 1000 meter level, the range of temperature for both analyses was $13.5^{\circ}\text{C} \leq T \leq 14.0^{\circ}\text{C}$. The presence of the Ionian Deep Water near 1600 meters was not reflected in either the GDEM or Atlantis analyses. This section is possibly a little too far south for its definite identification.

o Salinity

Winter comparisons of salinity revealed in both the GDEM and the Atlantis 275 and Wust analyses the presence of known isohalines ($\leq 38.6^{\circ}/\text{oo}$, $38.7^{\circ}/\text{oo}$ and $\geq 38.8^{\circ}/\text{oo}$) in this region. All three analyses reflected the surface layer of salinity minimum (≤ 38.6) toward Sicily between the surface down to approximately 200 meters.

Also, all three analyses reflected the subsurface salinity maximum ($\geq 38.8^{\circ}/\text{oo}$) layer which protrudes northwestward from the lower Ionian Basin. This layer of salinity maximum was reflected in both analyses as existing between the 100 meter and 700 meter levels. All three analyses reflected a region of $\geq 38.9^{\circ}/\text{oo}$ to the right (toward Crete) at approximately the 200 meter to 400 meter levels. Locating itself around the 1000 meter level in both analyses was the $38.7^{\circ}/\text{oo}$ isohaline with a region $\leq 38.7^{\circ}/\text{oo}$ below. The presence of the Ionian Deep Water near 1600 meters was not reflected in either the GDEM or Atlantis analyses. This section is probably a little too far south for its definite identification.

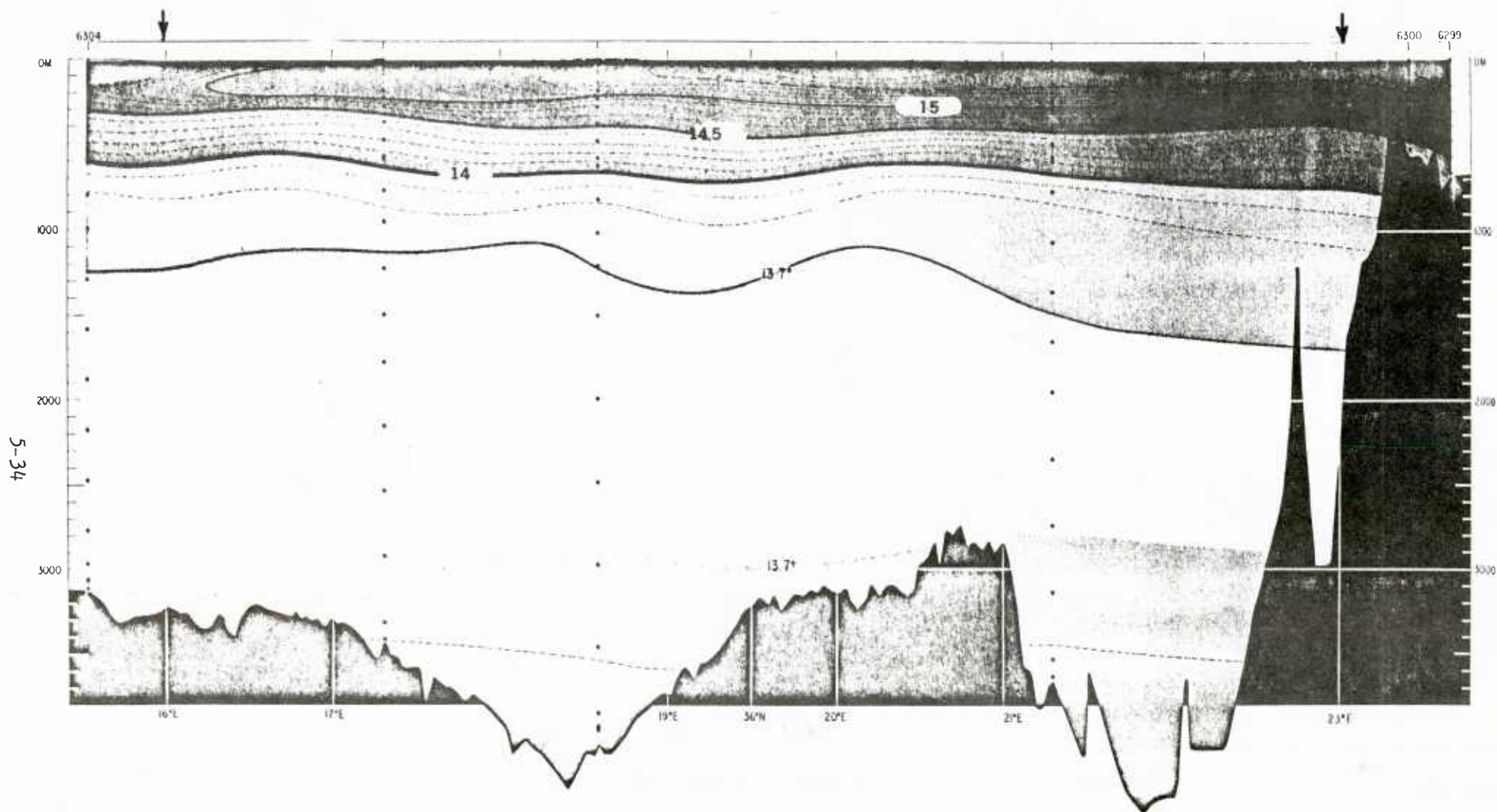


FIGURE 5-18: WINTER VERTICAL TEMPERATURE CROSS-SECTION ALONG GREAT CIRCLE TRACK MX-04

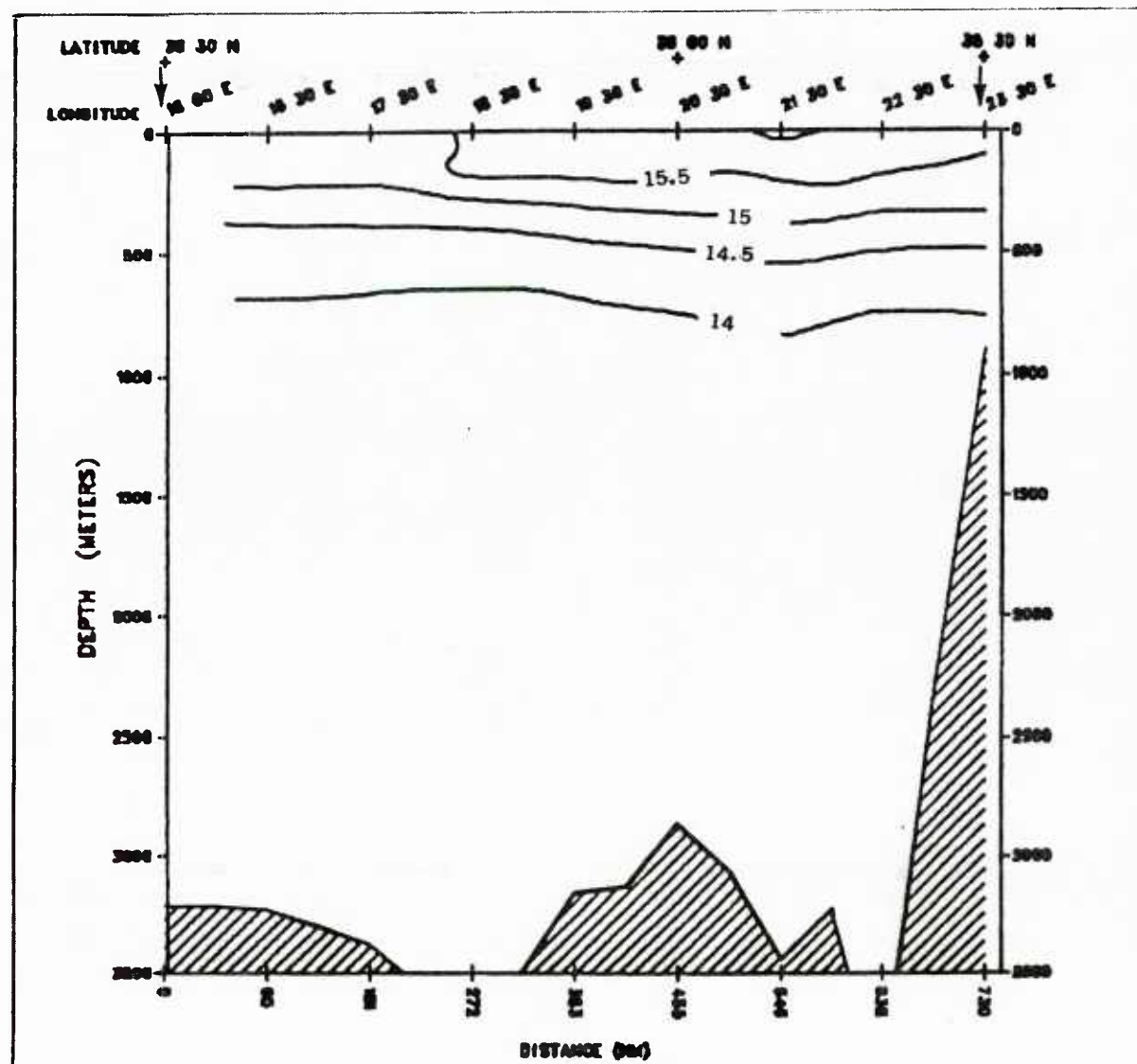


FIGURE 5-19: GDEM - WINTER VERTICAL TEMPERATURE CROSS-SECTION ALONG GREAT CIRCLE TRACK MX-04

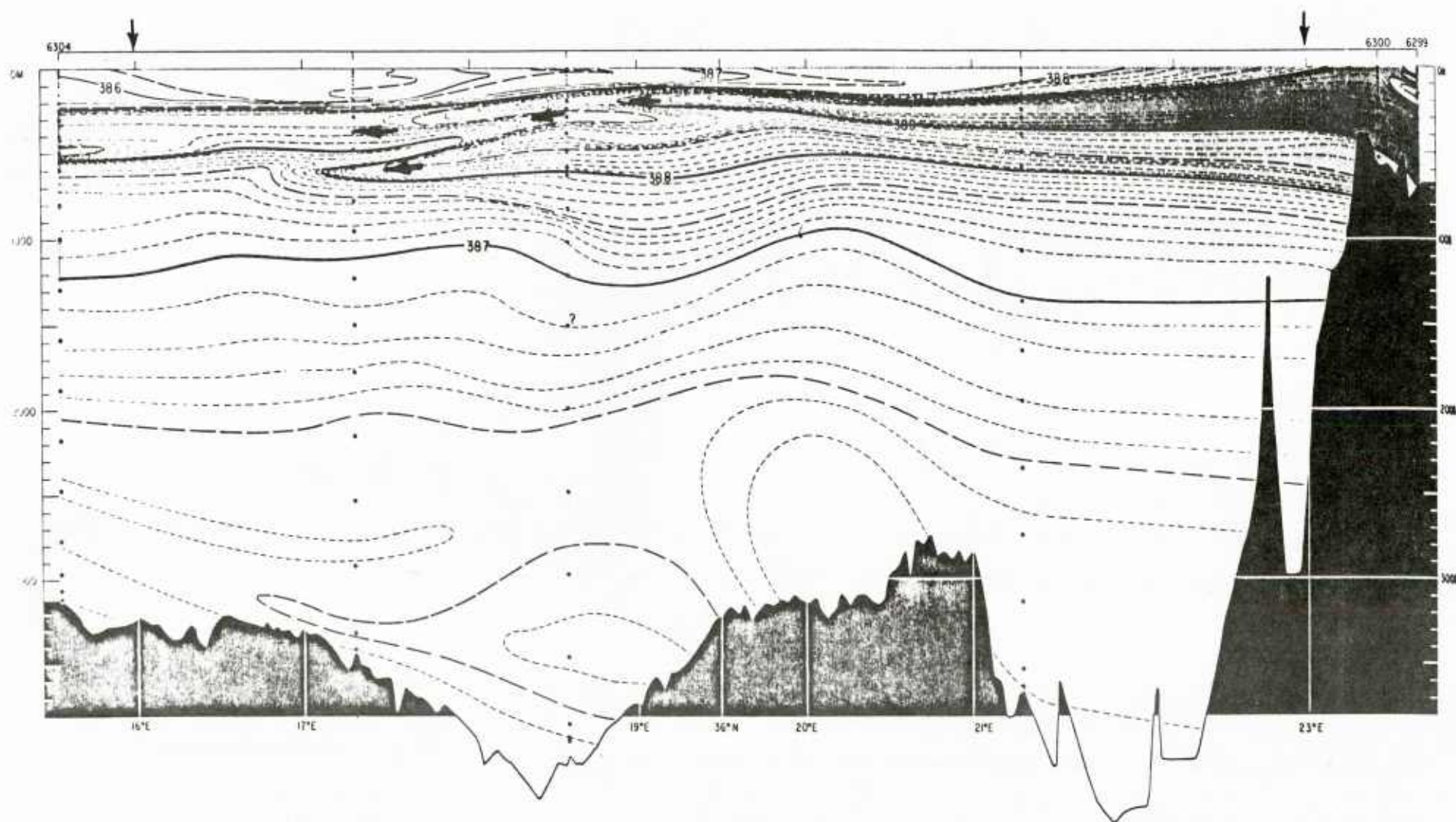


FIGURE 5-20: WINTER VERTICAL SALINITY CROSS-SECTION ALONG GREAT CIRCLE TRACK MX-04

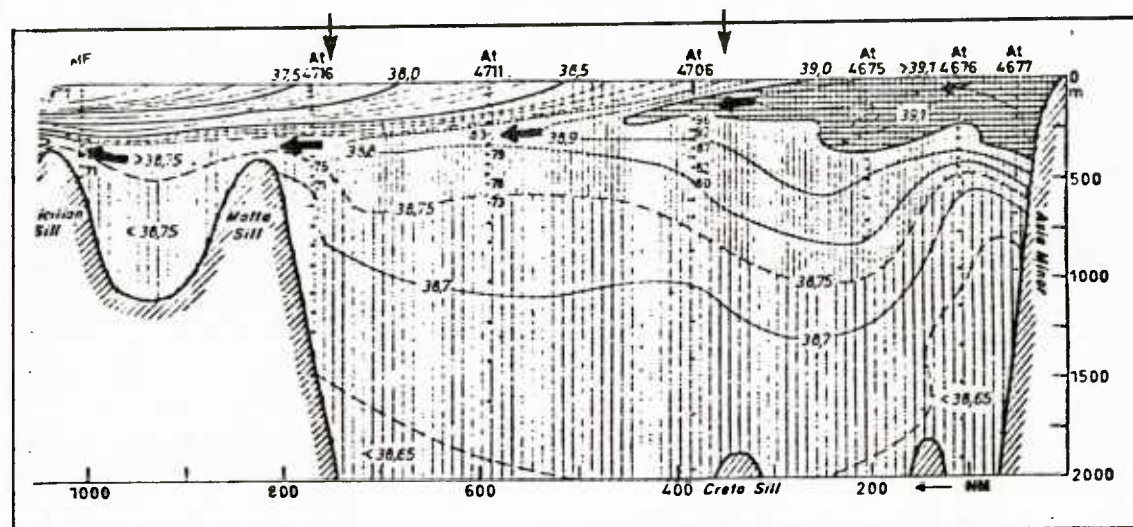


FIGURE 5-21: WINTER VERTICAL SALINITY CROSS-SECTION
ALONG GREAT CIRCLE TRACK MX-04

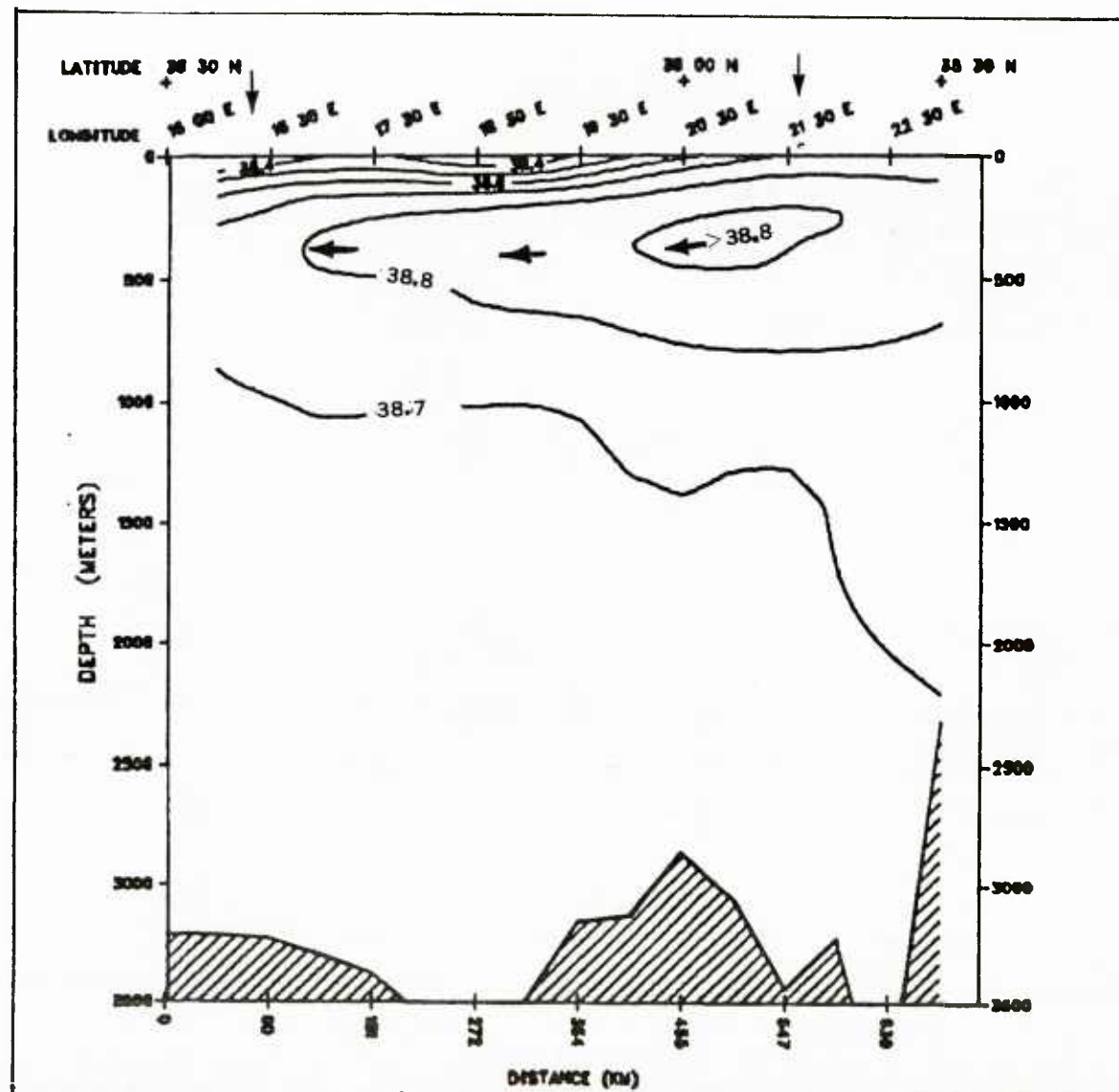


FIGURE 5-22: GDEM - WINTER VERTICAL SALINITY CROSS-SECTION ALONG GREAT CIRCLE TRACK MX-04

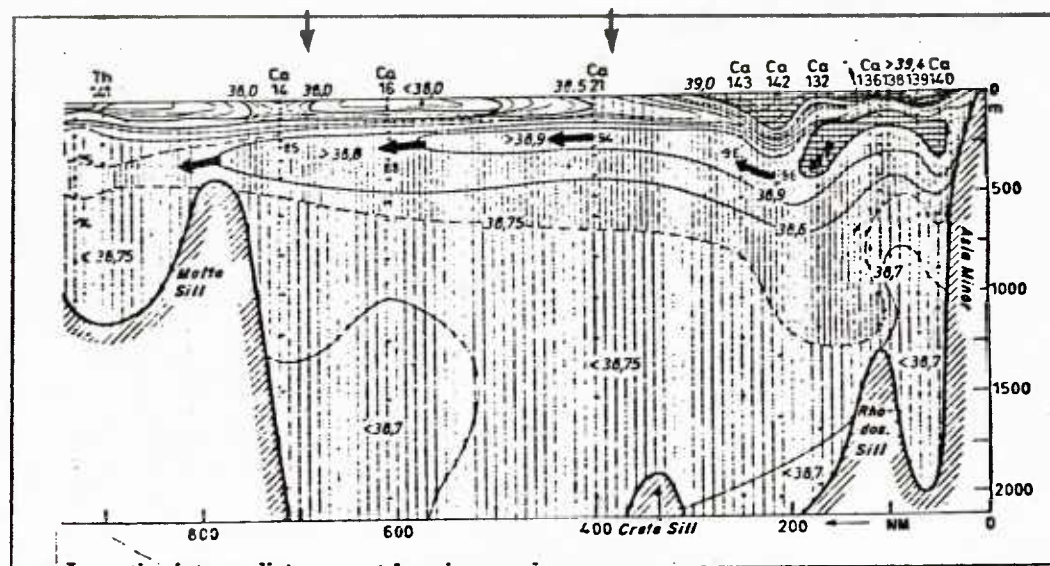


FIGURE 5-23: SUMMER VERTICAL SALINITY CROSS-SECTION
ALONG GREAT CIRCLE TRACK MX-04

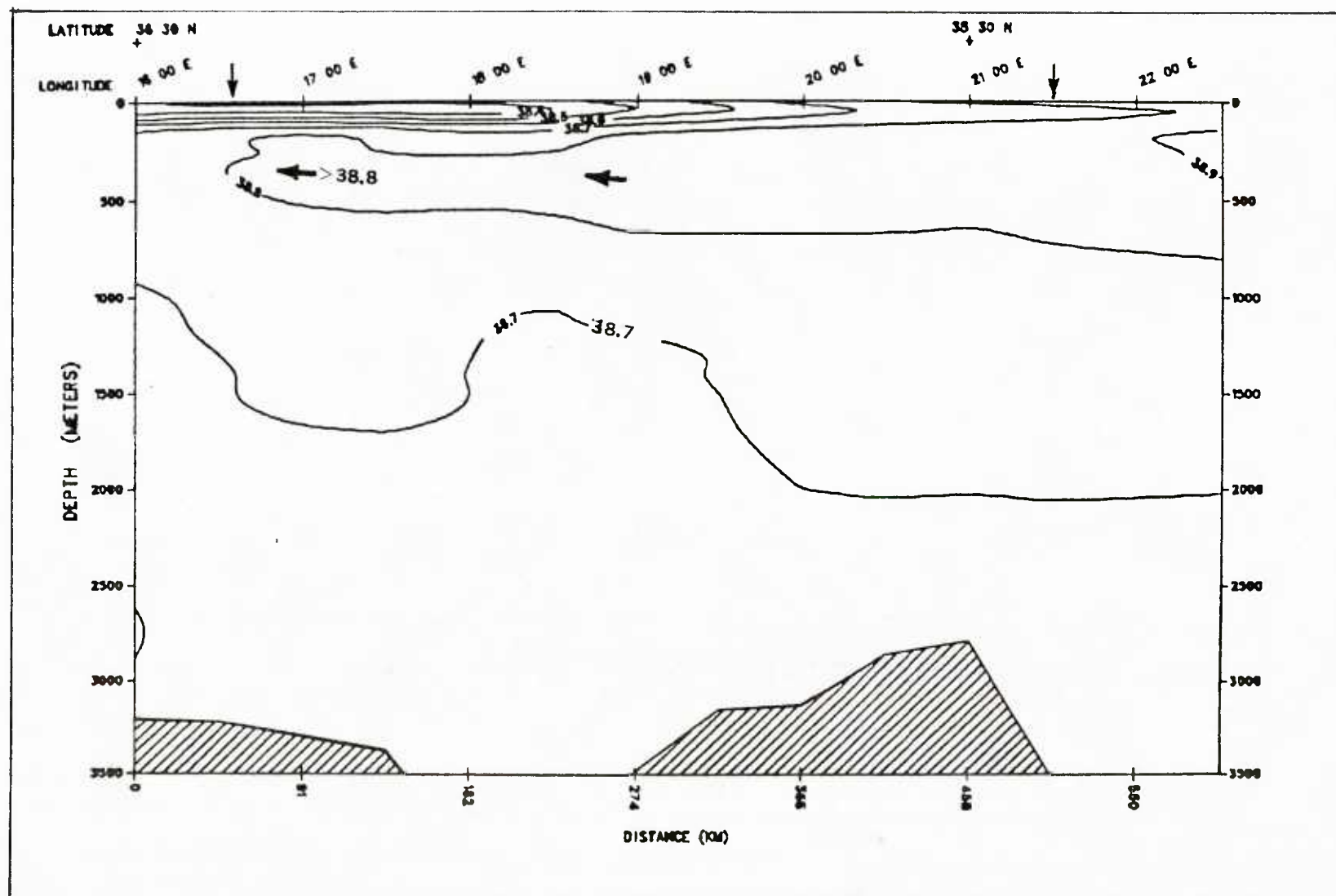


FIGURE 5-24: GDEM - SUMMER VERTICAL SALINITY CROSS-SECTION ALONG GREAT CIRCLE TRACK MX-04

5.5 Vertical Temperature and Salinity Comparisons for MX-05 (Aegean Sea)

Vertical cross-sections of salinity (S) for the fall time period were compared. The survey cross-sections were taken during the R.V. Chain cruise of 1961.

5.5.1. Regional Description

Section MX-05 was selected from the Aegean Sea region of the Mediterranean Sea. The vertical cross-sections are defined by a great circle track which originates at $38^{\circ}00'N$, $24^{\circ}00'E$, and terminates at $38^{\circ}00'N$, $27^{\circ}00'E$ longitude. The locations of the Aegean Sea and Section MX-05 are depicted on Figure 1-1.

Oceanographically, this region is considered semi-active and semi-variable. The authors consider this region as a bay of the eastern Mediterranean Sea characterized by relative shallowness and possessing many island barriers. The primary oceanographic contribution is that it acts as a passageway to the Black Sea. Dynamics leading toward the development of water mass contributions appear relatively minor in importance. This region does not appear to have a significant influence on the general oceanography of the eastern Mediterranean Sea.

Relatively shallow in depth, the Aegean Sea bathymetric configuration can be defined as being developed through a series of complex faulting and apparently a great deal of subsidence. The combination of these physical processes has resulted in the unique irregular topography for this region (Hill). Pollack (1951) conducted a brief survey in the southern Aegean Sea to determine the degree of exchange between the northern Mediterranean with the southern Aegean. In the upper 400 meters of the Aegean, the thermo-haline structure closely resembled that of the northern Mediterranean. The oxygen, however, reflected a somewhat different and less agreement - possibly due to noticeable biological activity in this zone.

into the Aegean Sea, which agrees with Nielsen's (1912) assumption regarding the movement of water in this region. The primary point of significance, however, is not that the surface waters of the Mediterranean flows into the Aegean Sea, but that there is no conclusive evidence, yet presented and based on existing data, which indicates a subsurface outflow of Aegean bottom water into the eastern Mediterranean via the channels between Asia Minor and the island of Crete. Due to the known relatively high values of oxygen and salinity in the southern Aegean, the presence of this parcel into the eastern Mediterranean would be readily detectable.

Meteorologically, this region is considered variable and seasonally active. The seasonal weather patterns are controlled to a degree by the monsoonal character of the Eurasian land mass. Cold outbreaks in winter are frequent due to the colder air mass to the north. Summer season is characterized by dry northerly to northwesterly flow over this region. The transitional seasons are different. Spring is relatively long (three months) when compared to fall (one month). The complex topographical features surrounding this region result in the channeling of air flow between island, mountain barriers, and coastal valleys.

5.5.2 Comparison

Due to the shallow water depths for this region and the short distance (less than 175 nautical miles) of the great circle track, comparisons of either temperature or salinity vertical cross-sections were not made.

5.6. Vertical Temperature and Salinity Comparisons for MX-06 (Levantine Sea)

Vertical cross-sections of temperature (T) and salinity (S) for the fall were compared. The survey cross-sections were taken during the R. V. Chain cruise of 1961.

5.6.1 Regional Description

Section MX-06 was selected from the Levantine Sea region of the Mediterranean Sea. The vertical cross-sections are defined by a great circle track which originates at $32^{\circ}30'N$, $32^{\circ}00'E$, and terminates at $36^{\circ}30'N$, $32^{\circ}00'E$. The locations of the Levantine Sea and Section MX-06 are depicted on Figure 1-1. Vertical cross-sections of temperature and salinity for MX-06 are shown on Figures 5-28 through 5-31.

Oceanographically, this region is considered to be active, variable and important to the overall surface distribution of salt and heat fluxes of the eastern Mediterranean basin. Within this region, processes leading to the development of Levantine Intermediate Water (L.I.W.), positive salt fluxes, localized near-surface stratifications in temperature and salinity from the Nile, and large-scale subsurface flow patterns (currents) are known to take place.

Nielsen (1912) presented a thesis that the source for the deep water of the Levantine Basin was the Aegean Sea. As further investigations were conducted in the years to follow, Nielsen's thesis became increasingly more unpopular. Schott (1915) reviewed Nielsen's work and doubted that there was a large enough flow of water out of the Aegean Sea to fill the Levantine Basin. Pollak (1951) conducted studies in the eastern Mediterranean basin which resulted in conclusions which were contrary to that of Nielsen. The Strait of Sicily was also eliminated as a source for Mediterranean deep water. This was due to the separation in the stratification of the vertical water column by an intervening layer of salinity maximum.

Pollak revealed that the source of Levantine Bottom Water was in the eastern basin proper. Confirmed by the distribution of oxygen in the deep layers of the entire eastern Mediterranean, considerable mixing appears to take place between the relatively fresh waters from the north with the saline waters of the upper hundred meters of the Ionian Sea. Sinking of this resultant parcel of water flows intermittently along the bottom into the major eastern basins in a counter-clockwise flow circulation.

If marked changes in gradients were to be used in determining the vertical limits of the Levantine Deep Water, a 700 meter depth could be viewed as the possible boundary layer. However, if absolute numerical values were to be used, approximately 1600 meters could be viewed as the possible upper limit for the deep water. Below 1600 m, dissolved oxygen values in the Ionian are found to be approximately 0.15 ml/l greater than those found in the Levantine Basin; the temperature and salinity structures are similar (e.g. temperature minimums near 13.57°C; salinity, isohaline near 38.65‰). For this report, the region between 750 to 1600 meters will be considered as a "transition zone" between the intermediate and deep waters of the eastern Mediterranean basins. This zone of transition is not applicable to the entire eastern Mediterranean, but predominantly in and near deep basin regions.

Wust (1961) presented an informative description of the vertical and horizontal distribution and flow of water parcels in the Levantine Basin. Identified were four different core masses, developed from the vertical distribution of temperature, salinity and oxygen: (1) the near-surface water, (2) the intermediate water, (3) the deep water, and (4) the bottom water. In discussions regarding the various watermasses which have been studied in the Mediterranean, the most popular is the Levantine Intermediate Water (L.I.W.). The most striking characteristic of the L.I.W. is the associated salinity maximum. During the winter period in the northern region of the Levantine Basin, studies have revealed that conditions for favorable water-mass formation exist. This region (located on both sides of the island of

Rhodes - sometimes spelled Rodhos) is where favorable surface conditions (low temperatures of 15.0°C ; high salinities of $39.1^{\circ}/\text{oo}$) for vertical thermal haline convective processes develop. The resultant newly formed winter parcel of water of high salinity spreads out within the core layer to all basins (eastern and western) of the Mediterranean. This process of water type formation appears to be a seasonal phenomenon (varying in degree from winter to winter) whose intensity and strength can be mapped from season to season. Figures 5-25, 5-26 and 5-27 illustrate the geographical placement of the core of the L.I.W. for winter and summer, respectively. The southerly displacement of the core in winter reflects a stronger presence in intensity, whereas the northerly displacement of the core in the summer reflects a weaker intensity of flow. The vertical spreading in the vicinity of formation changes to horizontal spreading while approaching the intermediate depths. The L.I.W. continues its general westerly direction passing through the Ionian Basin, over the Malta Sill, over the Strait of Sicily (system of sills) and into the western Mediterranean basin. This L.I.W. has been confirmed by investigators to flow out over the Gibraltar sill into the eastern North Atlantic Ocean. This westerly undercurrent flow of L.I.W. over the Gibraltar sill has been observed to be of measurable strength, at times reaching high velocities of more than 100 cm/sec near 275 meters in depth (Wust). This undercurrent on occasion has been referred to as the Levantine Intermediate Undercurrent. The presence and influence of this L.I.W. appears to be most strongly felt at depths that correspond to potential densities near 29.10 (Morel).

Treatment on the sources of deep and bottom waters for the eastern Mediterranean (which includes the Levantine Basin) have been discussed and presented in the oceanographic description of the Ionian Sea. Other features observed and measured in the Levantine Sea were thermal fronts and subsurface intrusions of less saline water. Levine and White (1972), during the cruise of the R. V. Chain in 1966, describe a thermal front, assumed continuous, which followed the general eastern coastline configuration of the Mediterranean, Figure 5-27. It is suggested by these investigators

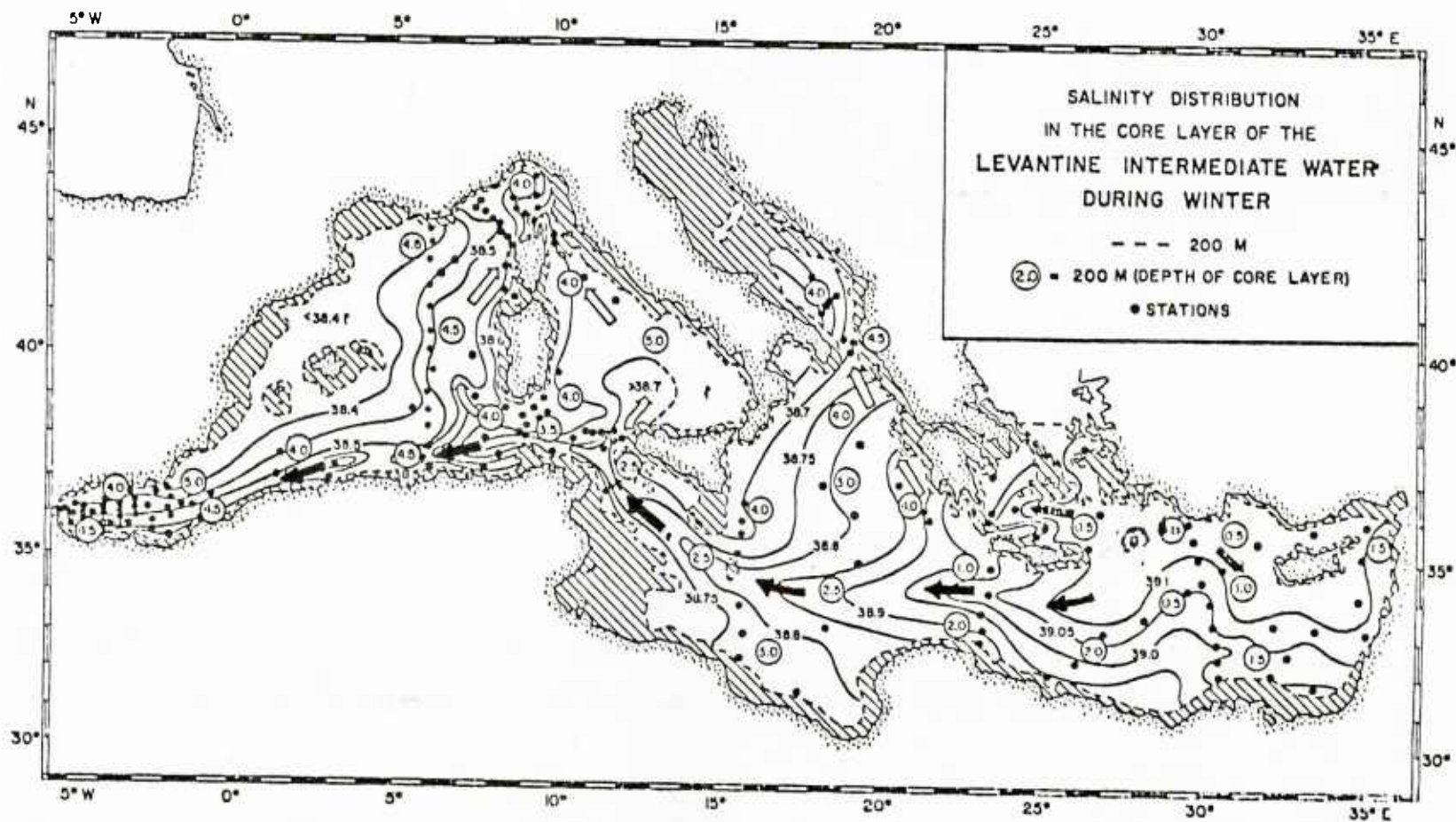


FIGURE 5-25: LOCATIONS OF THE SALINITY CORE LAYER
WITHIN THE LEVANTINE INTERMEDIATE WATER
IN THE WINTER (WUST, 1961)

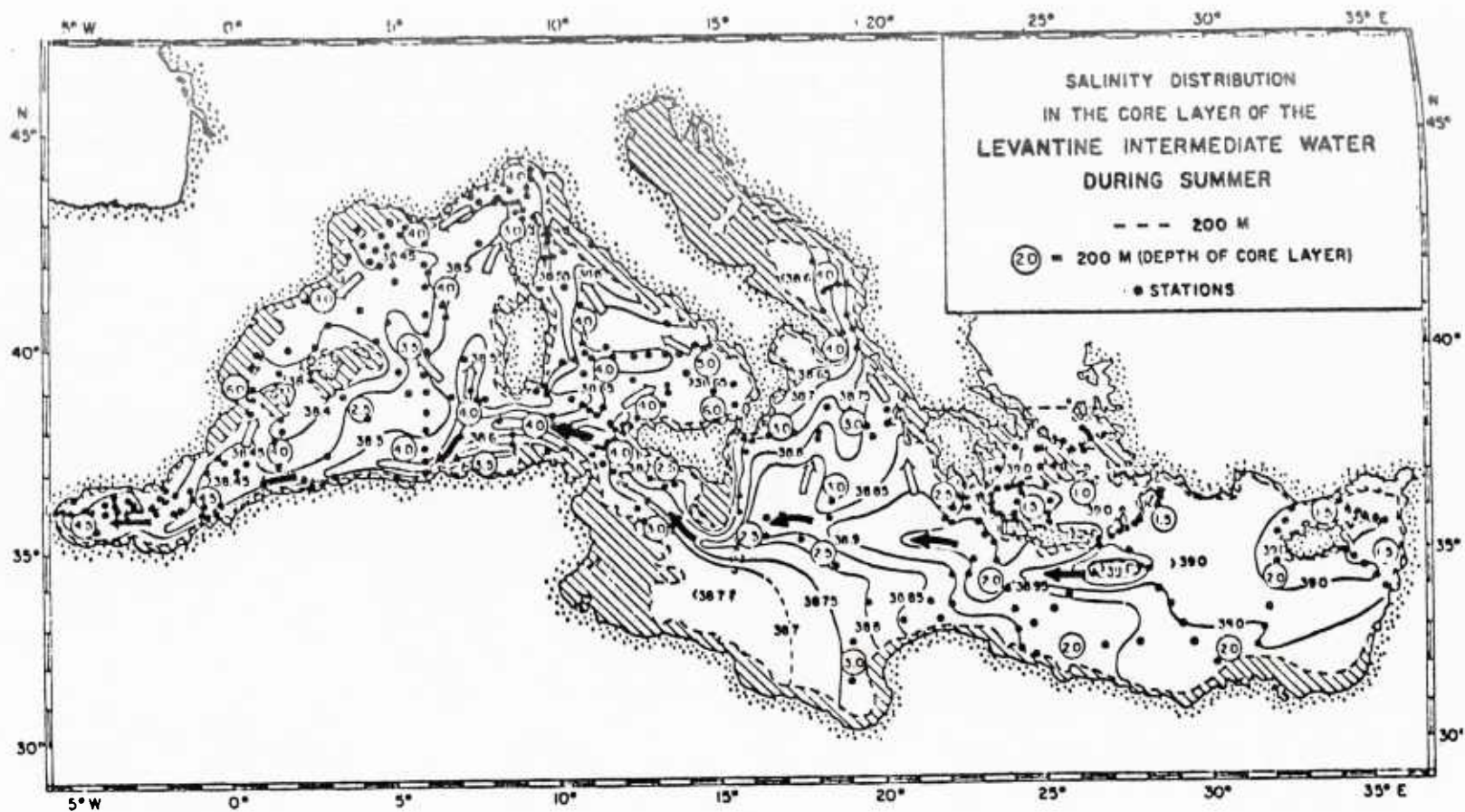


FIGURE 5-26: LOCATIONS OF THE SALINITY CORE LAYER
WITHIN THE LEVANTINE INTERMEDIATE WATER
IN THE SUMMER (WUST, 1961)

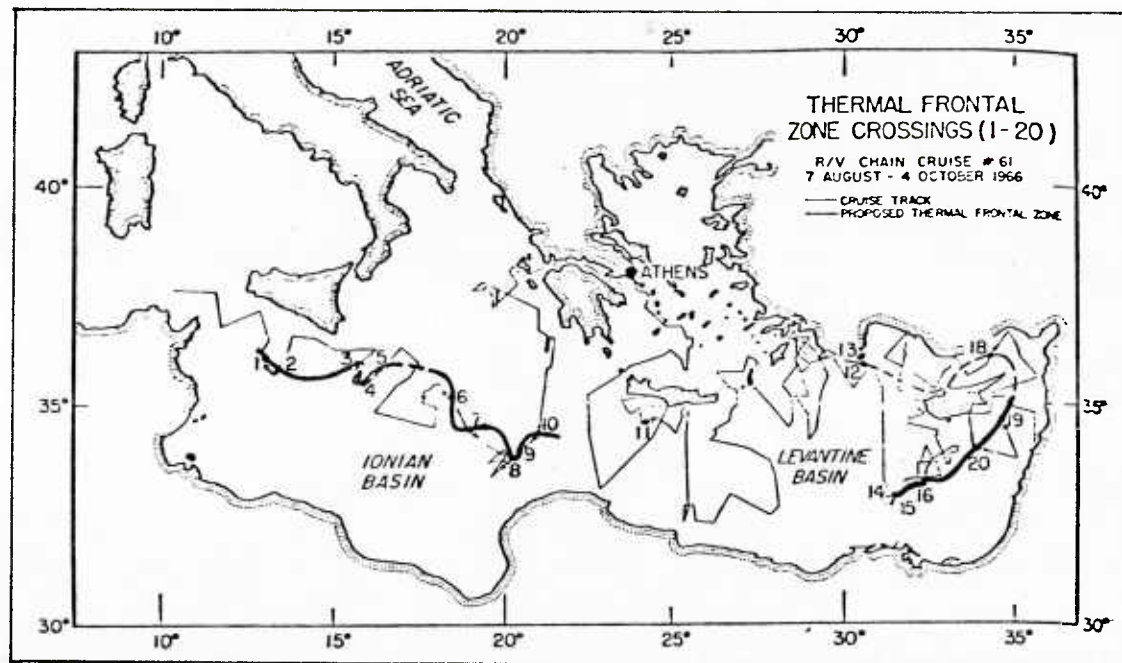


FIGURE 5-27: LOCATIONS OF THE THERMAL FRONTS
 IN THE IONIAN AND LEVANTINE SEAS
 (LEVINE AND WHITE, 1972)

that this thermal front is associated with the general counter-clockwise circulation around the eastern Mediterranean basin. Miller, Tschernia and Charnock have mapped the eastern Levantine basin. Their study revealed several features, one of which was the presence of fresh water intrusions at subsurface levels. A possible explanation for these intrusive layers of fresh water is that these parcels are related to large quantities of fresh water river run-off or discharge. Unfortunately, neither the persistence nor degree of temporal variability of this particular feature is adequately known.

Meteorologically, this region is considered variable. Seasonal weather patterns are largely influenced by patterns that develop over the adjacent land masses. Cyclogenesis development, in general, is limited and originates at other distant regions (i.e. Ionian Sea and the Aegean Sea regions). A minor region is located over Cyprus. The winter patterns are very cold (relative to the sea surface temperatures), unsettled, and have associated strong winds. The summer patterns are dry and with heated air masses having persistent surface winds.

5.6.2 Comparison

GDEM temperature and salinity vertical cross sections along great circle track MX-06 were compared with the Chain #21 data of October 18, 1961, to November 11, 1961, and evaluated as follows:

- Temperature

Fall comparisons of temperature revealed in both the GDEM and Chain 21 analyses the presence of known isotherms in this region. Both analyses properly reflected the 17.0°C isotherm, the 15.0°C isotherm, and the 14.0°C isotherm. Below 800 meters both analyses reflected the deep region as $13.5 \leq T < 14.0^\circ\text{C}$.

- Salinity

Fall comparisons of salinity revealed in both the GDEM and Chain #21 analyses the presence of similar isohalines in this region. Both analyses properly reflected the surface as a region of surface salinity maximum and followed below by a layer of

lower salinity (separating a subsurface layer of higher salinity) between approximately the 200 - 300 meter levels. The only difference was that this subsurface layer of higher salinity in GDEM was not reflected as being quite as extensive along the track as that reflected by the Chain. In both analyses (near the 600 meter level + 200 meters) the $38.8^{\circ}/\text{oo}$ isohaline is noted. GDEM isohaline ($38.8^{\circ}/\text{oo}$) did penetrate deeper near $34^{\circ}30'N$ latitude than in the Chain analysis. Both analyses (below 1000 meters) reflected a similar deep region as $38.6^{\circ}/\text{oo} \leq S^{\circ}/\text{oo} \leq 38.8^{\circ}/\text{oo}$.

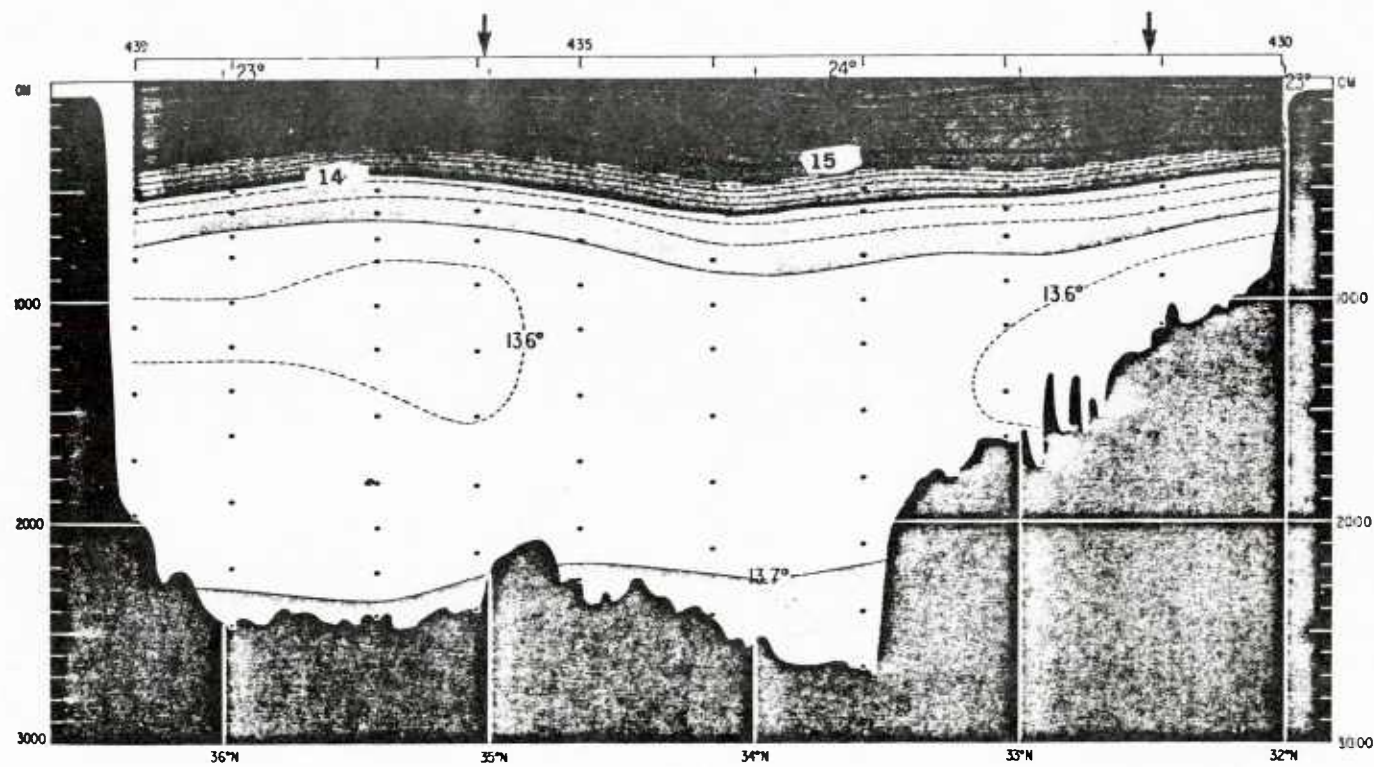


FIGURE 5-28: FALL VERTICAL TEMPERATURE CROSS-SECTION
ALONG GREAT CIRCLE TRACK MX-06

MED MODEL(MOD 3) TEMP 38 SON TO 32 OON ALONG 32E-AUTUMN.

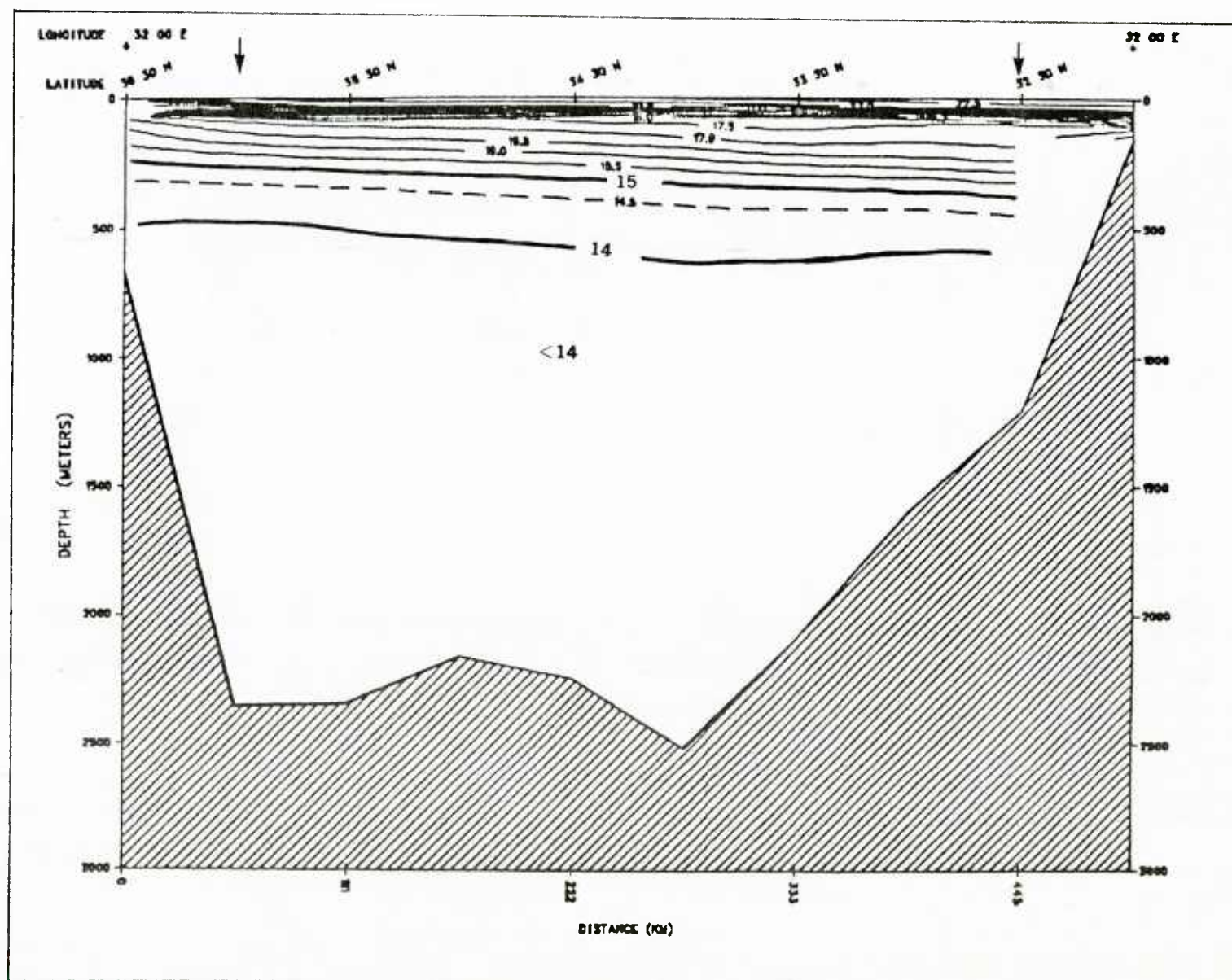


FIGURE 5-29: GDEM FALL VERTICAL TEMPERATURE CROSS-SECTION ALONG GREAT CIRCLE TRACK MX-06

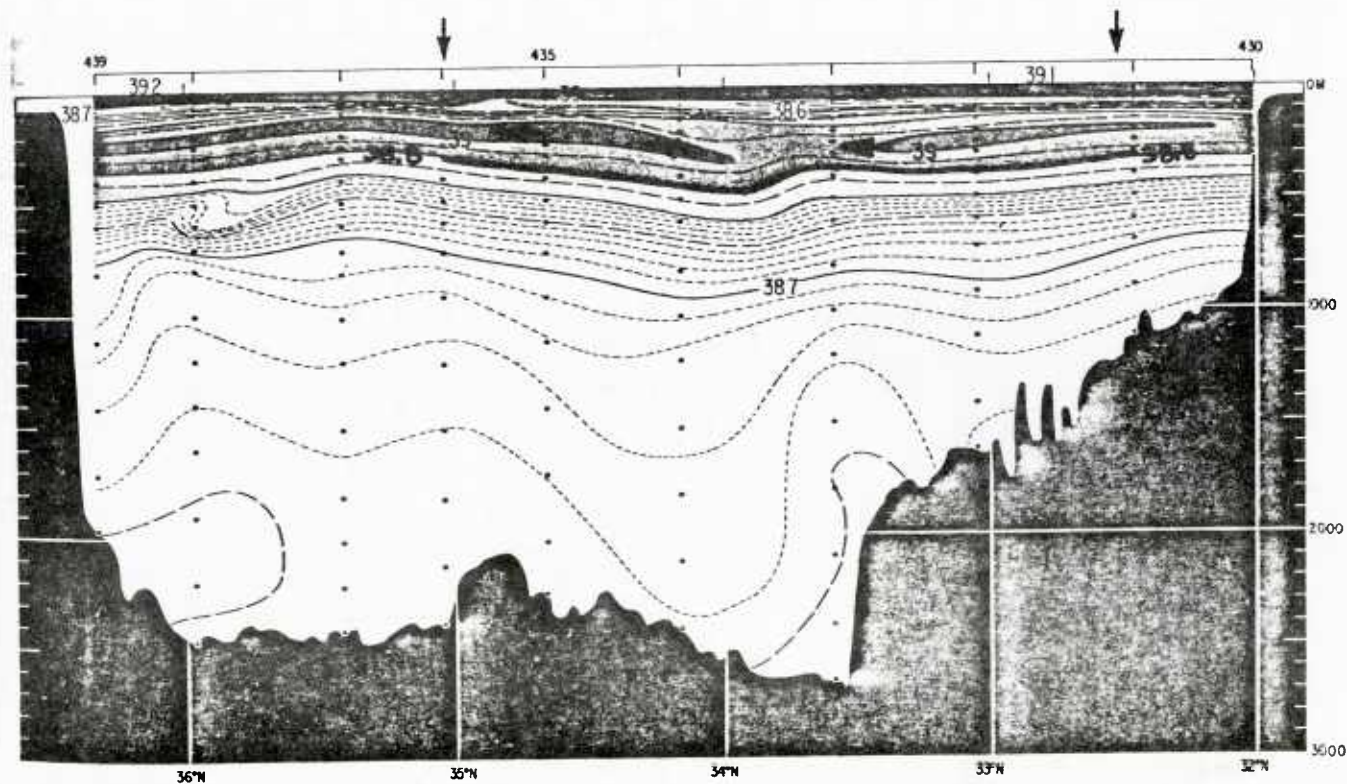


FIGURE 5-30: FALL VERTICAL SALINITY CROSS-SECTION
ALONG GREAT CIRCLE TRACK MX-06

understood. Also, it is suggested by Katz that one possible exit of the L.I.W. from the Balearic Sea may be located in the southern region near the island of Mallorca.

In reviewing the works by Wust and Miller, Tschernia, and Charnock, the Balearic appears to provide for two separate regions for the formation of two distinct Mediterranean water masses: the North Balearic Deep Water and the North Balearic Bottom Water. Analysis of oxygen distribution in the core layer of the Mediterranean Deep Water, from the studies by Wust and Miller, Tschernia and Charnock, indicates that the region north-east of the island of Mallorca and south of France (near the Golfe du Lion at approximately $42^{\circ}00'N$ latitude and $5^{\circ}00'E$ longitude) is the primary source and location for the formation of the North Balearic Deep Water. Other investigations (French naval vessel ORIGNY, 1903; R. V. ATLANTIS, U.S.A., 1961; and six vessels from the U.S.A., France, U.K. and Italy in 1969 of the MEDOC Group) have all revealed the same conclusion. The conclusion was that the winter formation and sinking of the deep water in this region follows three distinct phases: pre-conditioning, violent mixing, and sinking/spreading. Salinity values range near $38.20^{\circ}/\text{oo}$ to $38.48^{\circ}/\text{oo}$; surface σ_t exceeds 29.00 ; potential temperatures were near $10.0^{\circ}C$ to $12.0^{\circ}C$; and the depths to which sinking extended occurs approximately down to 1400 meters. Oxygen contents exceeding 4.6 ml/l were reported by Wust.

Analysis of potential temperature indicated that the Ligurian Sea north of the island of Corsica yielded itself as the location for the source and formation of the North Balearic Bottom Water. This bottom water contains relatively high oxygen and high salinity levels. Balearic Bottom Water is characterized by temperatures of $12.6^{\circ}C$ to $12.7^{\circ}C$, salinities of $38.35^{\circ}/\text{oo}$ to $38.45^{\circ}/\text{oo}$, and σ_t of 29.1 below 1500 meters.

Meteorologically, this region is considered active, variable, and seasonally influenced by an area that is known for cyclogenesis. This area is located off the eastern coast of Spain in the Balearic Sea and encompasses the Balearic Islands. Cyclogenesis over the Balearic Sea is frequently found in the winter, with common occurrences in the spring and fall.

5.7.2 Comparison

GDEM temperature and salinity vertical sections along great circle track MX-07 were compared with the Atlantis #263 data of February 4, 1961 to March 10, 1961 and evaluated as follows:

- Temperature

Winter comparisons of temperature revealed in both the GDEM and Atlantis #263 analyses the presence of known isotherms in this region. At the surface, both analyses reflected a layer of temperature maximum ($\geq 14.0^{\circ}\text{C}$) originating from the south and extending northward up to approximately the $39^{\circ}50'\text{N}$ latitude.

Below this surface layer ($\geq 14.0^{\circ}\text{C}$), the 13.5°C isotherm appeared in both analyses with GDEM being slightly deeper and extending to the surface at approximately $40^{\circ}45'\text{N}$ latitude. Both the analyses reflected a minimum temperature region (between 1000 meters to 2000 meters) of $12.5 \leq T^{\circ}\text{C} \leq 13.5^{\circ}\text{C}$. Below 2000 meters, both analyses reflected the deep region as $\geq 13.0^{\circ}\text{C}$.

- Salinity

Winter comparisons of salinity revealed in both the GDEM and Atlantis #263 analyses the presence of known isohalines in this region. At the surface, both analyses properly reflected a surface wedge of $\geq 38^{\circ}/\text{oo}$ extending northward and surfacing near $41^{\circ}00'\text{N}$ latitude. Surface salinity minimums in both analyses were to the right hand side of the track (southern portion). The continuous subsurface isohaline ($38.4^{\circ}/\text{oo}$) in both analyses was reflected around the 200 meter level.

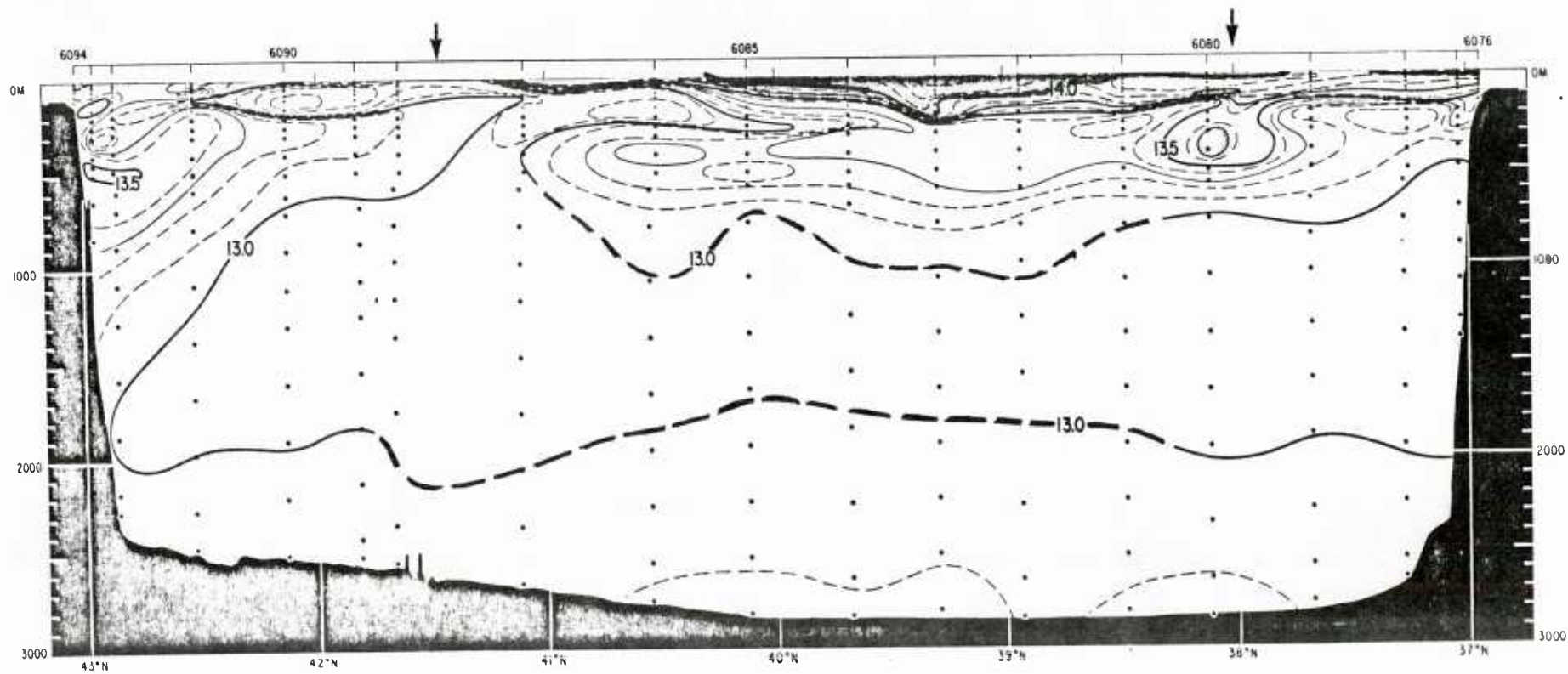


FIGURE 5-32: WINTER VERTICAL TEMPERATURE CROSS-SECTION
ALONG GREAT CIRCLE TRACK MX-07

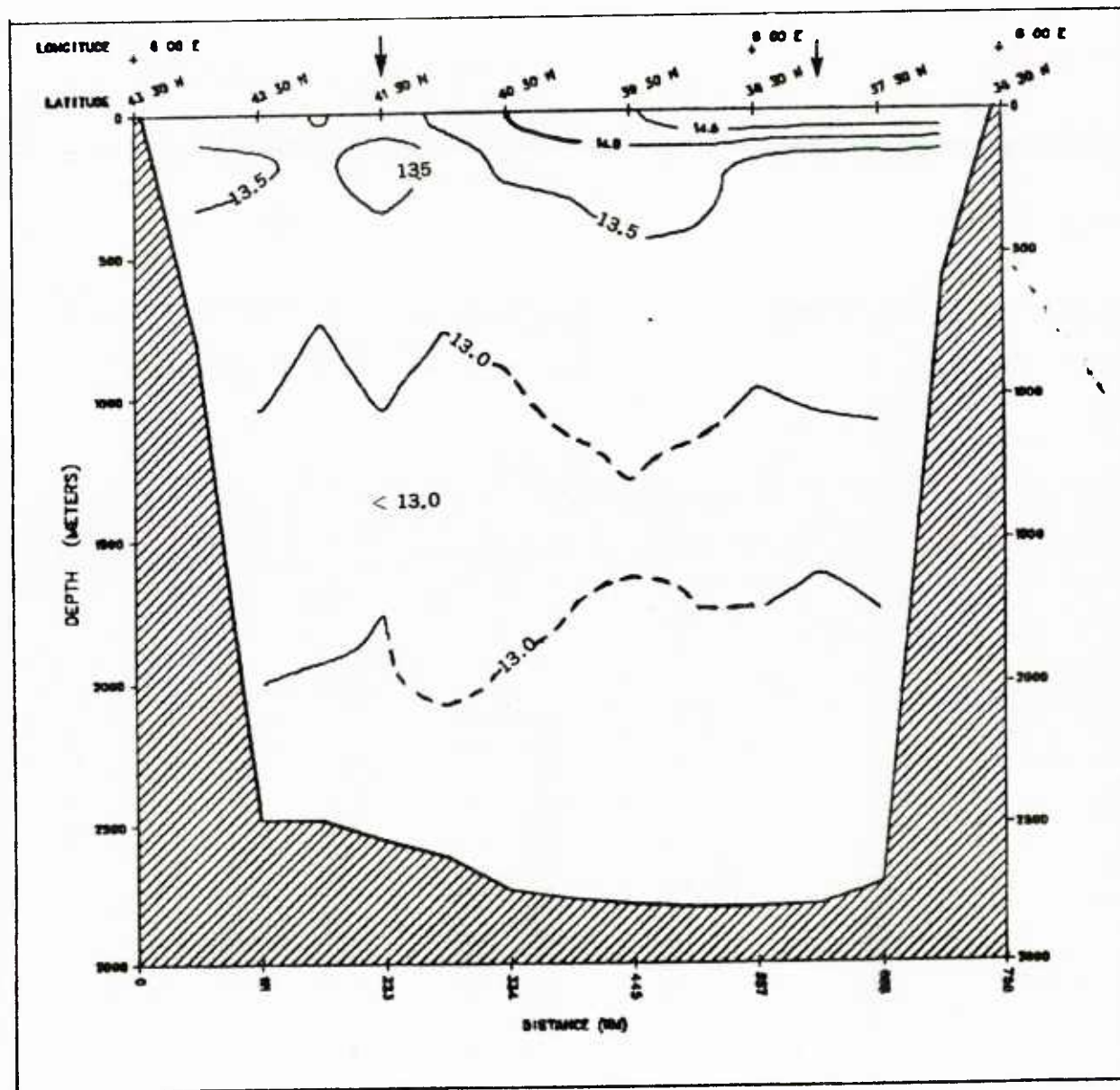


FIGURE 5-33: GDEM WINTER VERTICAL TEMPERATURE CROSS-SECTION ALONG GREAT CIRCLE TRACK MX-07

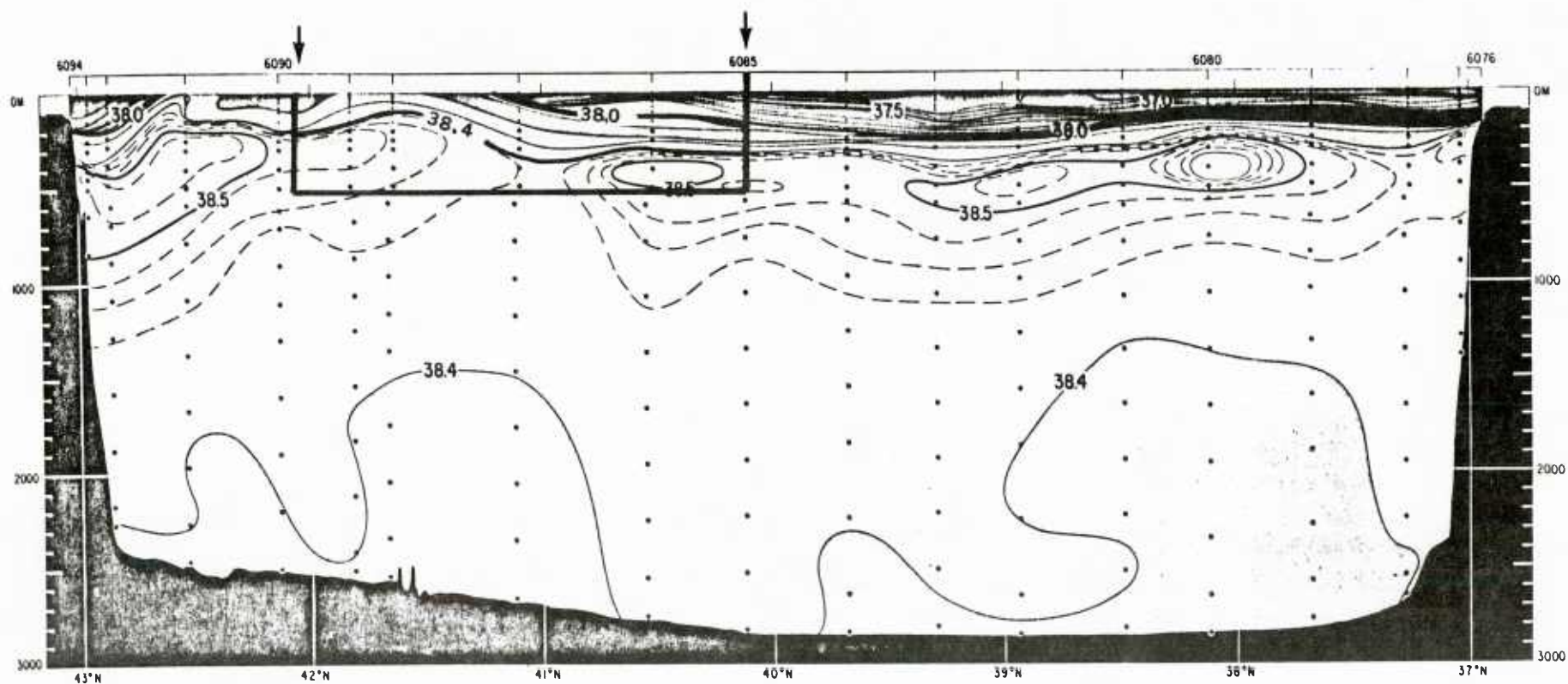


FIGURE 5-34: WINTER VERTICAL SALINITY CROSS-SECTION
ALONG GREAT CIRCLE TRACK MX-07

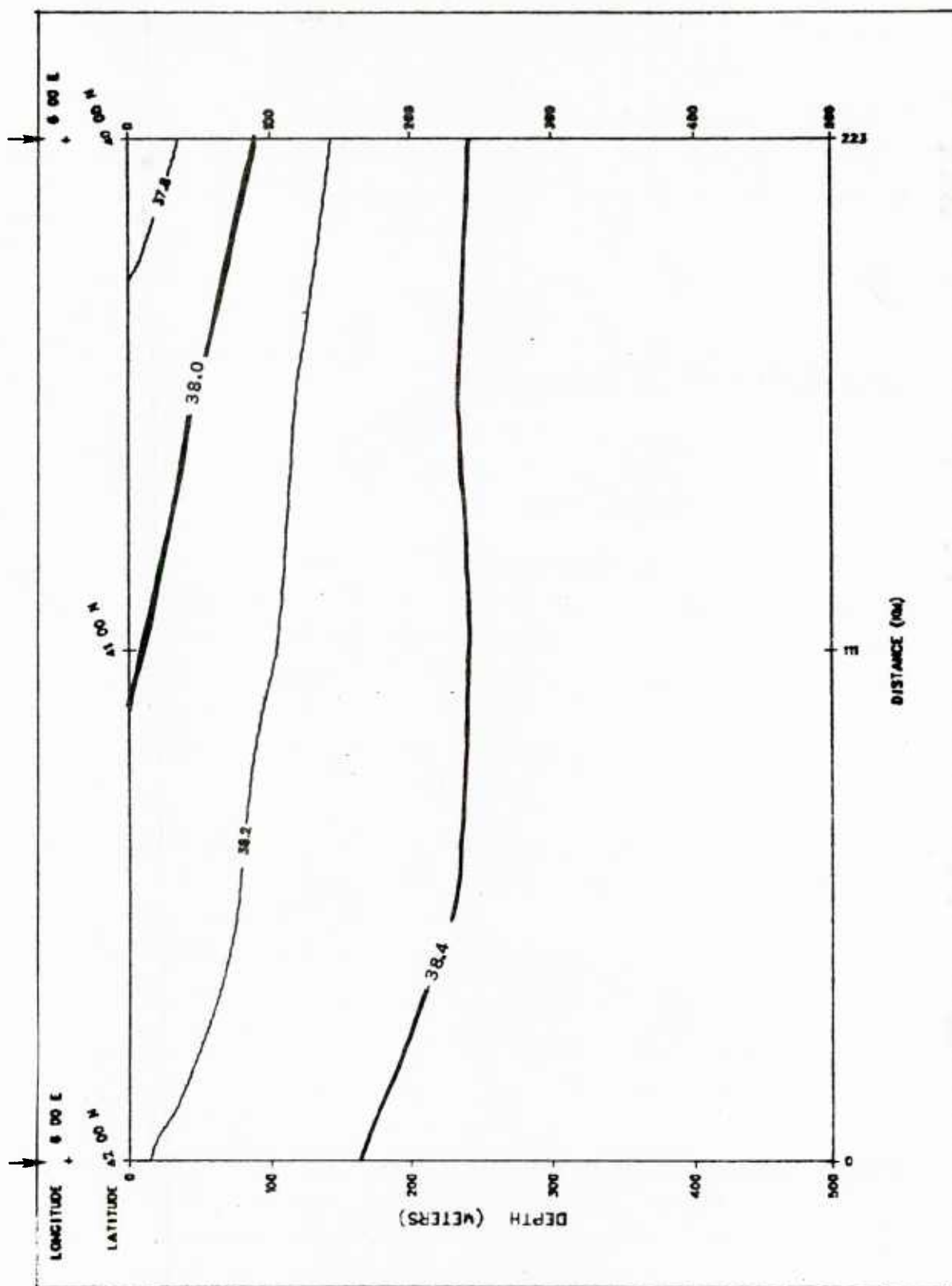


FIGURE 5-35: GDEM WINTER VERTICAL SALINITY CROSS-SECTION ALONG GREAT CIRCLE TRACK MX-07

5.8 Vertical Temperature and Salinity Comparisons for MX-08 (Ionian Sea)

Vertical cross-sections of temperature (T) and salinity (S) for the winter time period were compared. The survey cross-sections were taken during the R. V. Atlantis I cruise of 1962.

5.8.1 Regional Description

Section MX-08 was selected from the Ionian Sea region of the Mediterranean Sea. The vertical cross-sections are defined by a great circle track which originates at $32^{\circ}00'N$, $20^{\circ}00'E$ and terminates at $40^{\circ}00'N$, $20^{\circ}00'E$. The locations of the Ionian Sea and Section MX-08 are depicted on Figure 1-1. Vertical cross-sections of temperature and salinity for MX-08 are shown on Figures 5-38 through 5-41.

Oceanographically, this region is considered variable. The ocean variability and changes in the near-surface vertical water column are directly influenced by the impulses received from the paths of cyclogenesis through mechanical mixing (especially in the winter and early spring). Because of the seasonal influence of surface air masses from the Sahara Desert, this area will reflect wide vertical variability in the surface and near-surface stratification, especially in salinity.

The Ionian Sea is an active basin and contributes toward Mediterranean watermass formations, thermal fronts, displacements of the proximity of the Levantine Intermediate Water (L.I.W.), etc. General surveys and in-depth studies have both been conducted in furthering our understanding of the above features.

Early studies by Nielsen (1912) indicate that the deep waters of the Ionian Sea are formed in the southern Aegean Sea (possibly north of Crete). Schott (1915) conducted a review of Nielsen's work. In his review, Schott agreed with Nielsen regarding the location of Ionian deep water formation, but doubted that sufficient quantities of water flow out from the southern Aegean Sea to fill the Levantine Basin. Pollak (1951) expressed a contrary opinion to those of Nielsen and Schott. Pollak concluded that the Ionian

Deep Water is formed north of the Ionian Basin proper and not in the southern Aegean Sea. In reviewing the work of Pollak as well as other foreign data sets available for this particular region, the authors are in agreement with the thesis of Pollak. Characteristics of the Ionian Deep Water existing at roughly 1600 meters are: for temperature, a minimum of 13.57°C ; for salinity, isohaline of $38.65^{\circ}/\text{oo}$; for oxygen, 3.9 ml/l to 4.0 ml/l . The physical characteristics of temperature, salinity and dissolved oxygen appear to reflect the properties of water found in the region near the southern limits of the Adriatic Sea (the Strait of Otranto). In this region, it is possible for mixing to occur of waters from a region of relatively fresh water (river effluent) from the north (Adriatic) with the more saline waters of the upper Ionian. This newly mixed parcel of water results due to sufficient surface cooling and vertical convection in winter. The resultant mixture eventually sinks towards the bottom and flows out through the Strait of Otranto into the Ionian Sea. The magnitude and quantity of this outflowing Ionian Deep Water is neither clearly understood nor adequately measured; however, there seems to be little doubt that the impulses of outflow are irregular depending to a large extent on the prevailing weather regimes from winter to winter. This deep water should be detectable throughout the major Ionian Sea Basin. The outflow originates along the bottom of the western side of the Strait, then flows in a counter-clockwise circulation pattern (Pollak, 1951; Wust, 1961). Further evidence of the outflow is that the water at the sill depth of the Strait of Otranto has a higher potential density (the majority of the time in winter) than the deep waters of the eastern Mediterranean. This differential in potential densities can allow for a net downslope flow into the Ionian Sea.

Although some flow has been measured and observed through the Strait of Messina by Nielsen (1912) and Vercelli (1925), this passageway into the Ionian Sea has been ruled out as a major channel for water transport between the eastern and western Mediterranean Basins. The amount of flow and exchange through the Strait of Messina when compared to that taking

place through the Strait of Sicily and the Strait of Otranto would be very small by comparison. In the past, investigations have been conducted by Frassetto (1964) revealing that the primary water exchange between the eastern and western Mediterranean Basins occurs in the region of the Strait of Sicily* over at least two sills (or systems of sills) and the exchanges are confined to depths not greater than 558 meters on the Eastern Sill (almost exactly along the $15^{\circ}00'E$ meridian) between the Medina Bank and south of Malta.

Zones of high thermal gradients were found and studied by Levine and White (1972) in the Ionian Sea. The most striking feature of these zones was that thermal fronts were measured and observed having thermal gradients exceeding $1^{\circ}C/10$ km at either the surface or in the seasonal thermocline. The thermal discontinuity appeared not to be continuous but discontinuous in a step-wise fashion. Other investigations have been conducted on specific regions of the thermal fronts described by Levine and White. Woods and Watson (1970); Woods (1972); Johannessen, De Strobel and Gehin (1971); Johannessen (1971); and Briscoe, Johannessen and Vincenzi (1974) all have studied the western portion known as the Maltese Front. This front extends from the southern tip of Sicily to about $35^{\circ}30'N$ and appears to coincide with the edge of the continental shelf. The northern region of this front revealed changes across the front of 1.0° to $1.5^{\circ}C$ in temperature; and 0.6 to $1.0^{\circ}/\text{oo}$ in salinity. The width was estimated at approximately eight to ten nautical miles.

The core of the L.I.W. flows in a predominantly westerly direction through the southern region of the Ionian Basin. The placement of the axis of the L.I.W. core layer appears to be seasonally variable. The core layer appears to be displaced southerly in the winter (indicating weaker in strength) and northerly in the summer (indicating stronger in strength). This seasonal displacement can be observed in Figures 5-36 and 5-37 (Wust 1961), and 5-42 (Levine and White 1972).

*Note: The "Strait of Sicily" in the text should be taken in the broadest meaning to include all the area between the Meridian of Malta (or Medina Bank) and a line joining Cape Bon to the Aegates Islands (Marittimo).

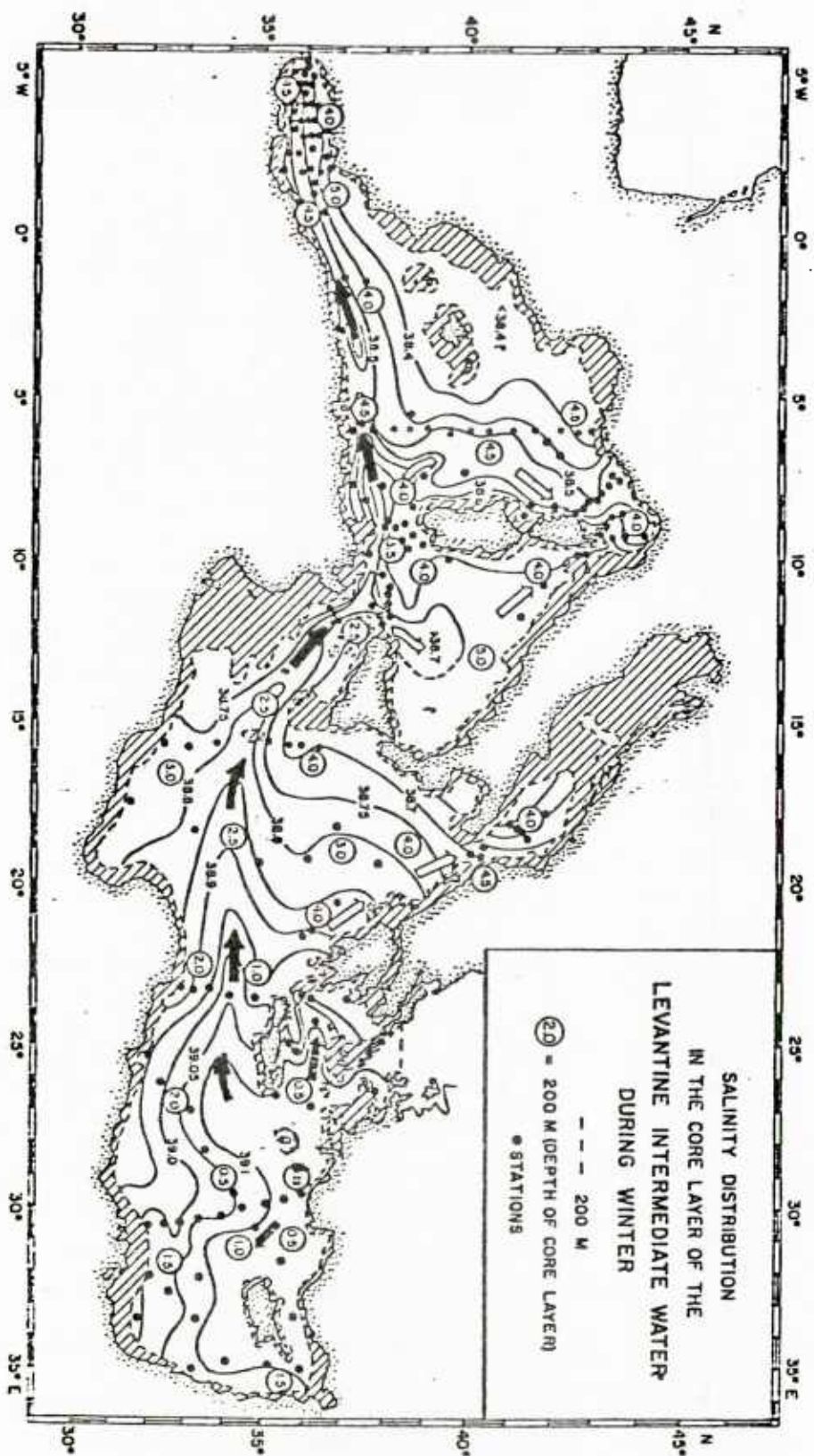


FIGURE 5-36: LOCATIONS OF THE SALINITY CORE LAYER WITHIN THE LEVANTINE INTERMEDIATE WATER IN THE WINTER (WUST, 1961)

FIGURE 5-37: LOCATIONS OF THE SALINITY CORE LAYER WITHIN THE LEVANTINE INTERMEDIATE WATER IN THE SUMMER (WUST, 1961)

Meteorologically, this region is considered variable and seasonally active. The seasonal patterns are controlled primarily by the monsoonal characteristics of the Sahara Desert to the south and the Eurasian land mass to the north. The winters are characterized by a dominant high pressure with associated unsettled, windy conditions. The summers are characterized by a relatively weak high pressure with associated warm, dry settled conditions and light winds. Cyclogenesis does occur over the Ionian Sea. With their origin in the Atlas Mountains of Algeria and Tunisia, the primary path for the North African cyclones is north-eastward across the Ionian Sea. A secondary zone for Ionian cyclogenesis is located over the northern portion of the Ionian Sea. This region is known to generate southeastward cyclones that are associated with the southerly invasion of cold-air-mass movements from the Adriatic Sea.

5.8.2 Comparison

GDEM temperature and salinity vertical cross sections along great circle track MX-08 were compared with the Atlantis #275 data of February 1, 1962 to March 24, 1962 and evaluated as follows:

- Temperature

Winter comparisons of temperature revealed in both the GDEM and Atlantis #275 analyses the presence of the known isotherms in this region. Both analyses properly reflected the surface temperature maximum ($>16^{\circ}\text{C}$) which exists below $35^{\circ}00'\text{N}$ latitude. The thickness of this surface maximum layer in both analyses was ≤ 200 meters. The 16.5°C isotherms in both analyses were realistic. Remaining above the 300 meter level in both analyses, as well as surfacing at approximately $\approx 36^{\circ}30'\text{N}$ latitude, both the GDEM and Atlantis #275 analyses were in agreement geographically with the thermal frontal zones in the Ionian as previously described by Levine and White (1972) during their R. V. Chain cruise #61 near station #7. Below the 16.5°C isotherm, both the 15.0°C and 14.5°C isotherms were similar and reflected in both analyses. Both analyses exhibited a southerly decrease in the thickness of the layer which exists between the 14.0°C and 15.0°C isotherms; below 1000 meters, the values for temperature in both analyses for the deep region were $13.5^{\circ}\text{C} \leq T^{\circ}\text{C} \leq 14.0^{\circ}\text{C}$.

- Salinity

Winter comparisons of salinity revealed in both the GDEM and Atlantis 275 analyses the presence of the known isohalines in this region. At the surface, both analyses properly reflected a known southern minimum layer of salinity ($\leq 38.4^{\circ}/\text{oo}$) below $34^{\circ}00'\text{N}$ latitude. At mid-depths between approximately the 200 meter and 700 meter levels, both analyses properly reflected the major known subsurface layer of salinity maximum ($>38.8^{\circ}/\text{oo}$) throughout the section. Both analyses properly reflected the core of this maximum to increase in depth (from approximately 200 meters down to 700 meters) along a northward track from $33^{\circ}00'\text{N}$ latitude to $38^{\circ}00'\text{N}$ latitude. Below 1000 meters, both analyses reflected the deep region as $38.6^{\circ}/\text{oo} \leq S^{\circ}/\text{oo} \leq 38.8^{\circ}/\text{oo}$.

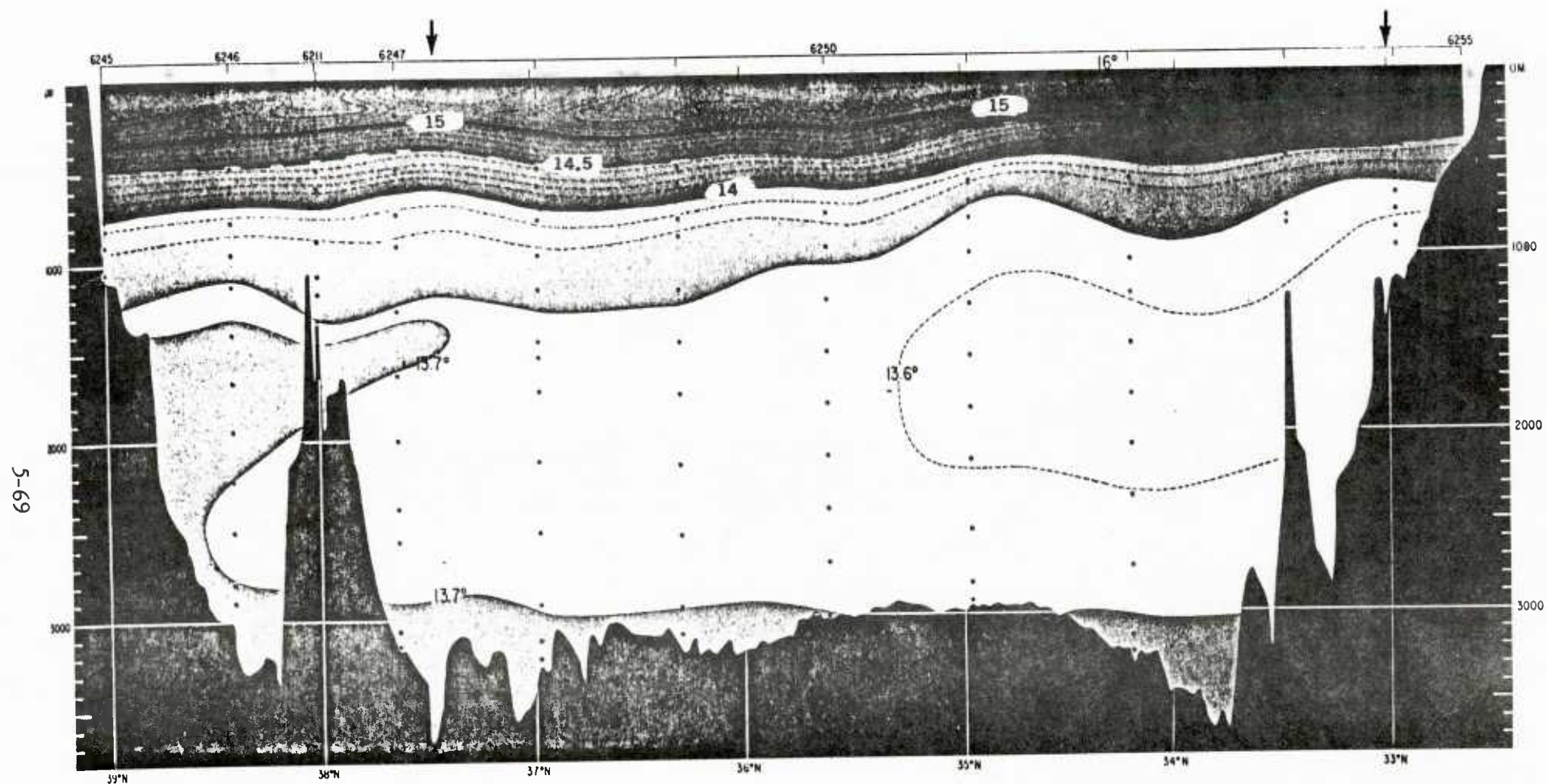


FIGURE 5-38: WINTER VERTICAL TEMPERATURE CROSS-SECTION ALONG GREAT CIRCLE TRACK MX-08

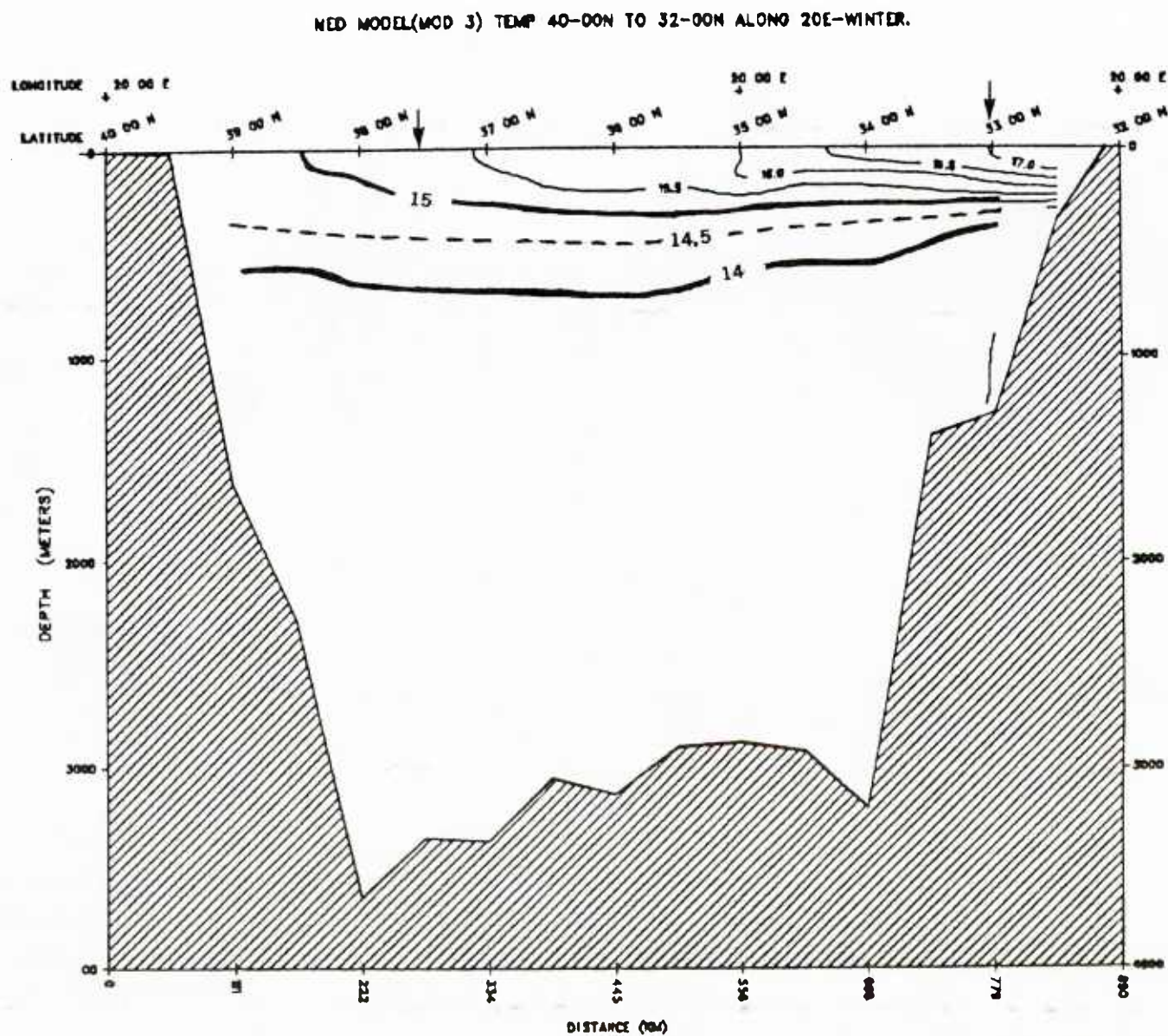


FIGURE 5-39: GDEM - WINTER VERTICAL TEMPERATURE CROSS-SECTION ALONG GREAT CIRCLE TRACK MX-08

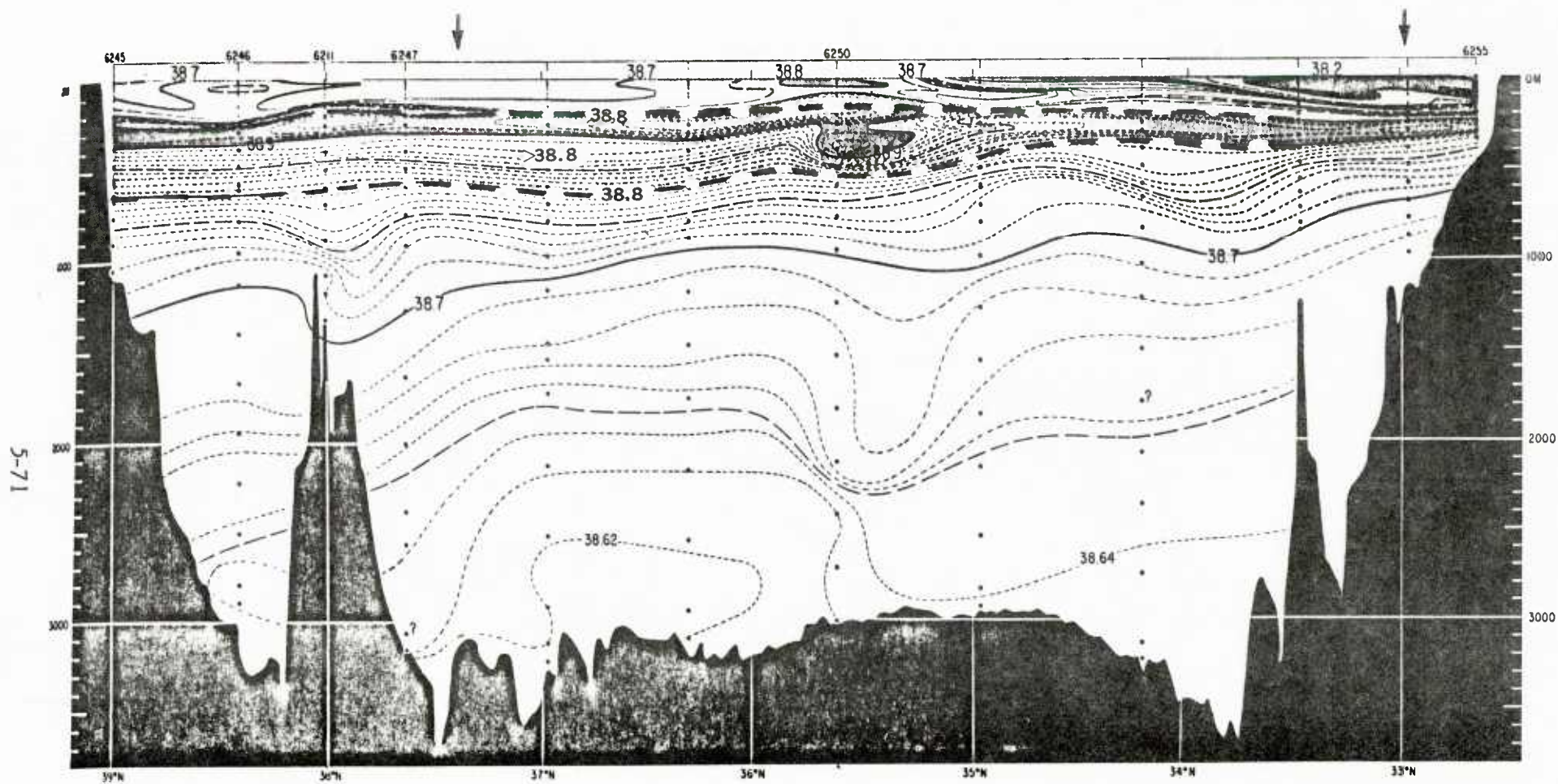


FIGURE 5-40: WINTER VERTICAL SALINITY CROSS-SECTION ALONG GREAT CIRCLE TRACK MX-08

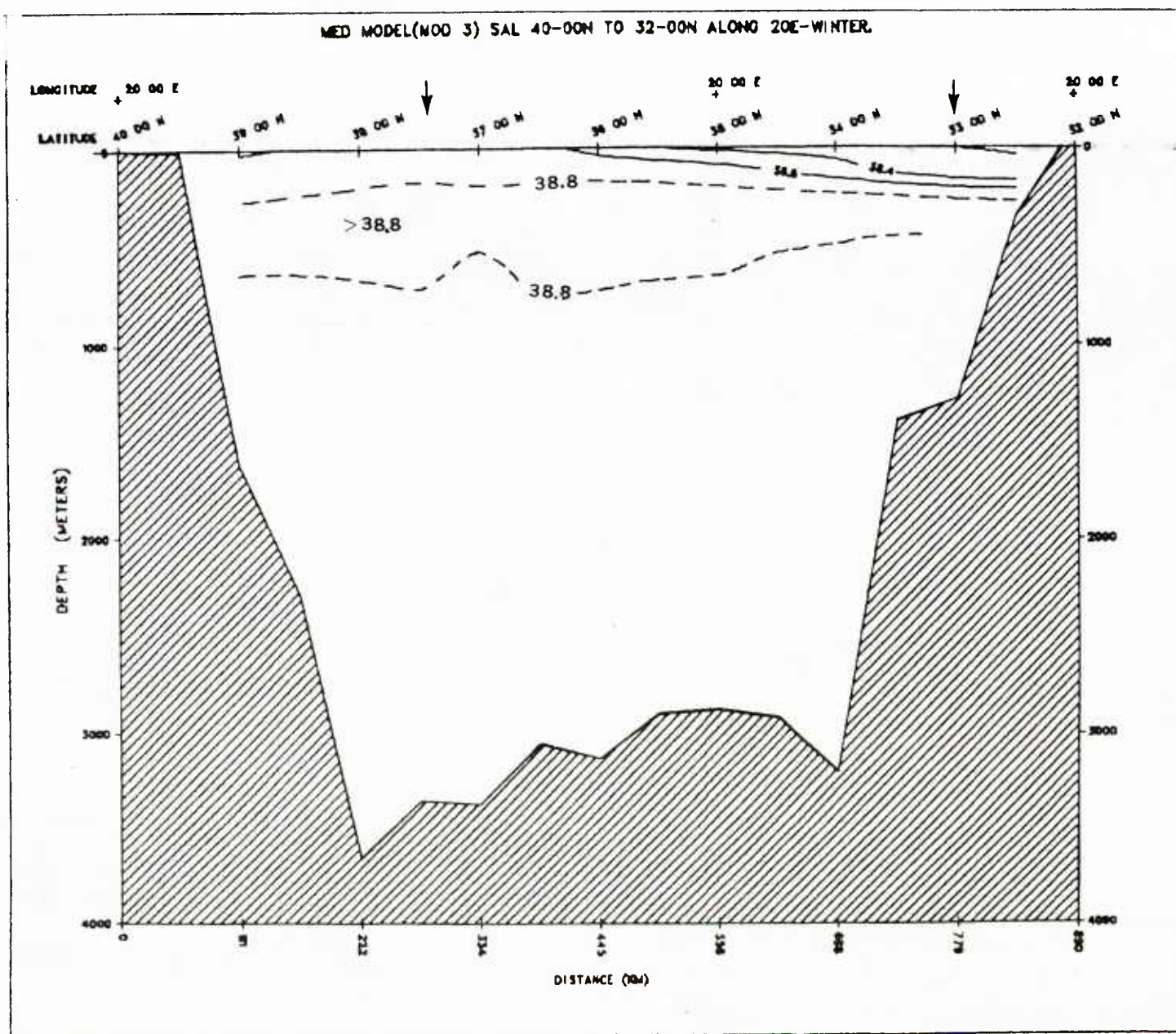


FIGURE 5-41: GDEM - WINTER VERTICAL SALINITY CROSS-SECTION ALONG GREAT CIRCLE TRACK MX-08

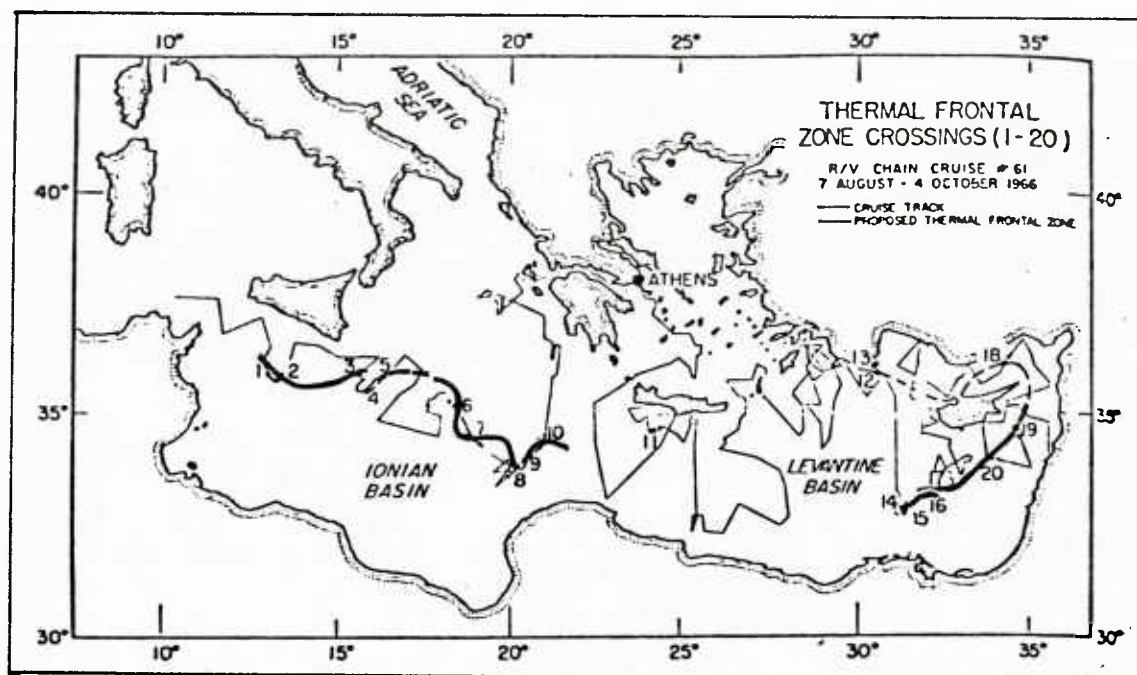


FIGURE 5-42: LOCATIONS OF THE THERMAL FRONTS
IN THE IONIAN AND LEVANTINE SEAS
(LEVINE AND WHITE)

5.9 Vertical Temperature and Salinity Comparisons for MX-09 (Levantine Sea)

Vertical cross-sections of temperature (T) and salinity (S) for the fall time period were compared. The survey cross-sections were taken during the R. V. Chain cruise of 1961.

5.9.1 Regional Description

Section MX-09 was selected from the Levantine Sea region of the Mediterranean Sea. The vertical cross-sections were defined by a great circle track which originates at $31^{\circ}30'N$, $27^{\circ}00'E$ and terminates at $36^{\circ}30'N$, $27^{\circ}00'E$. The locations of the Levantine Sea and Section MX-09 are depicted on Figure 1-1. Vertical cross-sections of temperature and salinity for MX-08 are shown on Figures 5-43 through 5-46.

Oceanographically, this region is considered to be active, variable and important to the overall surface distribution of salt and heat fluxes of the eastern Mediterranean basin. Within this region, processes leading to the development of Levantine Intermediate Water (L.I.W.), positive salt fluxes, localized near-surface stratifications in temperature and salinity from the Nile, and large-scale subsurface flow patterns (currents) are known to take place.

Nielsen (1912) had presented a thesis that the source for the deep water of the Levantine Basin was the Aegean Sea. As further investigations were conducted in the years to follow, Nielsen's thesis became increasingly more unpopular. Schott (1915) reviewed Nielsen's work and doubted that there was a large enough flow of water out of the Aegean Sea to fill the Levantine Basin. Pollack (1951) conducted studies in the eastern Mediterranean basin which resulted in conclusions which were contrary to that of Nielsen. The Strait of Sicily was also eliminated as a source for Mediterranean deep water. This was due to the separation in the stratification of the vertical water column by an intervening layer of salinity maximum. Pollack revealed that the source of Levantine Bottom Water was in the eastern basin proper. Confirmed by the distribution of oxygen in the deep

layers of the entire eastern Mediterranean, considerable mixing appears to take place between the relatively fresh waters from the north with the saline waters of the upper hundred meters of the Ionian Sea. Sinking of this resultant parcel of water flows intermittently along the bottom into the major eastern basins in a counter-clockwise flow circulation.

If marked changes in gradients were to be used in determining the vertical limits of the Levantine Deep Water, a 700 meter depth could be viewed as the possible boundary layer. However, if absolute numerical values were to be used, approximately 1600 meters could be viewed as possibly the upper limit for the deep water. Below 1600 m, dissolved oxygen values in the Ionian are found to be approximately 0.15 ml/l greater than those found in the Levantine Basin; the temperature and salinity structures are similar (e.g. temperature minimums near 13.57°C; salinity, isohaline near 38.65‰). For this report, the region between 750 to 1600 meters will be considered as a "transition zone" between the intermediate and deep waters of the eastern Mediterranean basins. This zone of transition is not applicable to the entire eastern Mediterranean, but predominantly in and near deep basin regions.

Wust (1961) presented an informative description of the vertical and horizontal distribution and flow of water parcels in the Levantine Basin. Identified were four different core masses, developed from the vertical distribution of temperature, salinity and oxygen: (1) the near-surface water, (2) the intermediate water, (3) the deep water, and (4) the bottom water. In discussions regarding the various watermasses which have been studied in the Mediterranean, the most popular is the Levantine Intermediate Water (L.I.W.). The most striking characteristic of the L.I.W. is the associated salinity maximum. During the winter period in the northern region of the Levantine Basin, studies have revealed that conditions for favorable water-mass formation exist. This region (located on both sides of the island of Rhodes) is where favorable surface conditions (low temperatures of 15.0°C; high salinities of 39.1‰) for vertical thermal haline convective processes

develop. The resultant newly formed winter parcel of water of high salinity spreads out within the core layer to all basins (eastern and western) of the Mediterranean. This process of water type formation appears to be a seasonal phenomenon (varying in degree from winter to winter) whose intensity and strength can be mapped from season to season. Figures 5-42 and 5-43 illustrate the geographical placement of the core of the L.I.W. for winter and summer, respectively. The southerly displacement of the core in winter reflects a stronger presence in intensity, whereas the northerly displacement of the core in the summer reflects a weaker intensity of flow. The vertical spreading in the vicinity of formation changes to horizontal spreading while approaching the intermediate depths. The L.I.W. continues its general westerly direction passing through the Ionian Basin, over the Malta Sill, over the Strait of Sicily (system of sills) and into the western Mediterranean basin. This L.I.W. has been confirmed by investigators to flow out over the Gibraltar sill into the eastern North Atlantic Ocean. This westerly undercurrent flow of L.I.W. over the Gibraltar sill has been observed to be of measurable strength, at times reaching high velocities of more than 100 cm/sec near 275 meters in depth (Wust). This undercurrent on occasion has been referred to as the Levantine Intermediate Undercurrent. The presence and influence of this L.I.W. appears to be most strongly felt at depths that correspond to potential densities near 29.10 (Morel).

Treatment on the sources of deep and bottom waters for the eastern Mediterranean (which includes the Levantine Basin) have been discussed and presented in the oceanographic description of the Ionian Sea. Other features observed and measured in the Levantine Sea were thermal fronts and subsurface intrusions of less saline water. Levine and White (1972), during the cruise of the R. V. Chain in 1966, describe a thermal front, assumed continuous, which followed the general eastern coastline configuration of the Mediterranean, Figure 5-44. It is suggested by these investigators that this thermal front is associated with the general counter-clockwise circulation around the eastern Mediterranean basin. Miller, Tschernia and

Charnock have mapped the eastern Levantine basin. Their study revealed several features, one of which was the presence of fresh water intrusions at subsurface levels. A possible explanation for these intrusive layers of fresh water is that these parcels are related to large quantities of fresh water river run-off or discharge. Unfortunately, neither the persistence nor degree of temporal variability of this particular feature is adequately known.

Meteorologically, this region is considered variable. Seasonal weather patterns are largely influenced by patterns that develop over the adjacent land masses. Cyclogenesis development, in general, is limited and originates at other distant regions (i.e. Ionian Sea and the Aegean Sea regions). A minor region is located over Cyprus. The winter patterns are very cold (relative to the sea surface temperatures), unsettled, and have associated strong winds. The summer patterns are dry and heated air masses have persistent surface winds.

5.9.2 Comparison

GDEM temperature and salinity vertical cross-sections along great circle track MX-09 were compared with the Chain #21 data of October 18, 1961 to November 11, 1961 and evaluated as follows:

- Temperature

Fall comparisons of temperature revealed in both the GDEM and Chain 21 analyses the presence of known isotherms in this region. At the surface, both analyses reflected two distinct regions of surface temperature maxima (a lens-like maximum centered near $34^{\circ}00'N$ latitude; and northward surface layer maximum extending from the south up to approximately $33^{\circ}15'N$ latitude). The thickness of these two surface maxima were also similar ≤ 100 meters. The $15.0^{\circ}C$ isotherm was reflected in both analyses between the 200 meter and 300 meter levels. The $14.0^{\circ}C$ isotherm was reflected in both analyses between the 450 meter and 650 meter levels. Below 1000 meters both analyses reflected the deep region as $13.5 \leq T^{\circ}C \leq 14.0^{\circ}C$.

- Salinity

Fall comparisons of salinity revealed in both the GDEM and Chain 21 analyses the presence of known isohalines in this region. At the surface, both analyses reflected the presence of a thin salinity maximum layer (≤ 100 meters in thickness) from the north and extending southward out to approximately $33^{\circ}00'N$ to $32^{\circ}00'N$ latitude. In the near subsurface region (≤ 500 meters) both analyses reflected three similar features. First, both reflected two regions of subsurface salinity maxima ($\geq 39.0^{\circ}/\text{oo}$, at approximately the 200 meter levels) near $35^{\circ}00'N$ and $33^{\circ}30'N$ latitude, respectively. Second, both reflected a thin (≤ 50 meters in thickness) subsurface salinity minimum ($\leq 38.8^{\circ}/\text{oo}$, at approximately the 100 meter level) near $32^{\circ}00'N$ latitude. Also, both analyses reflected the major subsurface $38.8^{\circ}/\text{oo}$ isohaline as extending throughout the cross section and present between the 500 meter and 600 meter depth levels. Below 1000 meters both analyses reflected the deep region as $38.6^{\circ}/\text{oo} \leq S^{\circ}/\text{oo} \leq 38.8^{\circ}/\text{oo}$.

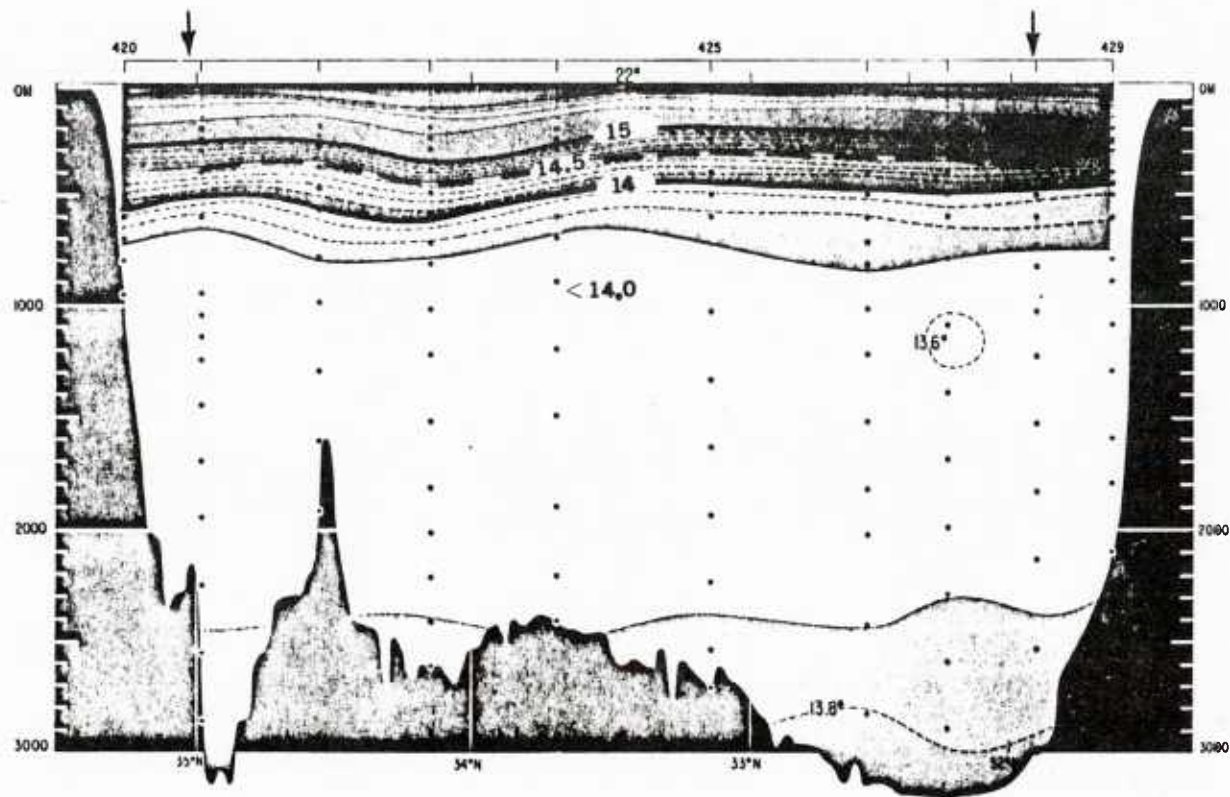


FIGURE 5-43: FALL VERTICAL TEMPERATURE CROSS-SECTION
ALONG GREAT CIRCLE TRACK MX-09

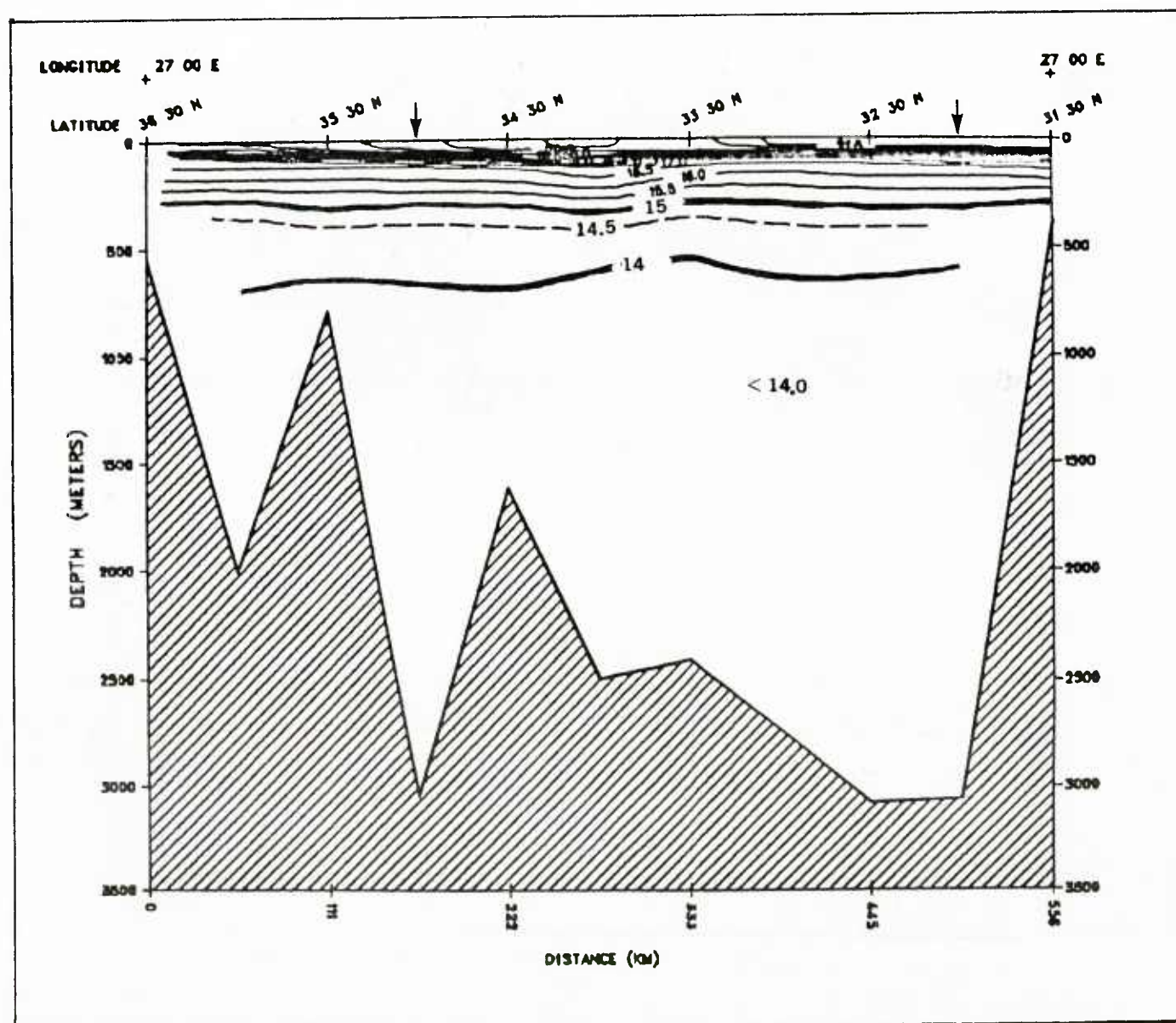


FIGURE 5-44: GDEM - FALL VERTICAL TEMPERATURE CROSS-SECTION
ALONG GREAT CIRCLE TRACK MX-09

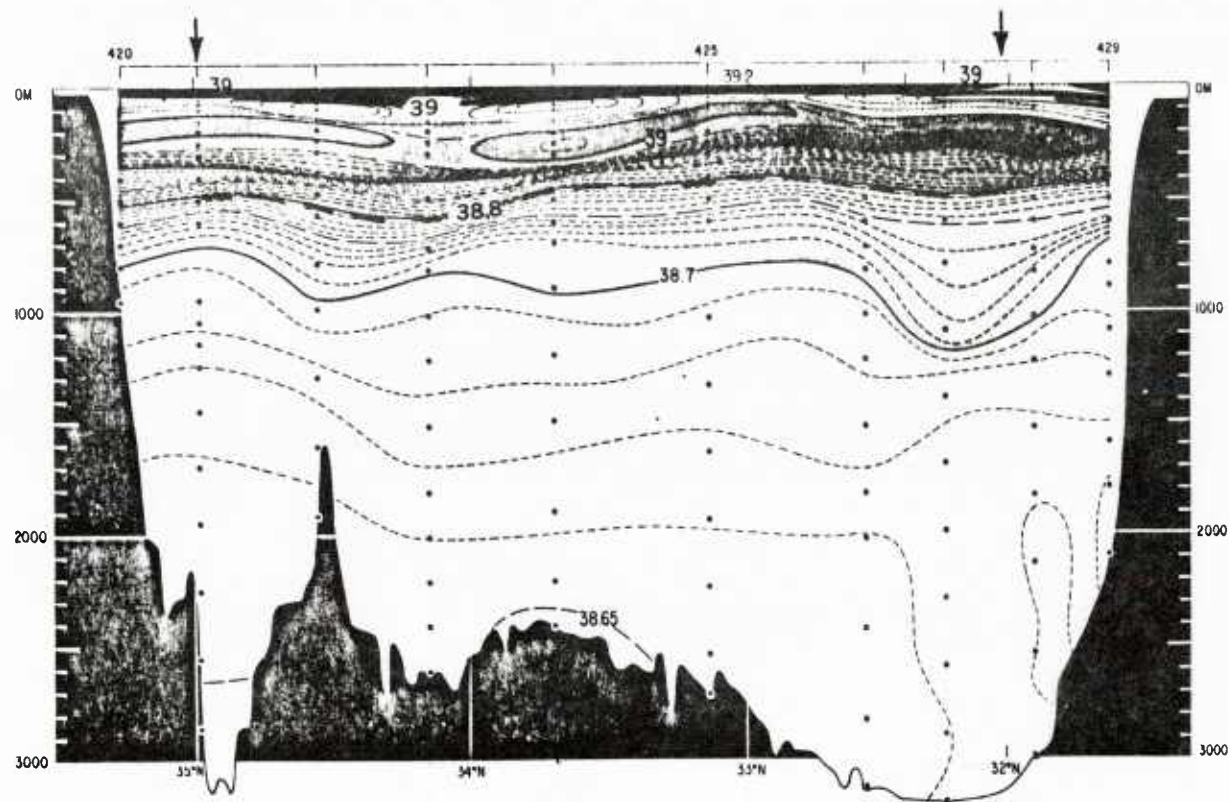


FIGURE 5-45: FALL VERTICAL SALINITY CROSS-SECTION
ALONG GREAT CIRCLE TRACK MX-09

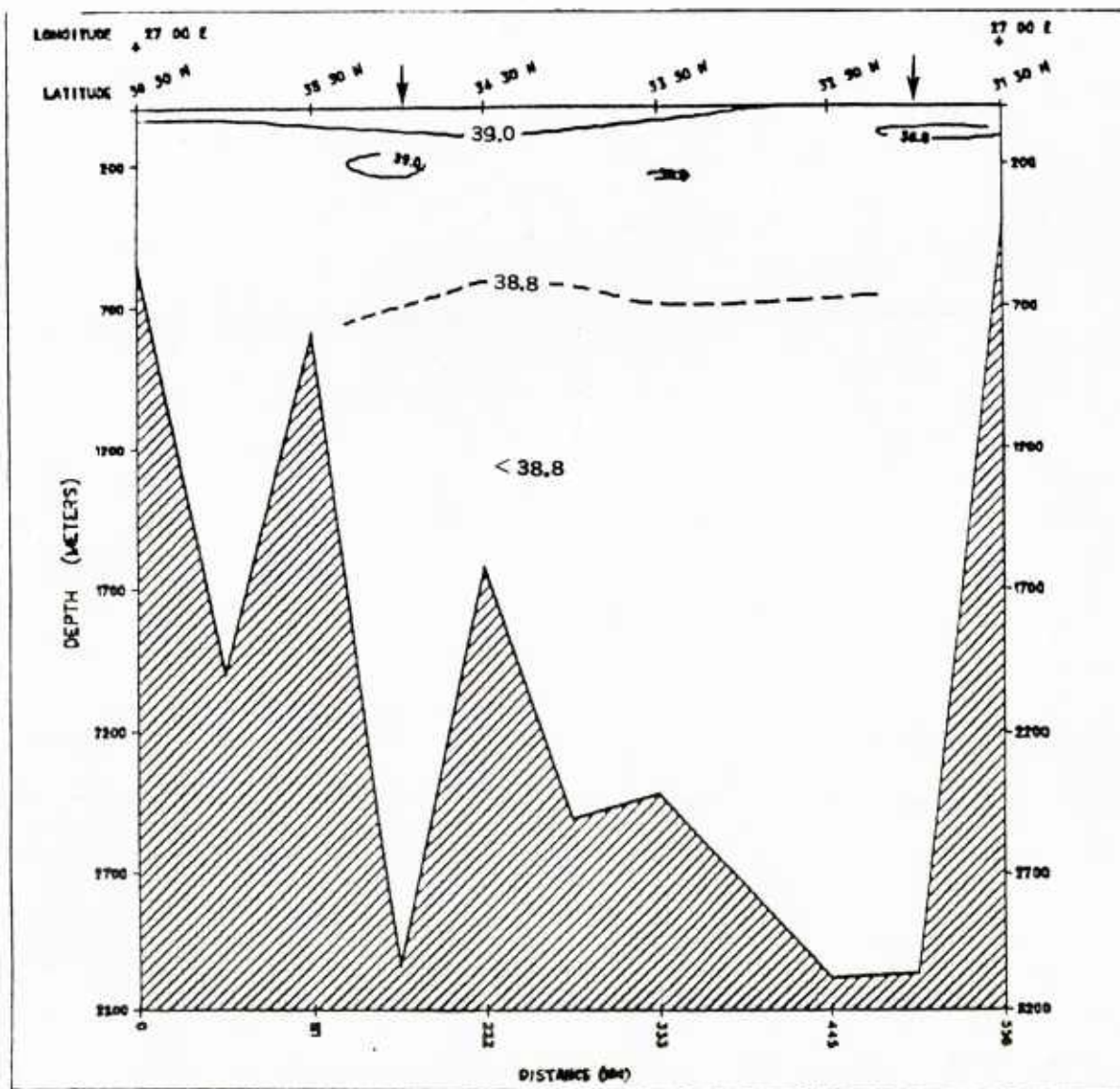


FIGURE 5-46: GDEM - FALL VERTICAL SALINITY CROSS-SECTION
ALONG GREAT CIRCLE TRACK MX-09

5.10 Vertical Temperature and Salinity Comparisons for MX-10 (Balearic Sea)

Vertical cross-sections of salinity (S) for the summer time period were compared. The survey cross-sections were taken during the R. V. Atlantis II cruise of 1970.

5.10.1 Regional Description

Section MX-10 was selected from the Balearic Sea region of the Mediterranean Sea. The vertical cross-sections are defined by a great circle track which originates at $38^{\circ}00'N$, $5^{\circ}00'E$ and terminates at $38^{\circ}00'N$, $9^{\circ}00'E$. The locations of the Balearic Sea and Section MX-10 are depicted on Figure 1-1. Vertical cross-sections of temperature and salinity for MX-10 are shown on Figures 5-47 through 5-48.

Oceanographically, this region is considered highly variable. The ocean variability and changes in the vertical and horizontal structuring are direct and substantial responses to the variable and seasonal impulses generated from the nearby zone of cyclogenesis. Seasonal effects of mechanical mixing are generally confined to the near-surface structure.

There is general agreement among investigators that the primary access (inflow) of the Levantine Intermediate Water (L.I.W.) is through the passageway between the island of Sardinia and the northern coastlines of Tunisia and Algeria. It has been accepted and studied that a predominantly westerly subsurface flow of L.I.W. follows the coastline of Algeria into the Alboran Sea by Wust, 1961, Katz, 1972; Molcard, 1972, and others.

Not thoroughly understood, however, is the actual northerly subsurface intrusion and its associated circulation pattern into the central and northern portions of the Balearic Sea. Indications of the northerly intrusion of L.I.W. can be detected in the work of Katz, 1972, where bifurcation southwest of Sardinia, at approximately 250 meters, of the most saline layer is recorded as turning north. The volume and pattern of this flow is not clearly

understood. Also, it is suggested, by Katz, that one possible exit of the L.I.W. from the Balearic Sea may be located in the southern region near the island of Mallorca.

In reviewing the works by Miller, Tschernia, Charnock and Wust, the Balearic appears to provide for two separate regions for the formation of two distinct Mediterranean water masses: the North Balearic Deep Water and the North Balearic Bottom Water. Analysis of oxygen distribution in the core layer of the Mediterranean Deep Water, from the studies by Wust and Miller, Tschernia and Charnock, indicate that the region northeast of the island of Mallorca and south of France (near the Golfe du Lion at approximately $42^{\circ}00'N$ latitude and $5^{\circ}00'E$ longitude) is the primary source and location for the formation of the North Balearic Deep Water. Other investigations (French naval vessel ORIGNY, 1903; R.V. ATLANTIS, U.S.A., 1961; and six vessels from the U.S.A., France, U.K. and Italy in 1969 of the MEDOC Group) have all revealed the same conclusion. The conclusion was that the winter formation and sinking of the deep water in this region follows three distinct phases: pre-conditioning, violent mixing, and sinking/spreading. Salinity values range near $38.20^{\circ}/\text{oo}$ to $38.48^{\circ}/\text{oo}$; surface σ_t exceed 29.00 ; potential temperatures were near 10.0° to $12.0^{\circ}C$; and the depths to which sinking extended occurs approximately down to 1400 meters. Oxygen contents exceeding 4.6 ml/l were reported by Wiess.

Analysis of potential temperature indicated that the Ligurian Sea north of the island of Corsica yielded itself as the location for the source and formation of the North Balearic Bottom Water. This bottom water contains relatively high oxygen and high salinity levels. Balearic Bottom Water is characterized by temperatures of 12.6° to $12.7^{\circ}C$, salinities of $38.35^{\circ}/\text{oo}$ to $38.45^{\circ}/\text{oo}$, and σ_t of 29.1 below 1500 meters.

Meteorologically, this region is considered active, variable, and seasonally influenced by an area that is known for cyclogenesis. This area is located off the eastern coast of Spain in the Balearic Sea and encompasses the Balearic Islands. Cyclogenesis over the Balearic Sea is frequently found in the winter, with common occurrences in the spring and fall.

5.10.2 Comparison

GDEM salinity vertical cross-section along great circle track MX-10 was compared with the R. V. Atlantis II, Cruise #59 data of July 1970 and evaluated as follows:

- Temperature

No GDEM temperature comparisons were made due to the lack of an appropriate R. V. Atlantis II temperature cross-section.

- Salinity

Summer comparisons of salinity revealed some similarities between the GDEM and R. V. Atlantis II analyses (by Katz). Both revealed a surface layer of $\leq 38.0^{\circ}/\text{oo}$. Both revealed a well-defined subsurface salinity maximum region ($\geq 38.5^{\circ}/\text{oo}$) throughout the cross-section having a vertical thickness of approximately 500 to 600 meters toward $8^{\circ}45'\text{E}$ longitude and thinning in thickness (down to approximately 100 to 150 meters) westward toward $5^{\circ}00'\text{E}$ longitude. Both analyses also revealed similarities in the vertical thicknesses of a subsurface salinity maximum region of between the 400 to 550 meter levels at $5^{\circ}00'\text{E}$ longitude and 250 to 850 meters at $8^{\circ}45'\text{E}$ longitude. The Atlantis analysis reflected the $38.5^{\circ}/\text{oo}$ subsurface maximum surfaces as having undulations between the $6^{\circ}00'\text{E}$ to $7^{\circ}00'\text{E}$ longitude. This may be simply a difference caused by a short wavelength feature instead of a historical persistent feature.

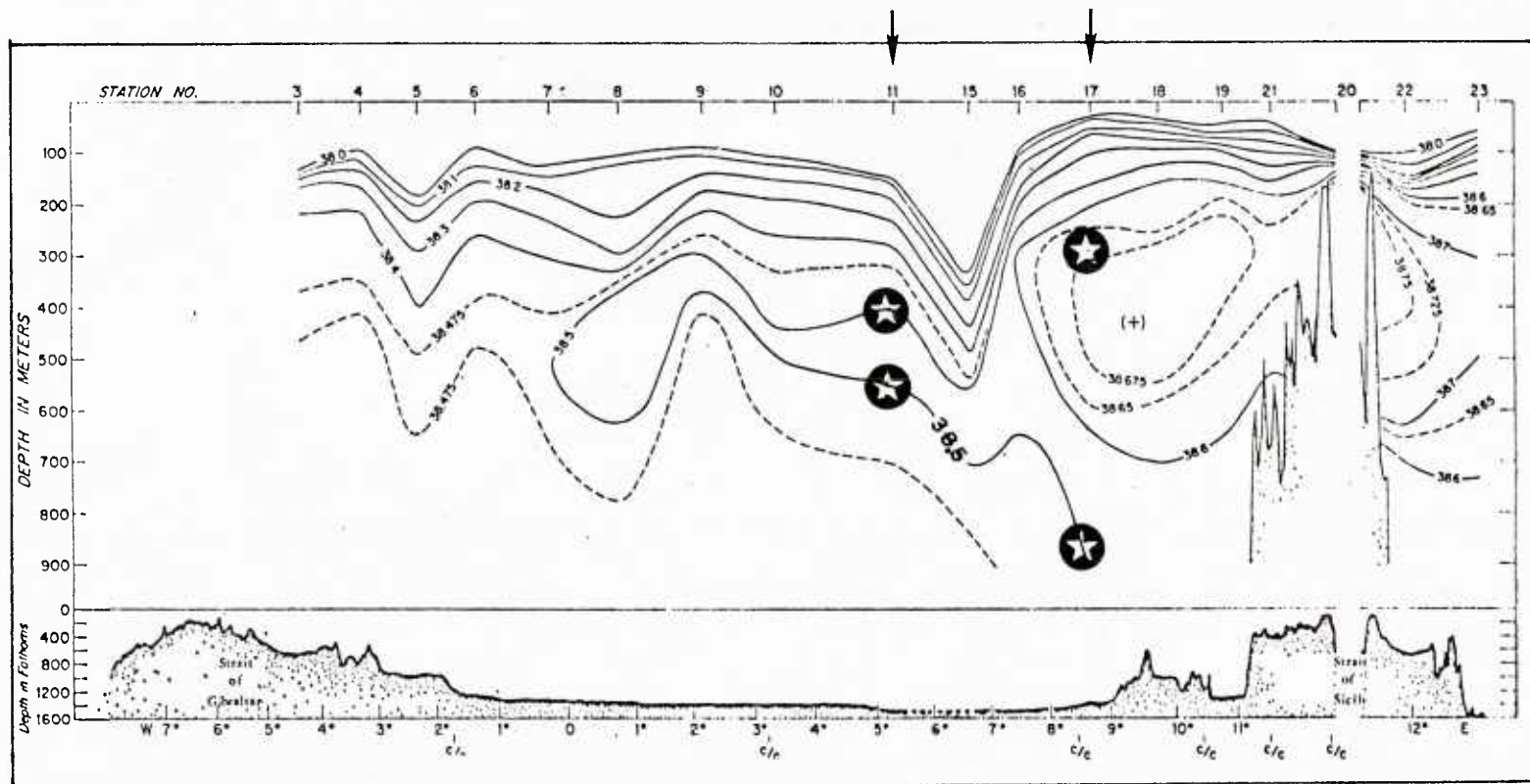


FIGURE 5-47: SUMMER VERTICAL SALINITY CROSS-SECTION
ALONG GREAT CIRCLE TRACK MX-10

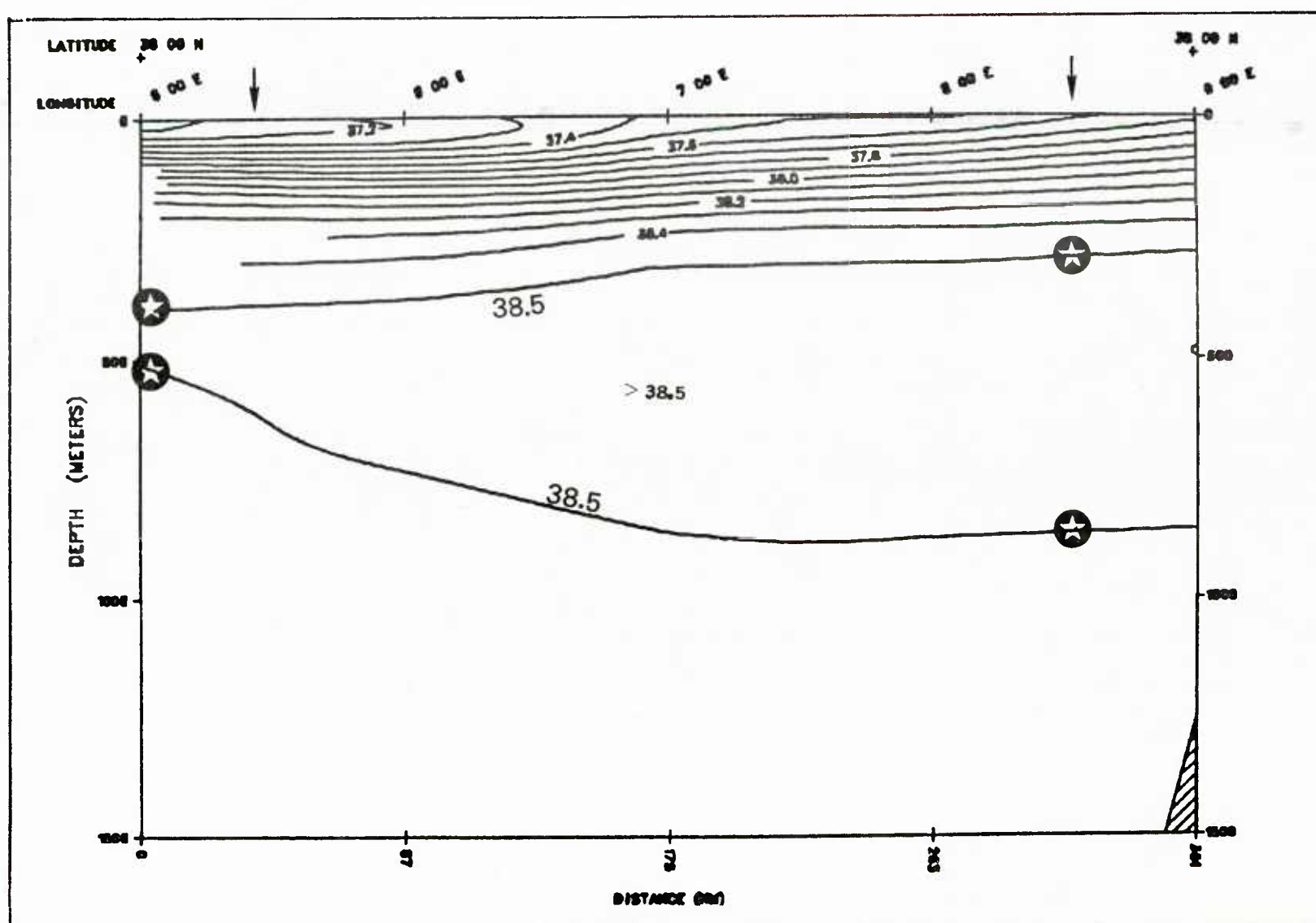


FIGURE 5-48: GDEM - SUMMER VERTICAL SALINITY CROSS-SECTION
ALONG GREAT CIRCLE TRACK MX-10

6.0 REFERENCES

AMBAR, I. and HOWE, M. R., "Observations of the Mediterranean Outflow-I., Mixing in the Mediterranean Outflow," Deep Sea Research, 26, 1979a, pp 535-554.

AMBAR, I. and HOWE, M. R., "Observations of the Mediterranean Outflow-II., The Deep Circulation in the Vicinity of the Gulf of Cadiz," Deep Sea Research, 26A, 1979b, pp 555-568.

AMBAR, E., HOWE, M. R., and ABDULLAH, M. I., "A Physical and Chemical Description of the Mediterranean Outflow in the Gulf of Cadiz," Deutsche Hydrographische Zeitschrift, 29, 1976, pp 58-68.

BRISCOE, M. G., JOHANNESSEN, O. M., and VINCENZI, S., "The Maltese Oceanic Front: A Surface Description by Ship and Aircraft," Deep Sea Research, 21, 1974, pp 247-262.

CHENEY, R. E., "Aerial Observations of Oceanic Fronts in the Western Mediterranean Sea," Tech. Note 3700-69-77, U. S. Naval Oceanographic Office, Washington, D. C., 1977.

DEFANT, A., "Scilla and Charybdis und die Gezeitenströmungen in der Strasse von Messina," Ann. Hydr. Marit. Met., 68, No. 5, 1940.

DEFANT, A., Physical Oceanography, Volume (2), 404, 1960.

DONGUY, J. R., "Hydrology of the Alboran Sea," Cahiers Oceanogr., 8, 1962, pp 573-578.

FAIRBRIDGE, V., Encyclopedia of Oceanography, Vol. I., Reinhold Publishing Corporation, N. Y., 1966.

FEDEROV, K. N., "Temperature Inversions in the Red and Mediterranean Sea," Oceanology, 12, No. 6, 1972, pp 795-803.

FEDEROV, K. N., "The Stepped Structure of Temperature Inversions in the Ocean," Izv. Akad. Nauk SSSR, Ser. Fiz. atmos. i Okeana, 6, No. 11, 1970.

FRASSETTO, R., "A Study of the Turbulent Flow and Character of the Water Masses Over the Sicilian Ridge in Both Summer and Winter," RAPP. PROC. VERB. C. I. E. S. M., XVIII, 3, 1964, pp 812-815.

GROUSSON, R., and FAROUX, J., "Surface Current Measurements in the Alboran Sea," Cahiers Oceanogr., 15 (10), 1963, pp 716-721.

HILL, M. N., "The Earth Beneath the Sea, History," The Sea, Volume (3), 253, 1963.

JOHANNESSEN, O. M., de STROBEL, F., and GEHIN, C., "Observations of an Oceanic Frontal System East of Malta in May, 1971 (MAYFROST)," SACLANT ASW Research Centre, Technical Memorandum No. 169, La Spezia, Italy, (NATO Unclassified), 1971.

JOHANNESSEN, O. M., "Oceanic Layered Micro-structures and Fronts. Geometrical Acoustics - Ray Tracing," SACLANT ASW Research Centre, Conference Proceedings No. 5, La Spezia, Italy, December 1971. pp 1-21.

KATZ, E. J., "The Levantine Intermediate Water Between the Strait of Sicily and the Strait of Gibraltar," Deep Sea Research, 19, 1972, pp 507-520.

LEVINE, E. R. and WHITE, W. B., "Thermal Frontal Zones in the Eastern Mediterranean Sea," Journal of Geophysical Research, 77 (6), 1972, pp 1081-1086.

LINDEN, P. F., "The Formation of Banded Salt Finger Structure," Journal of Geophysical Research, 83 (C6), 1978, pp 2902-2912.

MEDOC GROUP, "Observation of the Formation of Deep Water in the Mediterranean Sea 1969," Nature, No. 5262, 1970, pp 227.

MILLER A. R., TSCHERNIA P., and CHARNOCK H., "Mediterranean Sea Atlas," Woods Hole Oceanographic Institute Atlas Series 3, 1970, pp 190.

MOLCARD, R., "The Strait of Sicily in Relation to the General Circulation of the Mediterranean," SACLANT ASW Research Centre, Proceeding No. 7, September 1972.

MOREL, A., "The Hydrological Characteristics of the Waters Exchanged Between the Eastern and Western Basins of the Mediterranean," SACLANT ASW Research Centre Proceeding No. 7, September 1972.

NIELSEN, J. N., "Hydrology of the Mediterranean and Adjacent Waters," Report of the Danish Oceanographical Expeditions 1908-1910 to the Mediterranean and Adjacent Seas, Copenhagen, Vol. 1, 1912, pp 77-192.

OVCHINNIKOV, I. M., "Circulation in the Surface and Intermediate Layers of the Mediterranean Sea," Okeanologiya, 6, 1976, pp 62-75.

OVCHINNIKOV, I. M., KRIVOSHEYA, V. G., and MASKALENKO, L. V., "Anomalous Features of the Water Circulation of the Alboran Sea During the Summer of 1962," Oceanology, 15 (1), 1976, pp 31-35.

POLLAK, M. J., "Sources for Deep Water of the Eastern Mediterranean Sea," Journal of Marine Research, Sears Foundation, 1951, pp 10.

ROBINSON M. K., BAUER, R. A. and SCHROEDER, E. H., "Atlas of North Atlantic - Indian Ocean Monthly Mean Temperatures and Mean Salinities of the Surface Layer," Naval Oceanographic Office Reference Publication #18, 1979.

ROMANOVSKY, V. and LE FLOCH, J., "L'eau Intermediare en mer Tyrrhenienne en regime d'ete.," Cahiers Oceanogr. No. 3, 1966, pp 18.

SCHOTT, G., "Die Gewasser des Mittelmeeres," Ann. Hydrogr. Berl., 43, 1915, pp 1-18, 63-79.

STEVENSON, R. E., "Huelva Front and Malaga, Spain Eddy Chain as Defined by Satellite and Oceanographic Data," Sonderuck Deut. Hydrogr. Z., 2, 1977, pp 51-53.

STOMMEL, H., VOORHIS, A., and WEBB, D., "Submarine Clouds in the Deep Ocean," American Science, 59, 1971, pp 716-722.

SVERDRUP, JOHNSON, and FLEMING, The Oceans, Prentice Hall, Inc., New Jersey, 1942.

TAIT, R. I. and HOWE, M. R., "Thermohaline Staircase," Nature, 231, 1971, pp 178-179.

VERCELLI, F., "Il regime delle correnti e delle maree nello Stretto di Messina," Commissione Internazionale del Mediterraneo, 1, 1925, pp 209.

WOODS, J. D., "The Structure of Fronts in the Seasonal Thermocline, Oceanography of the Strait of Sicily," SACLANT ASW Research Centre, Conference Proceeding No. 7, La Spezia, Italy, September 1972, pp 144-152.

WOODS, J. D. and WATSON, N. R., "Measurement of Thermocline Fronts From the Air," Underwater Science and Technology (now Underwater Journal), 2, 1970, pp 90-99.

WUST, G., "On the Vertical Circulation of the Mediterranean Sea," Journal of Geophysical Research, 66, No. 10, , 1961, pp 3261-3271.

U206191